THE UNIVERSITY OF TURKISH AERONAUTICAL ASSOCIATION
INSTITUTE OF SCIENCE AND TECHNOLOGY

UTILIZATION OF SMART PHOTOVOLTAIC SYSTEMS FOR POWER QUALITY IMPROVEMENT IN DAY AND NIGHT

MASTER THESIS

RAAD DHAHI ABDULLAH

**A THESIS SUBMITTED IN PARTIAL FULFILLMENT OF THE REQUIREMENTS FOR THE DEGREE OF
MASTER SCIENCE OF IN
ELECTRICAL AND ELECTRONICS ENGINEERING**

OCTOBER 2017

THE UNIVERSITY OF TURKISH AERONAUTICAL ASSOCIATION
INSTITUTE OF SCIENCE AND TECHNOLOGY

UTILIZATION OF SMART PHOTOVOLTAIC SYSTEMS FOR POWER QUALITY IMPROVEMENT IN DAY AND NIGHT

MASTER THESIS

Raad Dhahi ABDULLAH

1406030002

A THESIS SUBMITTED IN PARTIAL FULFILLMENT OF THE REQUIREMENTS FOR THE DEGREE OF MASTER OF SCIENCE IN ELECTRICAL AND ELECTRONICS ENGINEERING

Supervisor: Prof. Dr. Doğan ÇALIKOĞLU

Raad Dhahi ABDULLAH, having student number **1406030002** and enrolled in the Master Program at the Institute of science and Technology at the University of Turkish Aeronautical Association, after meeting all of the required conditions contained in the related regulations, has successfully accomplished, in front of jury, the presentation of the thesis prepared with the title of: "**Utilization of Smart Photovoltaic Systems For Power Quality Improvement In Day And Night**".

Supervisor : **Prof. Dr. Doğan ÇALIKOĞLU**
University of Turkish Aeronautical Association ....

Jury Member : **Prof. Dr. Doğan ÇALIKOĞLU**
University of Turkish Aeronautical Association ....

: **Assist. Prof. Dr. Ozan KEYSAN**
Middle East Technical University ....

: **Assist. Prof. Dr. Ibrahim MAHARIQ**
University of Turkish Aeronautical Association ....

Thesis Defense Date: 06 .10.2017

THE UNIVERSITY OF TURKISH AERONAUTICAL ASSOCIATION
INSTITUTE OF SCIENCE AND TECHNOLOGY

I hereby declare that all information in the study I presented as my Master's Thesis, called; **UTILIZATION OF SMART PHOTOVOLTAIC SYSTEMS FOR POWER QUALITY IMPROVEMENT IN DAY AND NIGHT** has been presented in accordance with the academic rules and ethical conduct. I also declare and clarify with my honor that I have fully cited and referenced all the sources I made use of in the present study.

06.10.2017
Raad Dhahi ABDULLAH

ACKNOWLEDGEMENTS

First of all, I thank Allah for helping me to complete this thesis.

I would like to acknowledge my thesis advisor Prof. Dr. Doğan ÇALIKOĞLU at University of Turkish Aeronautical Association for his guidance and encouragement through my research for this thesis. Also, I would like to acknowledge and thank for my parents and my brother and sisters for their help and support during my study.

October 2017 Raad Dhahi ABDULLAH

TBALE CONTENTS

ACKNOWLEDGEMENTS .... **iv**
TBALE CONTENTS .... **v**
LIST OF TABLES .... **vii**
LIST OF FIGURES .... **viii**
LIST OF ABBRIVIATION .... **xi**
ABSTRACT .... **xii**
ÖZET .... **xiv**
CHAPTER ONE **1**
1. INTRODUCTION **1**
1.1 Presentation of the Work 1
1.2 Main Component 1
1.2.1 PV Cells 2
1.2.2 Voltage Source Converters (VSC): 4
1.3 Literature Review 4
1.4 The Main Aspects of the Work 6
1.5. Thesis Contents 7
CHAPTER TWO **8**
POWER QUALITY **8**
2.1 Overview 8
2.2 Why is The Interest About Power Quality? 8
2.3 Power Quality Problems Types 8
2.4 Power Quality Problems Discussion 9
2.4.1 Power Quality Due to Voltage Waveform Distortion 9
2.4.2 Power Quality Due To Current Waveforms Distortion 10
2.4.3 Power Quality Problems Due Non Unity Power Factor 10
2.5 Impact of Harmonics in Recent Buildings 11
2.6 Offer of Harmonic Voltage Distortions in New Buildings Include 12
2.7 Power Quality Measurement 12
2.8 Power Quality Standards 13
CHAPTER THREE **14**
3. MATHEMATICAL ANALYSIS OF SMART PV SYSTEM **14**
3.1 System Analysis 14
3.2 Smart PV System Analysis 15
3.3 System Analysis in Case of Linear Inductive Load and Idle PV system (In Night) 17
3.4 System Analyses in Case of Nonlinear Load and PV System Idle (in Night) 19
3.5 Power Components Calculation in Case of Linear Load and Real Power Production By the Pv System For Three Cases (Real Produced Power Less Than, Equal, Or More Than The Load Real Power 21
3.5.1 In Case That The Real Power Produced Less Than The Load Demand 21
3.5.2 In Case The Produced Real Power Equal to The Load Demand 22

3.6 Power Components Calculation in Case of Nonlinear Load and Real Power Production By The Pv System For Three Cases (Real Produced Power Less Than, Equal, Or More Than The Load Real Power 28
CHAPTER FOUR **32**
4. SMART PV SYSTEM SIMULATION **32**
4.1 Photo Voltaic PV Cell Simulation 32
4.2 Modified System Capacity 36
4.3 Capacitor Bank 37
4.4 Single Phase Voltage Source Converter 37
4.5 Power Transistors Switching and Control Circuits 38
4.6 AC Power Source 40
CHAPTER FIVE **42**
5. SIMULATION RESULTS DISCUSSION **42**
5.1 Linear Load Case 42
5.1.1 The First Case Idle PV Cells (in Night) 42
5.1.2 The Second Case 45
5.1.3 The Third Case 48
5.1.4 The Fourth Case 51
5.2 Nonlinear Load Case 54
5.2.1 The First Case Idle PV Cells (in Night) 54
5.2.2 The Second Case 57
5.2.3 The Third Case 60
5.2.4 The Fourth Case 63
5.3 Simulated Results Study 66
CHAPTER SIX **69**
CONCLUSION AND FUTURE WORKS **69**
REFERENCES **70**
CURRICULUM VITAE **73**

LIST OF TABLES

Table 2.1 : IEEE stander 519-1992. 13
Table 3.1 : System power components for nonlinear load. 21
Table 3.2 : Load power components. 21
Table 3.3 : Source power components. 23
Table 3.4 : Smart PV system power components. 24
Table 3.5 : Load power components. 28
Table 3.6 : Source power components. 28
Table 3.7 : Smart PV system power components. 28
Table 5.1 : System power components of linear load for first case. 43
Table 5.2 : System power components of linear load for second case. 46
Table 5.3 : System power components of linear load for third case. 49
Table 5.4 : System power components of linear load for fourth case. 52
Table 5.5 : System power components of nonlinear and idle PV cells. 55
Table 5.8 : System power of nonlinear load for fourth case. 64

LIST OF FIGURES

Figure1.1: PV cell module, and matrix. 2
Figure 1.2: PV equivalent circuit. 3
Figure 2.1: Voltage sag. 9
Figure 2.2: Voltage swell. 9
Figure 2.3: Distorted current waveform. 10
Figure 2.4: Non-unity power factor. 11
Figure 3.1: Smart PV system. 15
Figure 3.2: Waveforms of source voltage and load current. 17
Figure 3.3: Waveforms of source voltage and smart PV current. 18
Figure 3.4: Waveforms of source voltage and current. 18
Figure 3.5: Waveforms of source voltage and load current. 20
Figure 3.6: Waveforms of source voltage and smart PV system current. 20
Figure 3.7: Waveforms of source voltage and current. 20
Figure 3.8: Waveforms of source voltage and load current. 24
Figure 3.9: Waveforms of source voltage and smart PV system current. 25
Figure 3.10: Waveforms of source voltage and current. 25
Figure 3.11: Waveforms of source voltage and smart PV system current. 26
Figure 3.12: Waveforms of source voltage and current. 26
Figure 3.13: Waveforms of source voltage and smart PV system current. 27
Figure 3.14: Waveforms of source voltage and current. 27
Figure3.15: Waveforms of source voltage and load current. 29
Figure 3.16: Waveforms of source voltage and smart PV system current. 29
Figure 3.17: Waveforms of source voltage and current. 30
Figure 3.19: Waveforms of source voltage and current. 30
Figure 3.20: Waveforms of source voltage and smart PV system current. 31
Figure 3.21: Waveforms of source voltage and current. 31
Figure 4.1: PV Cell equivalent circuit. 32
Figure 4.2: Block diagram for PV cell and the values irradiance, and temperature. 33

Figure 4.3: Matlab PV equivalent circuit. 34

Figure 4.4: Diode and shunt resister circuit. 34

Figure 4.5: V&I and V&P characteristics lines. 35

Figure 4.6: V&I and P&V for PV matrix.. 35

Figure 4.7: V&I and V&P line or the PV matrix. 36

Figure 4.8: Full bridge voltage source converters.. 38

Figure 4.9: Power transistors switching and control circuit. 39

Figure 4.10: Switching signal sample. 39

Figure 4.11: Samples for wanted and actual currents and modulated signal. ... 39

Figure 4.12: Spectrum analyses for a-actual smart PV system current and b-wanted current. 40

Figure 4.13: Overall system components. 41

Figure 5.1: Show system implementation by Matlab/ Simulink program. 43

Figure 5.2: Shows the waveforms of source voltage, source current, load current and smart PV current respectively. 43

Figure 5.3: A and B show FFT analysis of the load current. 44

Figure 5.4: A and B show FFT analysis for source current. 45

Figure 5.5: Show system implementation by Matlab/ Simulink program. 46

Figure 5.6: Shows the waveforms of source voltage, source current, load current and smart PV current respectively. 47

Figure 5.7: A and B show FFT analysis for source current. 47

Figure 5.8: A and B show FFT for load current... 48

Figure 5.9: Show system implementation by Matlab/Simulink program. 49

Figure 5.10: Waveforms of source voltage, source current, load current and smart PV current respectively. 50

Figure 5.11: A and B show FFT for load current... 50

Figure 5.12: A and B show FFT for load current... 51

Figure 5.13: Show system implementation by Matlab/ Simulink program. 52

Figure 5.14: shows the waveforms of source voltage, source current, load current and smart PV current respectively. 53

Figure 5.15: A and B show FFT for load current... 53

Figure 5.16: A and B show FFT for smart PV current..................................... 54

Figure 5.17: Show system implementation by Maltab/Simulink program. 55

Figure 5.18: Waveforms of the source voltage, source current, smart PV current, and load current respectively. 56

Figure 5.19: A and B FFT of load current. 56

Figure 5.20: A and B FFT of source current. 57

Figure 5.21: Show system implementation by Matlab/Simulink program. 58

Figure 5.22: Waveforms of the source voltage, source current, smart PV current and load current respectively. 59

Figure 5.24: A and B FFT of source current. 60

Figure 5.25: System implementation by Matlab/Simulink program. 61

Figure 5.26: Waveforms of the source voltage, source current, load current and smart PV converter current respectively. 62

Figure 5.27: A and B show FFT of load current. 62

Figure 5.28: A and B show FFT of source current. 63

Figure 5.29: System implementation by Matlab/ Simulink program. 64

Figure 5.30: Waveforms of source voltage, source current, load current and smart PV current respectively. 65

Figure 5.31: B and B FFT analysis of the load current. 65

Figure 5.32: A and B FFT analysis of the smart PV current............................ 66

Figure 5.33: Apparent powers waveforms for load, SPV and source. 67

Figure 5.34: Real power waveforms for load, PV and source. 67

Figure 5.35: Reactive power waveforms for load, SPV and source. 68

LIST OF ABBRIVIATION

SPVS	:	Smart photovoltaic system
PQ	:	Power Quality
THD	:	Total Harmonic Distortion
CPD	:	Costumer Power Device
VSC	:	Voltage Source Converter
AC	:	Alternating Current
ASD	:	Adjustable Speed Drive
UPS	:	Uninterrupted Power Supply
FACTS	:	Flexible Ac Transmission system
PWM	:	Pulse with Modulation
SVM	:	Space vector Modulation
DG	:	Distributed Generation
DC	:	Direct Current
RMS	:	Root Mean Square
P.F	:	Power Factor
p.u	:	per unit values
UPQC	:	Unified power Quality Condition
PCC	:	Power component compensation
SMPS	:	Switch Mode Power Supply
IEEE	:	Institute of Electrical and Electronic Engineering
IEC	:	International Electro technical Engineering

ABSTRACT

UTILIZATION OF SMART PHOTOVOLTAIC SYSTEMS FOR POWER QUALITY IMPROVEMENT IN DAY AND NIGHT

ABDULLAH, Raad Dhahi

Master, Department of Electrical and Electronics Engineering

Supervisor: Prof. Dr. Doğan ÇALIKOĞLU

October 2017, 71 pages

Power quality enhancement nowadays is one of very important consideration in power system solutions, one of the major power quality causes is the customer power devices CPD, therefore the study takes into consideration that the solution can be performed from the power system end point, by solving the power problem caused by the user and to make the user a part of the aimed solution.

Solar energy is sustainable and one of the cleanest types of energy in spite of its high cost. It produces real power in the day time only; therefore, many studies focus on utilizing solar cell systems for the maximum possible time. One of the proposed topologies was to use the PV system as a STATCOM during the night to compensate for load reactive power. Most of these topologies are implemented in three-phase systems or for specific loads.

This study deals with two points, the first is to modify the system proposed by Arun Kumar and Bhim Singhin (2016) [11] in such way that split the system into three single-phase systems, that leads us to turn method of control driving for transistors, in order to be convenient for handing any type of loads and give it the ability to overcome the power quality problems caused by customer power devices which are almost single phase devices and also to minimize the overall system cost and volume and to increase the benefits. The second is to simulate the modified system and study the results of the simulation.

Keywords: Smart PV system (SPVS), Harmonic detection, Reactive current compensation, Power quality

ÖZET

GECE VE GÜNDÜZDE GÜÇ KALİTESİ GELİŞİMİ İÇİN AKILLI FOTOVOLTAİK SİSTEM KULLANIMI

ABDULLAH, Raad Dhahi

Yüksek Lisans, Elektrik ve Elektronik Mühendisliği

Tez Danışmanı: Prof. Dr. Doğan ÇALIKOĞLU

Ekim 2017, 71 sayfa

Günümüzde güç sistemleri çözümlerinde çok önemli bir husus olan güç kalitesi geliştirmeki ana güç kalitesi faktörlerinden birisi müşteri güç cihazları olan CPD'dir, bu nedenle bu çalışma çözüme enerji sistemi son noktasından bakılabileceği, kullanıcı tarafından kaynaklanan güç problemini çözülmesi, amaçlanan çözümün bir parçası olarak kullanıcıya yardımcı olması açısından önemlidir.

Güneş enerjisi yalnızca gündüz gerçek gücü üretmesi ve yüksek maliyetine rağmen sürdürülebilir ve en temiz enerji türlerinden biridir, böylece bu tez, güneş sistemlerini 24 saat boyunca kullanmak için topolojileri önermektedir. Bu topolojilerden biri, yük tarafından ihtiyaç duyulan reaktif gücün telafi edilmesi ve üç fazlı sistemlerin hepsindeki ızgaradaki gerilim seviyesini kontrol etmesi için onu bir STATCOM olarak kullanmaktır. Bu tezde önerilen topoloji yük dengesizlik problemlerini çözmek için üç tek fazlı sistemler olarak üç fazlı system ile ilgilenmektedir.

Bu çalışma iki nokta ile ilgiliydi, ilki üç fazlı sistemden tek bir faz için akıllı PV sistemi önermek, sistem PV hücresi, voltaj kaynağı dönüştürücü VSC, kontrol sistemi, yük ve AC güç kaynağından oluşmaktadır ve daha sonra sistemi analiz etmek için önemli denklemleri yazmaktır.

İkinci şey, önerilen sistemi Matlab / Simulink programını kullanarak taklit edilmesi ve güneş ve gece zamanında PV hücrelerinin davranışları arasında yük doğası değişimi (doğrusal, doğrusal olmayan, gerçek miktar yükün bir kısmı ile PV hücreleri tarafından üretilen gerçek güç ile karşılaştırılması), güç faktörünü birlik veya birliğe çok yakın tutarak en yüksek güç kalitesine sahip olması ve kaynak akımında minimum toplam harmonik bozulma THD' yi sağlaması gibi birçok olgu için simülasyonun sonuçlarını incelemektir.

Anahtar Kelimeler: akıllı PV sistemi (SPVS), harmonik algılama, reaktif akım telafisi, güç kalitesi

CHAPTER ONE

INTRODUCTION

1.1 Presentation of the Work

In this thesis work, the system proposed by Arun Kumar and Bhim Singhin (2016) [11] is studied and a modification is introduced to make it better for dealing with each phase of the three single phase system separately. This technique gives the system the ability to overcome the unbalanced load problem, to have a better utilization of the PV system in 24 hours for power quality improvement, and increase the number of users due to low cost. As a result the power factor for all studied cases was near unity and the total harmonic distortion was less than 5%.

The original system consisted of a solar PV system, a boost DC/DC converter, a four-leg voltage source converter (VSC) and a three-phase nonlinear load consisting of an RL load connected through three single-phase bridge uncontrolled rectifiers. The system was a symmetrical system [11]. The original system was simulated in two specified cases: the first was the balanced load and the second was a short interval unbalanced load. In both cases, the solar PV system was producing real power, the system capacity of which was 50 KW, 415V, 50Hz.

The modified system consists of a PV matrix, a boost DC/DC converter, a single-phase full bridge voltage source converter (VSC) and a nonlinear load. The system was simulated using the Matlab/Simulink program under all possible cases of operation taking into account the load nature (linear and nonlinear load) and real power production. For all these cases, the system currents were analyzed and the results show that the total harmonic distortion was less than 5% and the power factor was close to unity. To achieve the desired source current, the smart PV system current must be estimated depending on the load current and the effective value of the PV matrix current. This estimated current was compared with the actual converter current so that the error signal would be used in the controller circuit to drive the converter. In such a technique, called random pulse width modulation (RPWM), the use of PWM for power transistors driving was to give the system fast response and fewer undesired harmonics. The word “random” refers to the method of modulated signal estimation because the system has two instantaneous changing variables which are the load current and the real power produced by the PV matrix.

The modified system operation principle is based on load current analysis to estimate the source current which will be forced to be real only and in a unity power factor. The study came in three parts, the first of which was the analytical part which included all mathematical analysis requirements. The second included the simulation and the third was the simulation results and comparison with the analytical results.

1.2 Main Component

1.2.1 PV Cells

The PV cells are connected in groups called modules. The modules are connected as matrices in parallel or in series to increase the produced current, to increase the produced voltage or to increase the two simultaneously [1]. Figure 1.1 shows the PV matrix. The equivalent circuit for the PV cell is shown in Figure 1.2. The PV cell consists of a current source, a diode (D) and a resistor connected in parallel representing the leakage current [2].

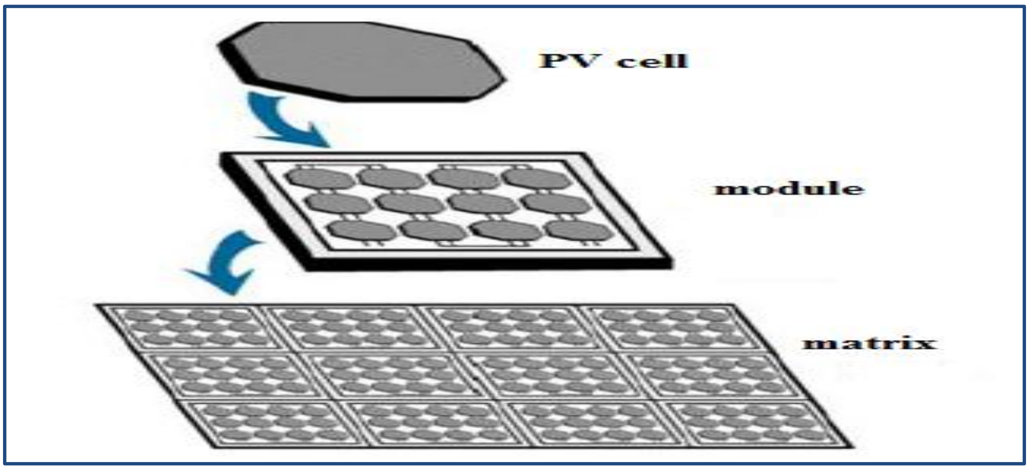

Figure1.1: PV cell module, and matrix.

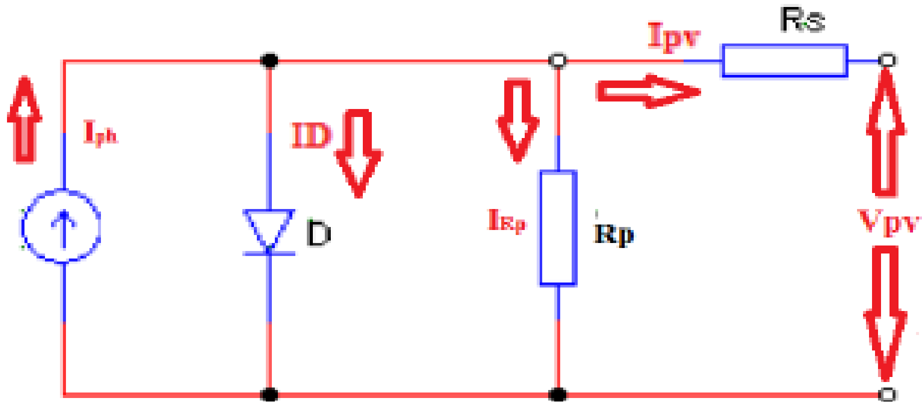

Figure 1.2: PV equivalent circuit.

The following equations are used to explain PV cell operation:

$$I_{PV} = I_{ph} - I_d - I_{Rp} \tag{1.1}$$

Where:

I_{PV} = PV cell current

I_{ph} = Photon current

I_d = diode current

I_{Rp} = leakage current

$$I_d = I_0 \left[\exp\left(\frac{V_d}{V_t}\right) - 1\right] \tag{1.2}$$

$$V_t = \frac{nKT}{q} \tag{1.3}$$

$$V_s = V_d = V_{pv} + I_{pv}R_s \tag{1.4}$$

so that PV cell current will be:

$$I_{pv} = I_{ph} - I_0 \left[\exp\left(\frac{V+IR_s}{\frac{nKT}{q}}\right) - 1\right] - \frac{V+IR_s}{R_s} \tag{1.5}$$

The module current can be calculated in Equation (1.6) [3].

$$I_{pv} = N_p I_{ph} - N_p I_0 (\exp\left[\frac{\left(\frac{V}{N_s}\right)}{\left(\frac{nKT}{q}\right)}\right]) \tag{1.6}$$

Np parallel connected cells

N_s series connected cells

1.2.2 Voltage Source Converters (VSC):

The main purpose of using a voltage source converter is to have the wanted AC waveforms from DC voltage sources. These generated waveforms are used in many applications, such as Adjustable Speed Drives (ASDs), Uninterruptable Power Supplies (UPSs), active filters, and Flexible AC Transmission Systems (FACTS). These voltage source converters have the ability to control voltage levels, frequencies and phase angles. Furthermore, the generated waveforms that are produced by these converters are not sinusoidal themselves but the fundamental components are sinusoidal. One of the important limitations to using these converters is Total Harmonic Distortion (THD) [4].

The voltage and current waveforms that are produced by those converters depend on switching method to produce the best waveforms and to achieve the optimum speed of operation and the best control method to make all that limitations match the switch ratings such as response time and switching losses so that many switching method proposed like Pulse Width Modulation (PWM).One of the most important advantages of this method is the reduced number of harmonics and the ability to eliminate harmonics selectively. The main drawback of this method is its high switching losses. Another method is Space Vector Modulation (SVM). In this method, the matter is not the same; here the switching losses are lower but but the response time is longer than in the pulse width modulation method [5].

1.3 Literature Review

In 2012, Rajiv K. Vorma studied the night-time use of the PV system as a STATCOM because the PV system produce real power during the day time only so that that system can be used to compensate for the converter capacity and the produced real power only of this type of system was implemented in the local distribution network in London hydro power stations. The system was simulated using the EMT/PSCAD program, with which he proposed the PV system reactive power for the load during the night to regulate the voltage level during that time, while in the day time, the PV system can be used as a STATCOM. However, it can compensate the reactive power with a limit such that the compensated reactive power, can be used in a flexible AC transmission flexible AC transmission system (FACTS)[6].

In 2013 V. Hima Leelaand S. Thai Subha studied the power quality improvement of a system by controlling the power converter in a grid connected PV system. They considered the PV as a distributed generator (DG). The study was conducted by means of two grids, one of which was 25 kV and the other 125 kV. They studied the system in a three considerations: firstly, they replaced the PV system with a DC voltage source and called it "DC fed to Grid." The DC voltage was 270 volts. This voltage was stepped up to 500 volts by using a boost converter and feeding it to a three-level converter which converts the DC voltage to the desired AC voltage. The second consideration was the "PV fed to 25 kV Grid." In this consideration, the DC voltage source was replaced by the PV system, the voltage of which was 270 volts and 100 kW of real power. The third consideration was called the "PV Fed to 125 kV Utility Grid." Here, the 25-kilovolt grid was replaced by a 125-kilovolt utility grid with two loads. In the three considerations, the reactive power was zero and compensation was performed as they mentioned [7].

In 2014 M. Sai Eswar and K. Obulreddy studied the utilization of a PV solar farm as a STATCOM during the night time hours in a distribution network. While the voltage source converter is the heart of a PV system, it is also the heart of the STATCOM. The researchers proposed a new control method to increase the utilization of the PV system. During the night, the system was used to control the reactive load power which was an induction machine, and to reduce the power losses, the proposed system was a three-phase system. The load was a linear induction load the compensation was carried out in the night hours only [8].

In same year, B. Mariappan et al. proposed a method to reduce the complexity and cost of the PV grid connected inverter. They suggested that if a single-stage power inverter was used to convert the DC power generated by the PV cells, even the DC voltage level would be lower than the RMS value of the grid voltage. They also proposed using a hybrid active filter system which consisted of a single-stage converter and a passive L-C filter which was tuned to a specific harmonic. The proposed system was simulated for a fixed nonlinear load which was a full-bridge uncontrolled rectifier and resistive load. The control system consisted of two control loops, one for the real power control which was based on the DQ method to inject the real power into the grid, and the other control loop was the harmonic control loop which was operated by the PID controller. The efficiency of the proposed PID controller. The efficiency of the proposed converter was about 94% [9].

In 2015 Prakash Vodapalli et al. proposed a new technique for using a unified power quality conditioner (UPQC). They proposed a reliable network model for the UPQC, which included the behavior of the system in four different intervals due to use or non-use of the UPQC and with real power generation during day time or without real power generation during the night. They studied how the UPQC can decide what type of current waveform to inject into the grid. The proposed system simulated using the Matlab/Simulink program [10].

In 2016 Arun Verma and Bhim Singh studied the harmonic and reactive detection in a grid connected with a PV system. The proposed system was based on a mathematical triangular function which can be used to estimate the power components. The given results were used to implement the desired functions, such as power quality improvement utilizing real power as high as possible and injecting it into the grid. In the simulation, they assumed the neutral current to be zero so as to make the solution easy. The proposed system was a three-phase, four-wire system. They also used a low-pass filter to eliminate high order harmonics and a PI controller to control the four-leg voltage source inverter [11].

1.4 The Main Aspects of the Work

The main purpose of this thesis is to propose a topology to utilize the smart PV system to overcome load demand and to inject real power into the AC source and control the power factor that can be achieved by controlling the voltage source converter. The proposed topology is to control the system in such manner that overcomes the load and real power variation simultaneously.

The study may be considered as follows:

1- Analyze the smart PV system mathematically and write all needed equations for power component calculations.
2- Design the proposed system and simulate it using the Matlab/Simulink program for all possible cases for load variations and PV cell behavior.

3- Study the simulation results and compare those results with the results of the mathematical calculations for all possible cases.

1.5. Thesis Contents

- This thesis consists of six chapters. The first chapter is an introduction of PV cells, PV systems, voltage source converters and a literature review of studies that deal with the same subject.
- The second chapter contains a brief study of power quality.
- The third chapter contains mathematical analyses and the important equation derivations that depend on power component calculations.
- The fourth chapter contains system simulations using the Matlab/ Simulink program.
- The fifth chapter contains the expected results for all possible cases for the PV (real power production or not) system, load nature (linear or nonlinear) and the produced real power relation with the load real power (less than, equal to and more than the load real power) and a discussion of the simulation results for all possible cases.
- The sixth chapter includes a conclusion and suggestions for future work.

CHAPTER TWO

POWER QUALITY

2.1 Overview

One of the important kinds of power limitations in the power system is the power quality. It refers to any change in both voltage and current waveforms or at last in one of them because the electric power is a quantity based on both voltage and current i.e. any problem in each waveform causes a power quality problem. The most important things in power quality consideration are the distortion in voltage and current waveforms, voltage sag, voltage swell and harmonics. Power quality problems always caused by the load.

2.2 Why is The Interest About Power Quality?

According to a Copper Development Association scanning, it is evaluation that power quality problems cost manufacture and business in the EU about €10 billion per year [12]. The cost goes to $ 50 billion per year in the USA because of power quality fall [13]. For example, a manufacturing company lost more than $ 3 million in one day in the summer of 1999 in Silicon Valley when the “lights switch off” [14]. Another example, a paper factory can rubbish a whole day of production of about $ 250,000 loss because of voltage sag [15]. Also power quality problems are the major causes of a half of all computer problems and one-third of all data loss [16]. In addition customer confidence increases with power quality increasing.

2.3 Power Quality Problems Types

Power quality problems can be classified according to the affected quantity into four types:

1. Power quality problems due to voltage waveform distortion,
2. power quality problems due to current distortion,
3. power quality problems due to power factor distortion
4. Power quality problems due to frequency distortion.

2.4 Power Quality Problems Discussion

2.4.1 Power Quality Due to Voltage Waveform Distortion

1) Voltage sag : which means a reduction in rms value of the AC voltage that can be continue from half cycle to few seconds it cause malfunction in many equipments like adjustable speed drives ADS, induction machines and control systems operation. This type of distortion can be solved or mitigated by using of D-STATCOM. Figure 2.1show voltage waveform in case of voltage sag.

2) Voltage swell: this type of disturbance with duration as above but here the voltage magnitude is more than the normal voltage for the three phase voltage. Figure 2.2 show voltage waveform in case of swell [17].

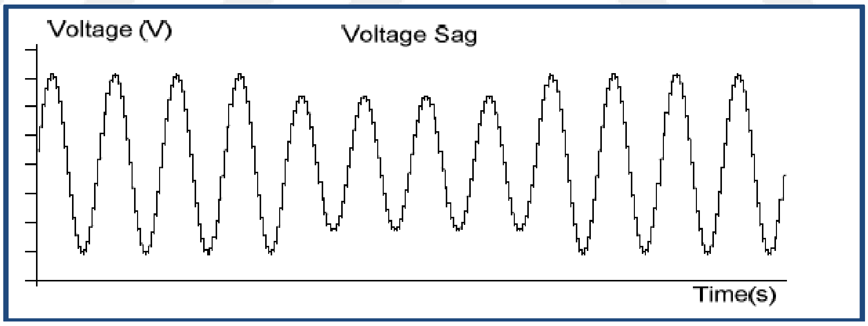

Figure 2.1: Voltage sag.

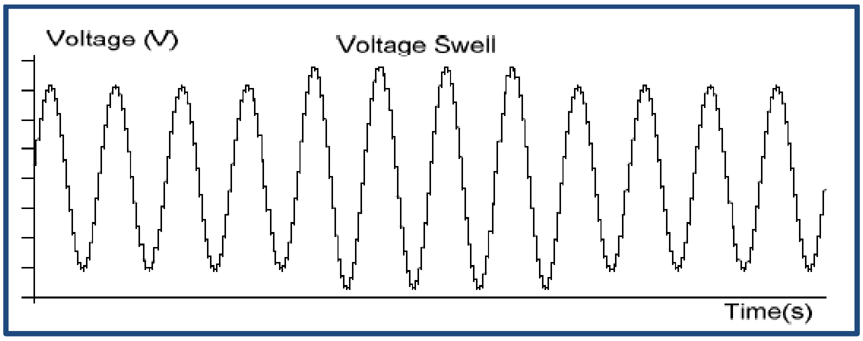

Figure 2.2: Voltage swell.

2.4.2 Power Quality Due To Current Waveforms Distortion

The electric power generator can control only voltage and frequency but the current depends on the connected loads, and nowadays there is a wide range in variety in load types like linear and nonlinear loads. The nonlinear loads are the main cause of current distortion because these loads drawn non sinusoidal currents from the power grid and those currents contain a lot of harmonics in wide range of frequencies in the range less than the fundamental frequency to some thousands of fundamental frequency, the worst case is that the frequencies near fundamental frequency due to the filtering difficulty in design. The main cause of this distortion type are switch mode power supplies, adjustable speed drives, ups, electric power modifiers, renewable power systems. The optimum solution for this type of distortion are the smart filters (the Smart PV System introduced in this thesis) because these systems can produce the harmonics needed by the nonlinear loads so that these systems have two advantages one is that the load will draw the wanted current with all needed harmonics and the other is that the electric power source will produce only sinusoidal waveforms currents, Figure 3.1 show distorted current waveform [18].

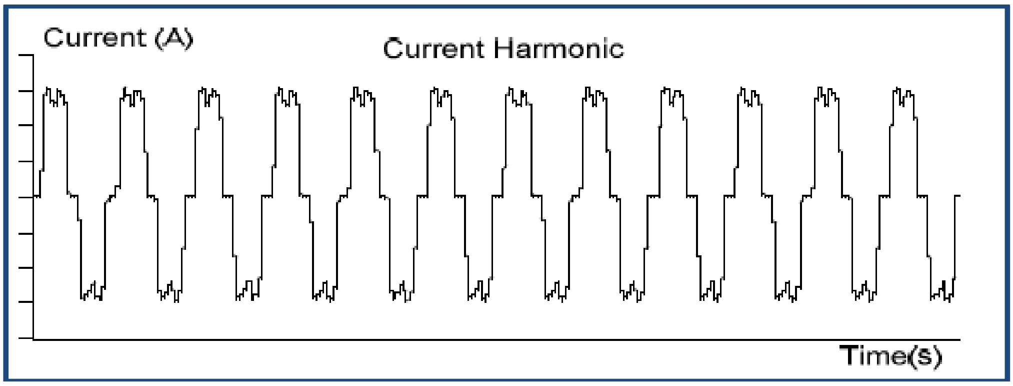

Figure 2.3: Distorted current waveform.

2.4.3 Power Quality Problems Due Non Unity Power Factor

This type of problems occur when the power factor is not unity, the total power factor is the result of production of displacement power factor and distortion power factor, where the first term caused by non-resistive loads (inductive or capacitive) while the other part caused by nonlinear loads. Figure 4.1 shows the non-unity power factor current waveform. This type of power quality problem caused by non-resistive linear loads. While the second term of power factor caused by nonlinear loads which discussed in the previous paragraph.

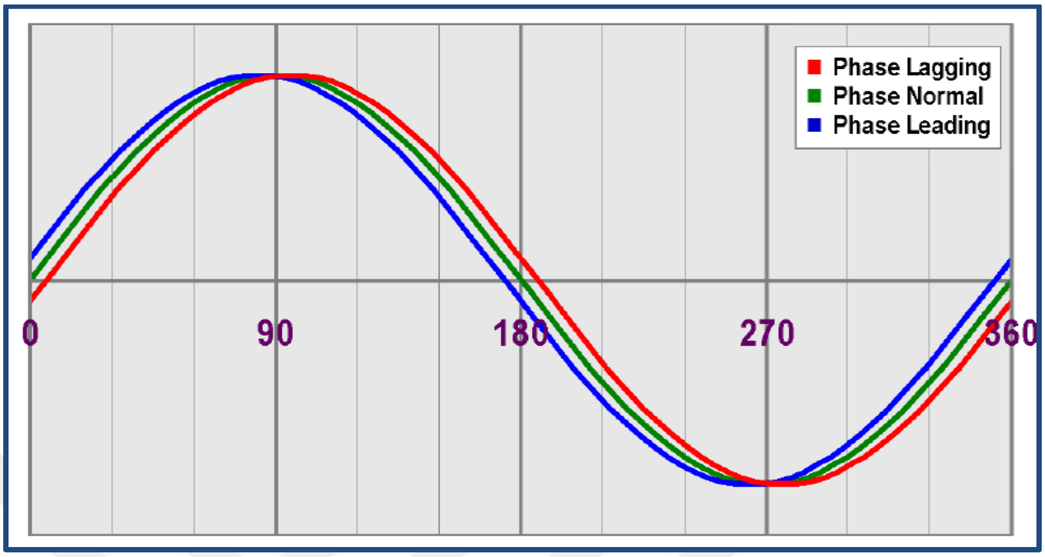

Figure 2.4: Non-unity power factor.

2.5 Impact of Harmonics in Recent Buildings

Almost all new buildings have non – linear loads which are of the following types:

a) Fluorescent lights.

b) Switched Mode Power Supplies (SMPS) for Computer, refrigerators, air conditioning units, etc.

c) Variable speed drives.

d) Uninterrupted power systems (UPS).

One of the major power quality problems in new buildings is the harmonics which could take the form of current and/or voltage harmonics. Usually harmonic currents are drowning by the nonlinear loads connected to the system which invariably lead to voltage harmonics in the system. Majority of harmonic problems affecting a building are generated within the building. But next door buildings with main harmonic generation can affect the harmonics of the building under consideration, hence the shape of power quality standards evolved.

2.6 Offer of Harmonic Voltage Distortions in New Buildings Include

1) Transformers may overheat without necessarily being overloaded.
2) Insulation in cable may be breakdown because of high temperature.
3) Occurrence of noise in the induction motors due to heat.
4) Capacitors can overheat.
5) Circuit breakers can trip.
6) Computers fail.
7) Metering devices may give false readings.
8) Electronic displays and lighting may flicker.

All these voltage distortions cause accelerated equipment ageing and metering error over a long period of high accumulated harmonic levels. Other forms of malfunctioning of sensitive electronics equipments could be caused by short bursts voltage waveforms. As mentioned earlier, power quality problems caused by an end user can adversely affect other end users. In order to prevent this and to set standards for sensitive electronic equipments, International Standards were set up to which power suppliers, end-users and manufacturers have to comply

2.7 Power Quality Measurement

There are many indicators which can be used to measure the electric power quality, because of load variety and electric power modifiers and also because of renewable energy systems, the power quality became more important than any time ago. The following parameters used to measure the power quality.

a) Crest Factor CF which defined as the ratio between the peak values of a waveform to the RMS of the same waveform.

$$CF = \frac{I_{peak}}{I_{rms}} \tag{2.1}$$

b) Power factor: power factor is the ratio of real power to apparent power or the product of distortion power factor and the displacement power factor, the first term related to nonlinear loads and the second term related to linear loads .optimum power factor equal to unity.

c) Total harmonic distortion (THD): this parameter describe the ratio of all harmonics without the fundamental harmonic to the fundamental harmonic

$$THD\% = \frac{\sqrt{\sum I_n^2 - I1^2}}{I1} \times 100 \qquad (2.2)$$

The minimum total harmonic distortion THD the highest power quality.

2.8 Power Quality Standards

IEC and IEEE and other institutes took the power quality in their consideration and write standard limitation tables for the power quality, table 2.1 presents some standards of power quality [19].

Table 2.1: IEEE stander 519-1992.

Maximum harmonic current distortion (in percent of I_L)						
Individual harmonic order (odd harmonics)						
I_{SC}/I_L	$h < 11$	$11 \le h < 17$	$17 \le h < 23$	$23 \le h < 35$	$35 \le h$	TDD (%)
<20*	4.0	2.0	1.5	0.6	0.3	5.0
20 to <50	7.0	3.5	2.5	1.0	0.5	8.0
50 to <100	10.0	4.5	4.0	1.5	0.7	12.0
100 to <1000	12.0	5.5	5.0	2.0	1.0	15.0
>1000	15.0	7.0	6.0	2.5	1.4	20.0

CHAPTER THREE

MATHEMATICAL ANALYSIS OF SMART PV SYSTEM

So as to know how the smart PV system working and which component it can be compensate the system must be analyzed:

3.1 System Analysis

From apparent power equation:

$$S^2 = V^2 I^2 \tag{3.1}$$

$$S^2 = \sum V_k^2 \sum I_n^2 \tag{3.2}$$

$$S^2 = P^2 + Q^2 + D^2 \tag{3.3}$$

Power components can be calculated by using Fourier transform:

Fundamental harmonic real power:

$$P_1 = V_1 I_1 \cos\theta_1 \tag{3.4}$$

Real power for the other harmonic

$$P_N = \sum_n V_n I_n \cos\theta_n \quad (n = 2,3,4,5,--) \tag{3.5}$$

Reactive power for all harmonics:

$$Q = \sum_n V_n I_n \sin\theta_n \quad \text{(n=1,2,3,- - - -)} \tag{3.6}$$

Distortion power:

$$D = \sum_{kn} V_k I_n \quad (k \neq n = 1, 2, 3,---) \qquad 3.7)$$

Equation 2.3 will be :

$$S^2 = \sum_n V_n^2 I_n^2 \cos^2(\theta_n) + \sum_n V_n^2 I_n^2 \sin^2(\theta_n) + \sum_{n,k,n\neq k} V_n^2 I_k^2 \tag{3.8}$$

Where:

S: apparent power.

P: real power.

Q: reactive power.

D: distortion power.

V_n: effective value of voltage.

I_n: effective value for current.

Power factor can be calculated from equation (2.9)

$$PF = \frac{P}{S} \tag{3.9}$$

The total harmonic distortion for both voltage and current can be calculated from equations (2.10) and (2.11) respectively:

$$THD_V = \frac{\sqrt{V_T^2 - V_1^2}}{V_1} \tag{3.10}$$

Where:

$$V_T^2 = \sum_{n=1}^{\infty} V_n^2$$

$$THD_I = \frac{\sqrt{I_T^2 - I_1^2}}{I_1} \tag{3.11}$$

Where:

$$I_T^2 = \sum_{n=1}^{\infty} I_n^2$$

3.2 Smart PV System Analysis

The smart PV system can do three tasks in same time which are:

Distortion reduction in source current, load reactive compensation and real power injection in to the power grid for any types of loads as shown in Figure 3.1.

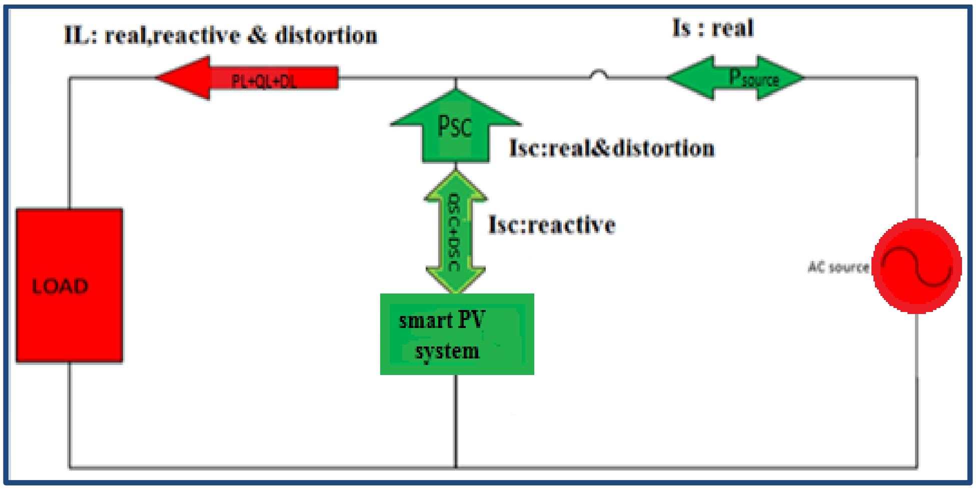

Figure 3.1: Smart PV system.

To analyze the smart PV system the voltage applied on load terminal and smart PV system is the source voltage itself.

$$i_s = \pm \hat{I}_s \sin(wt) \quad (3.12)$$

Or

$$i_s = \pm(\hat{I}_{L1} \cos(\theta_{L1}) - \hat{I}_{PV}) \sin(wt) \quad (3.13)$$

$$i_L = \sum_n [\hat{I}_L \cos(nwt) + \hat{I}_L \sin(nwt)] \quad (3.14)$$

Smart PV wanted current can be calculated from equation (2.15)

$$i_{spv} = i_L - i_s \quad (3.15)$$

Or

$$i_{spv} = (\hat{I}_{L1} \sin(\theta_{L1}) + \hat{I}_{PV}) \sin(wt) + \sum_{n=2} \hat{I}_{Ln} \sin(nwt \pm \theta_{Ln}) \quad (3.16)$$

Where:

i_{spv} : Smart PV system current.

: Load current.

: Source current.

: Effective value of PV cell which converted to AC current.

As in figure (2-1) the smart PV system was designed to work as foll owing:

In case that the PV system produce real power the real power which can be supplied by or injected to the source is the difference between the real power of the load and the real power produced by the PV system.

$$P_{source} = P_{Load} - P_{spv} \quad (3.17)$$

The real power delivered by the source or the real power injected to it depends on the real power produced by the PV system which converted to AC power in same frequency, while if the PV system is idle the source will deliver only the real power of the load in this case equation (3.17) can be write as :

$$P_{source=}P_{Load} \quad (3.18)$$

$$Q_{source} = Q_{spv} - Q_{Load} \quad (319)$$

$$D_{source} = D_{spv} - D_{Load} \quad (3.20)$$

Equations (3.19 &3.20) show the relation between the other power components of both smart PV system source and load. But the smart PV system designed to compensate the reactive and distortion power components of the load, so that the mentioned equations will be re-write as follow:

$$Q_{source} \cong 0$$

$$D_{source} \cong 0$$

$$Q_{sco} = Q_{Load} \tag{3.21}$$

$$D_{sco} = D_{Load} \tag{3.22}$$

3.3 System Analysis in Case of Linear Inductive Load and Idle PV system (In Night)

Figure 3.2 shows the waveforms of source voltage and load current which is a sinusoidal with lag power factor, while figure3.3 shows the waveforms of source voltage and smart PV system. Figure 2.4 shows the waveforms of source voltage and current respectively.

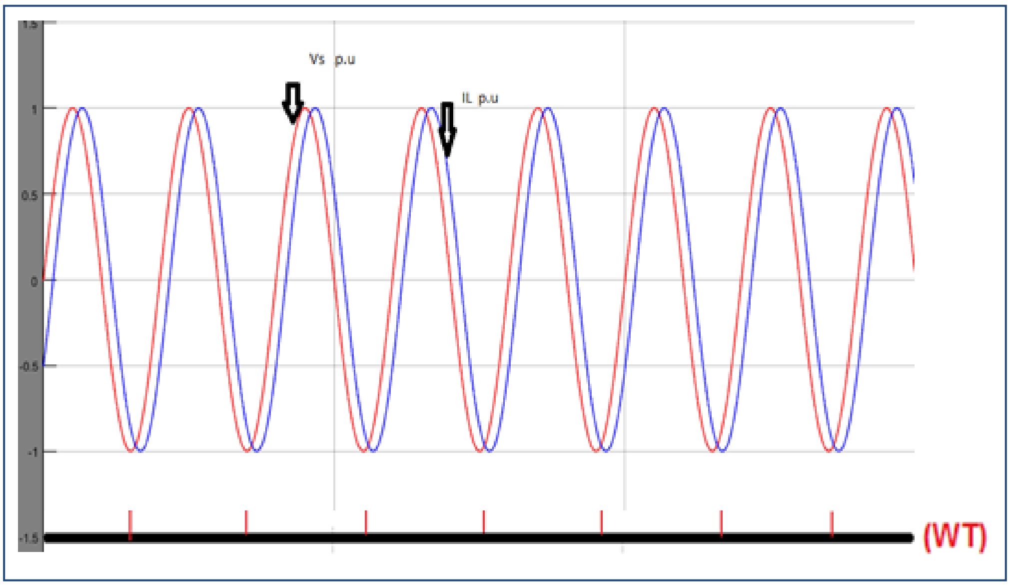

Figure 3.2: Waveforms of source voltage and load current.

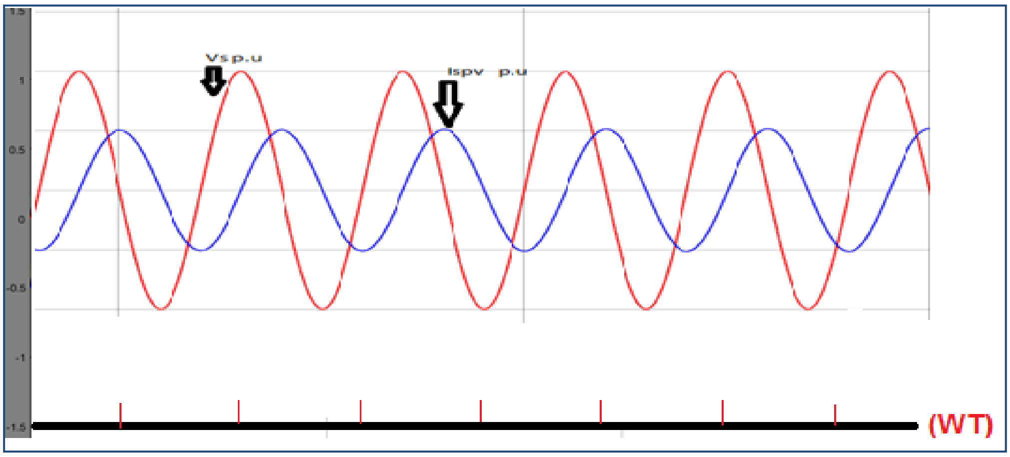

Figure 3.3: Waveforms of source voltage and smart PV current.

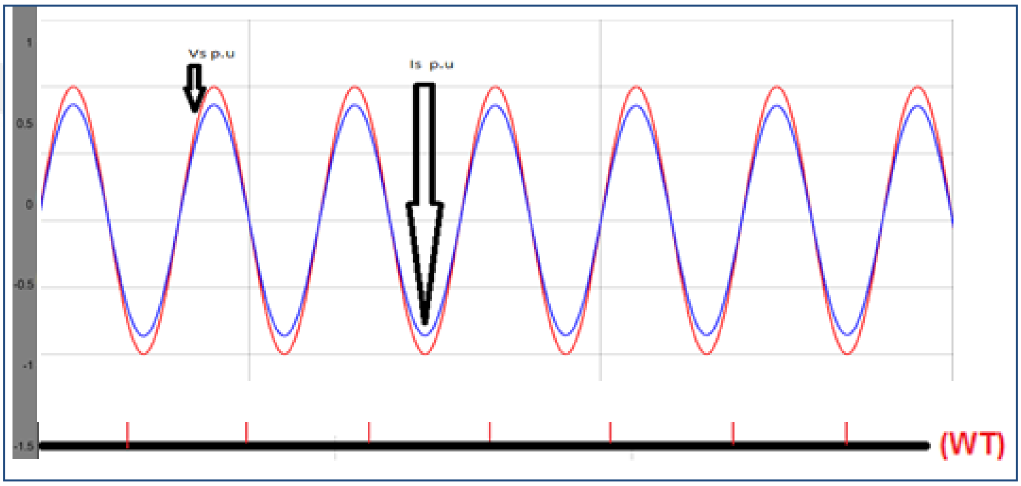

Figure 3.4: Waveforms of source voltage and current.

When equation 3.13 is applied on the system, the results show that the source current is a sinusoidal in a unity power factor and effective value is 0.866p.u while the load current is 1 p.u

$i_s = (8\cos(30) - 0)\sin(wt))$

$i_s = 6.928\sin(wt)$

$S_{source} = V_S(rms) * I_{source}(rms)$

$= \frac{220}{\sqrt{2}} \times \frac{6.928}{\sqrt{2}}$ =762.08 VA

$S_{source} = 0.866$ p.u

$P_{source} = V_S(rms) * I_{1source}(rms)\cos\theta_{1source}$, $\theta_{1source} = 0$

$P_{source} = 0.866$ p.u

$Q_{source} = D_{source} = 0$

But the load is linear load and its current is sinusoidal waveform, so that equation can be re-write as below (for this case only):

$S_{Load} = V_S(rms) * I_{Load}(rms)$

$S_L = \frac{220}{\sqrt{2}} \times \frac{8}{\sqrt{2}}$ = 880 VA

S_L = 1 p.u

$P_{Load} = V_{source} I_{Load} \cos\theta_{1Load}$

$P_{Load} = 762.08$Watt

P_{Load} = 0.866 p.u

$Q_{Load} = \sqrt{S_{Load}^2 - P_{Load}^2 - D_{Load}^2}$

Distortion power neglected due to the load was linear load.

$Q_{Load} = \sqrt{(880)^2 - (762.08)^2 - 0}$

$Q_{Load} = 440\ VAr$

$Q_{Load} = 0.5\ \ p.u$

From equation 2.17 smart PV system power components can be calculated.

$P_{SPV} = P_L - P_S$

$P_{SPV} = 0$ p.u

And the PV system does not produce real power

$Q_{SPV} = Q_L - Q_S$

Where $Q_{SPV=0}$

$Q_{SPV} = 0.5 - 0$

$Q_{SPV} = 0.5\ \ p.u$

$$S_{SPV} = \sqrt{{P_{SPV}}^2 + {Q_{SPV}}^2}$$

= 0.5 p.u

3.4 System Analyses in Case of Nonlinear Load and PV System Idle (in Night)

Figures 3.5, 3.6, and 3.7 shows the waveform of source voltage, load current, smart PV current and source current respectively [19].

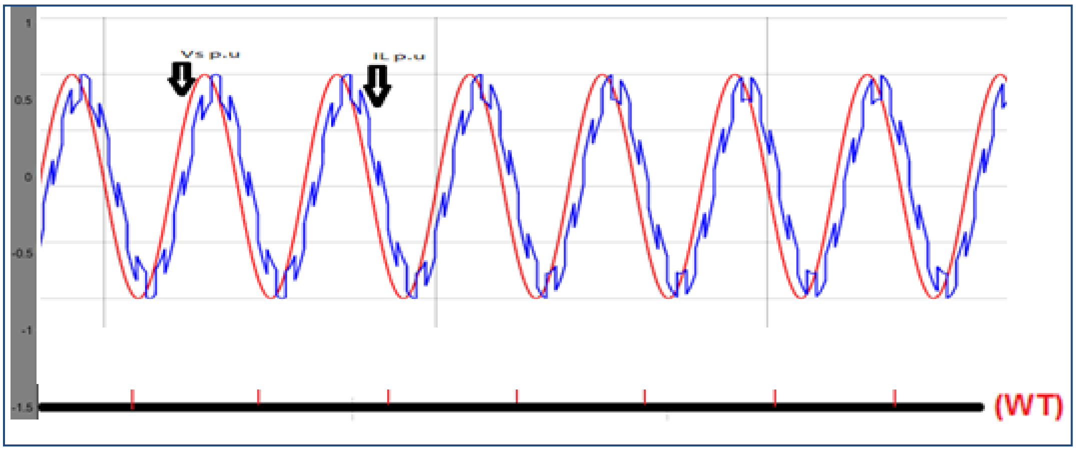

Figure 3.5: Waveforms of source voltage and load current.

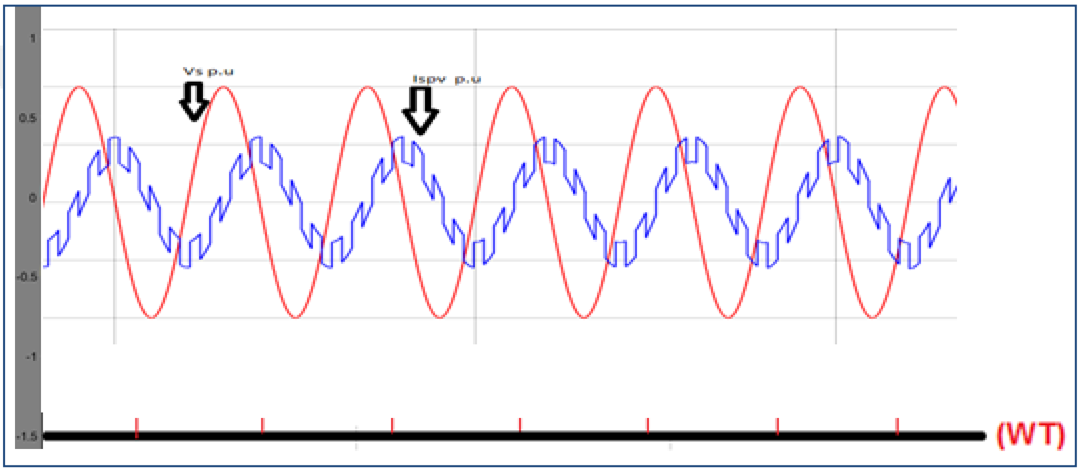

Figure 3.6: Waveforms of source voltage and smart PV system current.

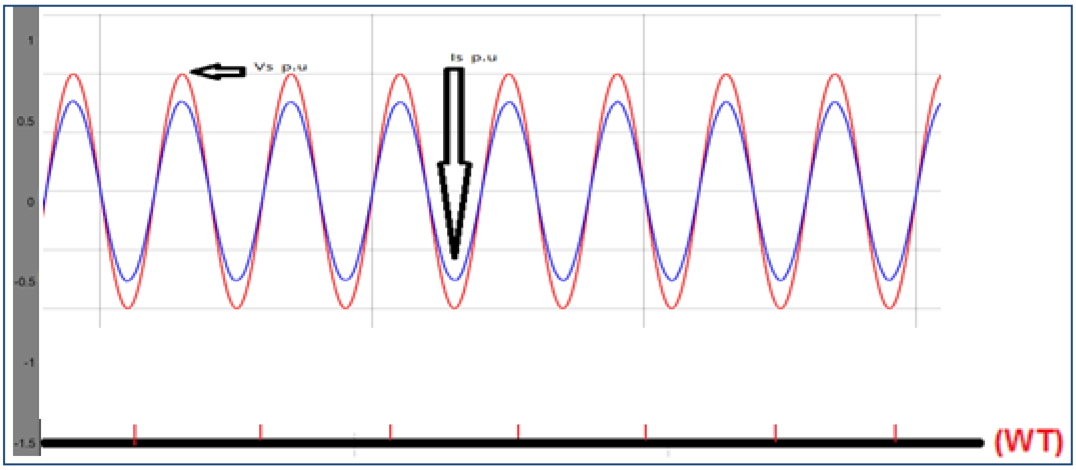

Figure 3.7: Waveforms of source voltage and current.

By applying equations 3.18, 3.22 the power components for load, smart PV system and source can be calculated, the results shown in table 3.1.

Table 3.1: System power components for nonlinear load.

Calculated value	Load	Smart PV system	source
Apparent power p.u	1	0.5773	0.8165
Real power p.u	0.8165	0	0.8165
Reactive power p.u	0.4714	0.4714	0
Distortion power p.u	0.3333	0.3333	0
Power factor	0.8303	0	1

3.5 Power Components Calculation in Case of Linear Load and Real Power Production By the Pv System For Three Cases (Real Produced Power Less Than, Equal, Or More Than The Load Real Power

Power components shown in each of tables 3.2 which contain load power components, table 3.3 contains power components for the source for three cases due to real power production while table 3.4 contains smart PV system power components for the same three cases.

Table 3.2: Load power components.

S_{Load}(pu)	**1**
P_{Load}(pu)	0.866
Q_{Load} (pu)	0.5
D_{Load} (pu)	0
PF_{Load}	0.866

From equation 3.13 the source current and the power components in the three cases of real power production can be calculated as follow:

$$i_s = \pm(\hat{I}_{L1}\cos(\theta_{L1}) - \hat{I}_{PV})\sin(wt)$$

3.5.1 In Case That The Real Power Produced Less Than The Load Demand

$\hat{I}pv$ = 4 A, $\hat{I}L$ = 8 A, $\theta 1_L$= 30 degree lag

Power components for the load:

$S_L = \frac{220 \times 8}{2}$ = 880 VA = 1 p.u

$P_L = 762.1\ Watt$ = 0.866 p.u,

$Q_L = 440\ VAr$ = 0.5 p.u

D_S = 0 due to linear load

Power components for the source:

$i_s = (8\cos(30) - 4)\sin(wt) = 2.928\sin(wt)$

S_S= $\frac{220 \times 2.928}{2}$ = 322.1 VA

S_S= $\frac{322.1}{880}$ = 0.366 p.u

$P_S = S_S \cos\theta_S$

= 322.1 Watt = 0.366 p.u

$Q_S = S_S \sin\theta_S$, but θ_S = 0

Q_S = 0

D_S = 0

Power components for the smart PV system:

P_{Spv}= $P_L - P_S$

= 762.1 -322.1

= 440 watt = 0.5 p.u

Q_{Spv}= $Q_L - Q_S$

= 440–0 = 440 VAr = 0.5 p.u

$S_{SPV} = \sqrt{(440)^2 + (440)^2}$

= 622.2 VA = 0.707 p.u

3.5.2 In Case The Produced Real Power Equal to The Load Demand

$i_s = (\hat{I}_{L1}\cos(\theta_{L1}) - \hat{I}_{PV})\sin(wt)$=0

$\hat{I}_{L1}\cos(\theta_{L1}) = \hat{I}_{PV}$ this the condition for this case, in this case the all source power components are equal to zero.

Power components for the smart PV system:

P_{Spv}= $P_L - P_S$

= 762.1 -0

= 762.1 watt = 0.866p.u

Q_{Spv}= $Q_L - Q_S$

= 440 – 0 = 440 VAr = 0.5 p.u

$S_{SPV} = \sqrt{(762.1)^2 + (440)^2}$

= 880 VA = 1p.u

1- The produced real power is more than the load demand :

In this case

$\hat{I}pv$ = 10 A, $\hat{I}L$ = 8 A, $\theta 1_L$= 30 degree lag

Power components for the source:

$$i_s = (\hat{I}_{L1} \cos(\theta_{L1}) - \hat{I}_{PV}) \sin(wt)$$

= (8*0.866- 6)sin(wt)

= - 3.072 sin(wt)

$S_S = \frac{220 \times 3.072}{2}$ =-337.92 VA

$P_S = S_S \cos\theta_S$

= -337.92Watt = -0.384p.u

$Q_S = S_S \sin\theta_S$, but θ_S = 0

Q_S = 0

D_S = 0

Power components for the smart PV system:

$P_{Spv} = P_L - P_S$

= 762.1 – (-337.92)

= 1100.02 watt = 1.25 p.u

$Q_{Spv} = Q_L - Q_S$

= 440 – 0 = 440 VAr = 0.5 p.u

$S_{SPV} = \sqrt{(1100.02)^2 + (440)^2}$ = 1184.75VA = 1.346p.u

Table 3.3: Source power components.

Calculated component	$P_{PV} < P_{Load}$	$P_{PV} = p_{Load}$	$P_{PV} > P_{Load}$
S_{source} (pu)	0.366	0	0.384
P_{source} (pu)	0.366	0	-0.384
Q_{source} (pu)	0	0	0
D_{source} (pu)	0	0	0
PF_{source}	1	-------	-1

Table 3.4: Smart PV system power components.

Calculated component	$P_{PV} < P_{lead}$	$p_{PV} = p_{lead}$	$P_{PV} > P_{lead}$
S_{PV}(pu)	0.707	1	1.346
P_{sPV} (pu)	0.5	0.866	1.25
Q_{sPV}(pu)	0.5	0.5	0.5
D_{sPV} (pu)	0	0	0
PF_{sPV}	0.707	0.866	0.928

Figure 3.8 shows the waveforms of source voltage and load current, in Figure3.9 shows waveforms of source voltage, smart PV system current and Figure 2.10 shows waveforms of source voltage and current in case that the real power produced by the PV system less than the load real power.

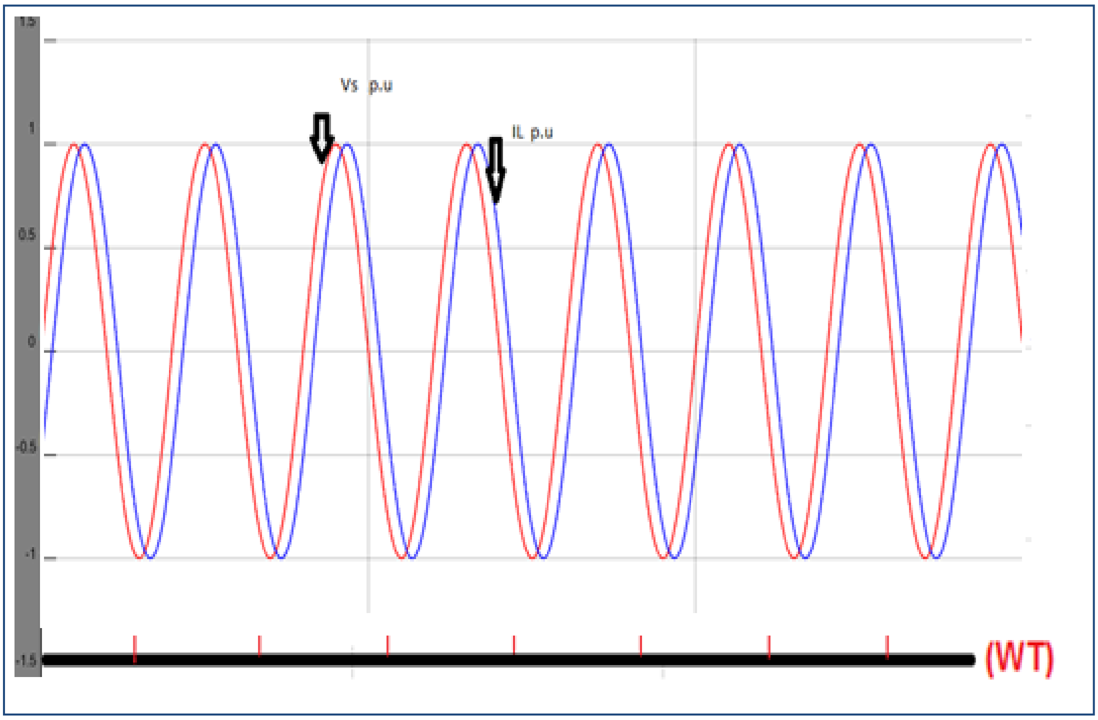

Figure 3.8: Waveforms of source voltage and load current.

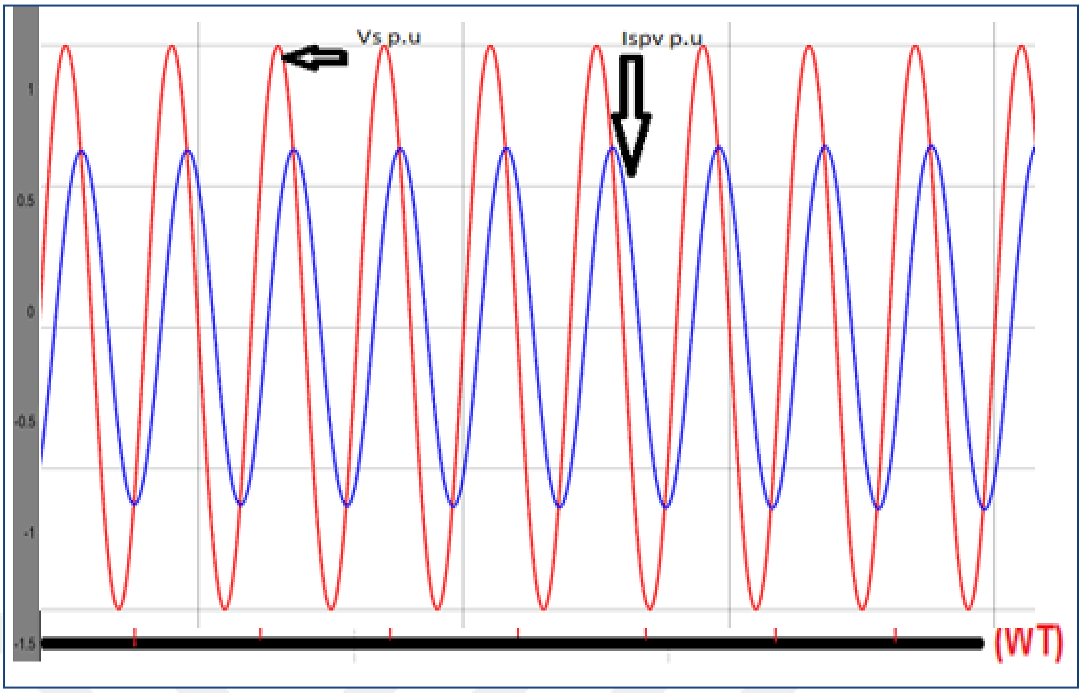

Figure 3.9: Waveforms of source voltage and smart PV system current.

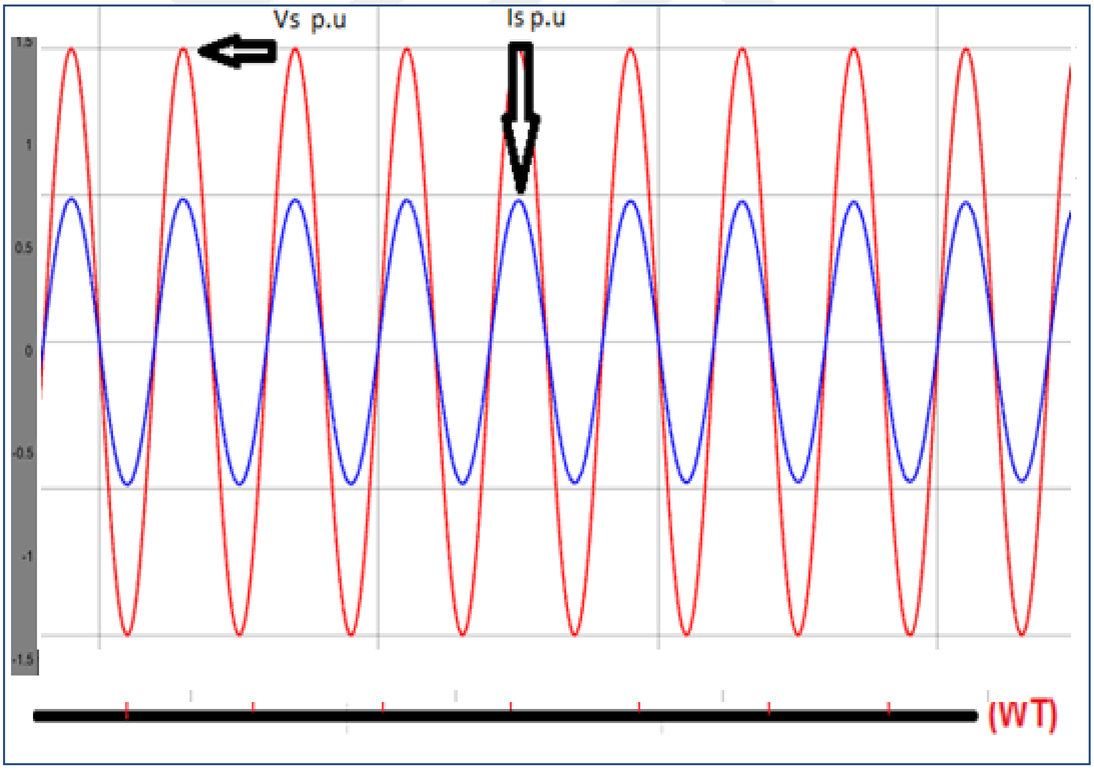

Figure 3.10: Waveforms of source voltage and current.

Figure 3.11 shows waveforms of source voltage and smart PV system current, and Figure 2.12 shows waveforms of source voltage and current in case that the real power produced by the PV system equal the load real power.

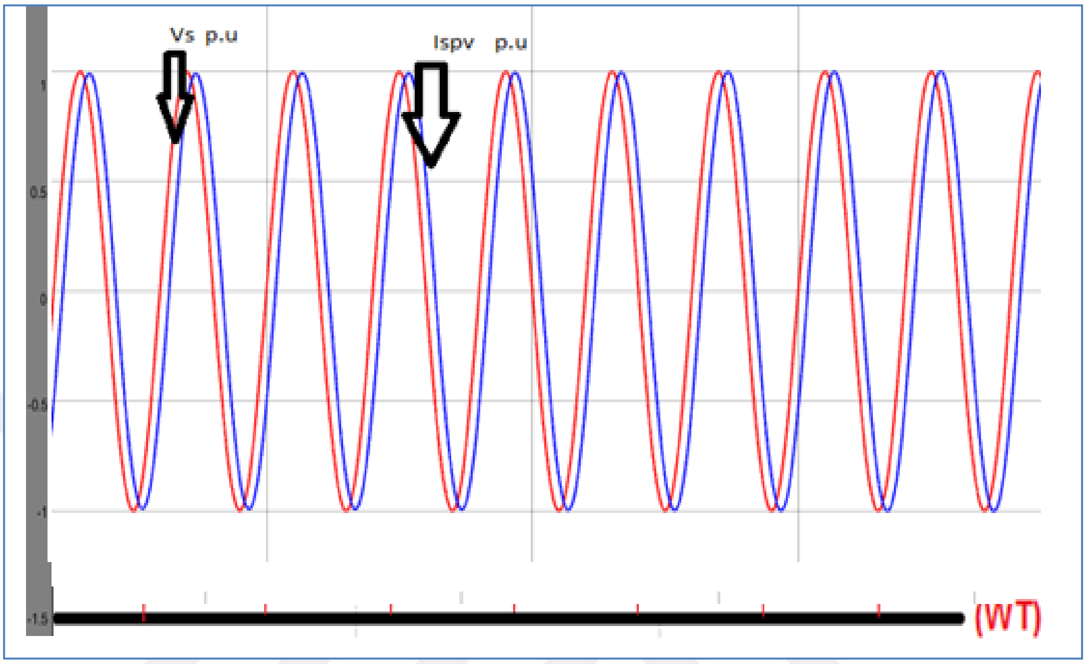

Figure 3.11: Waveforms of source voltage and smart PV system current.

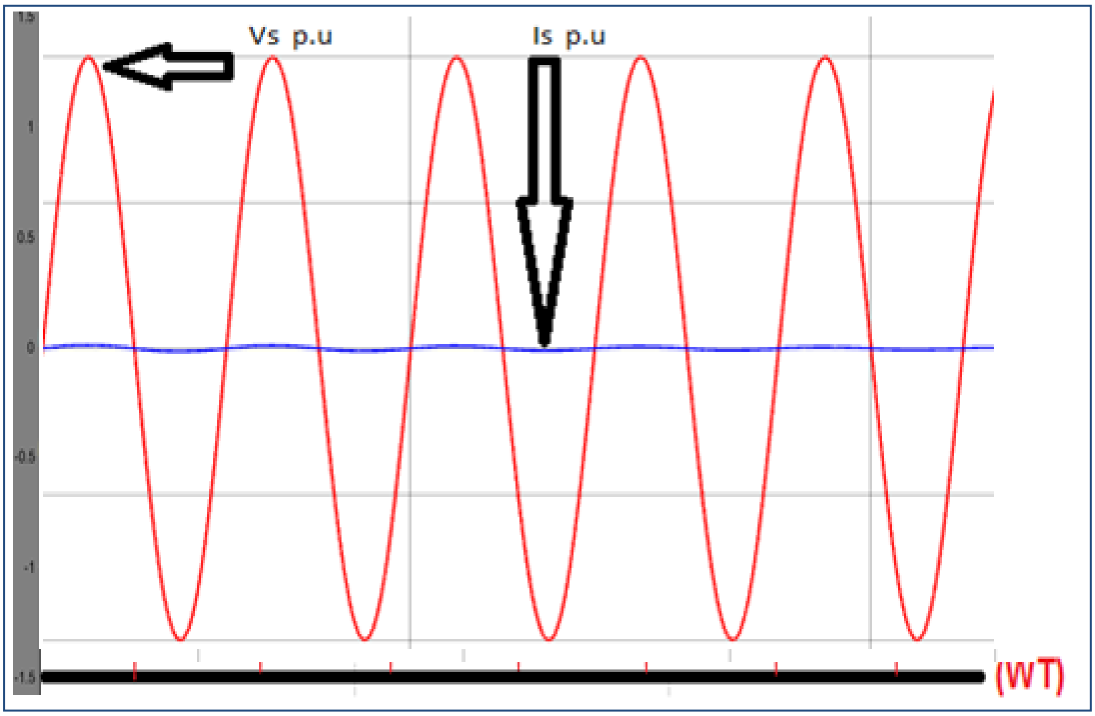

Figure 3.12: Waveforms of source voltage and current.

Figure 3.13 shows waveforms of source voltage and smart PV system current, and Figure3.14 show waveforms of source voltage and current in case that the real power produced by the PV system more than real power.

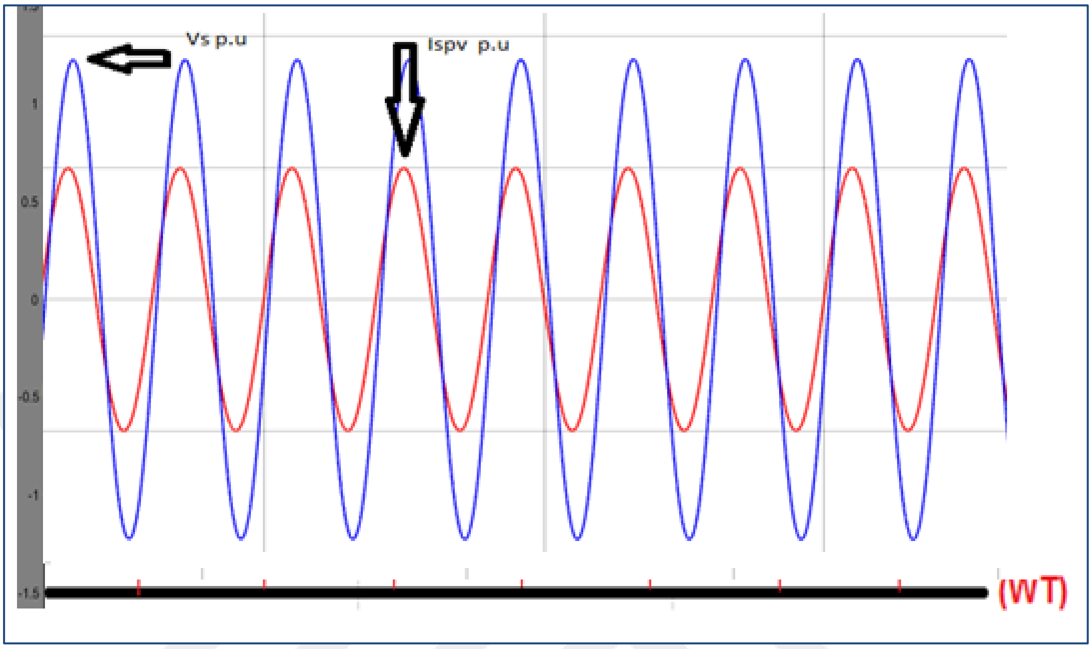

Figure 3.13: Waveforms of source voltage and smart PV system current.

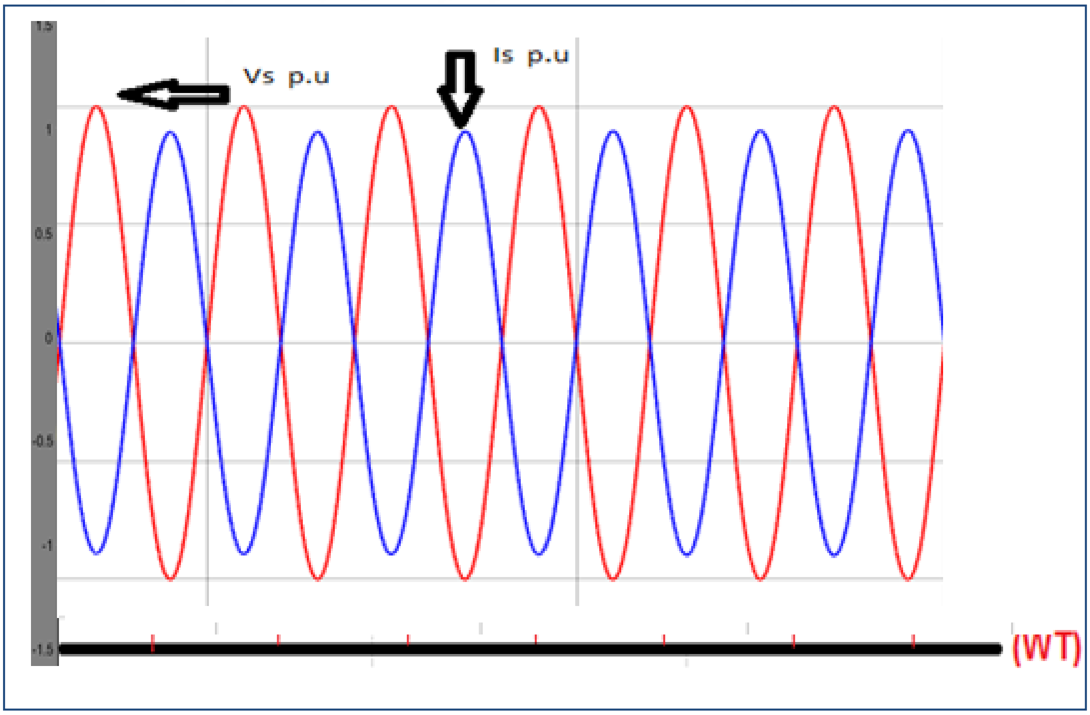

Figure 3.14: Waveforms of source voltage and current.

3.6 Power Components Calculation in Case of Nonlinear Load and Real Power Production By The Pv System For Three Cases (Real Produced Power Less Than, Equal, Or More Than The Load Real Power

Power components shown in each of tables 3.5 which contain load power components, table 3.6 contain power components for the source for three cases due to real power production while table 3.7 contain smart PV system power components.

Table 3.5: Load power components.

S_{Load}(pu)	1
P_{Load}(pu)	0.8165
Q_{Load} (pu)	0.4714
D_{Load} (pu)	0.3333
PF_{Load}	0.8165

Table 3.6 Source power components.

Calculated component	$P_{PV} < P_{Load}$	$P_{PV} = p_{Load}$	$P_{PV} > P_{Load}$
S_{source} (pu)	0.3451	0	0.362
P_{source} (pu)	0.3451	0	-0.362
Q_{source} (pu)	0	0	0
D_{source} (pu)	0	0	0
PF_{source}	1	-------	-1

Table 3.7: Smart PV system power components.

Calculated component	$P_{PV} < P_{Load}$	$P_{PV} = p_{Load}$	$P_{PV} > P_{Load}$
S_{sPV}(pu)	0.7454	1	1.312
P_{sPV} (pu)	0.4714	0.8165	1.179
Q_{sPV}(pu)	0.4713	0.4714	0.4714
D_{sPV} (pu)	0.3333	0.3333	0.3333
PF_{sPV}	0.6324	0.8165	0.898

Figure 3.15 shows waveforms of source voltage and load current, Figure 3.16 shows waveforms of source voltage and smart PV system current and Figure 3.17 show waveforms of source voltage and current in case that the real power produced by the PV system less than the load real power.

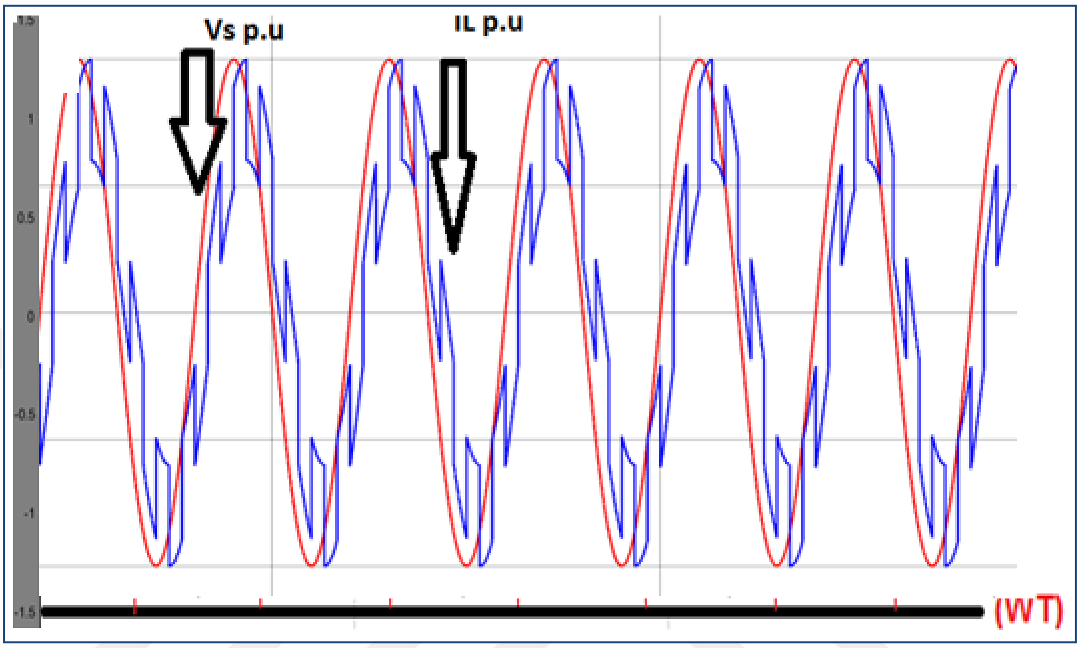

Figure3.15: Waveforms of source voltage and load current.

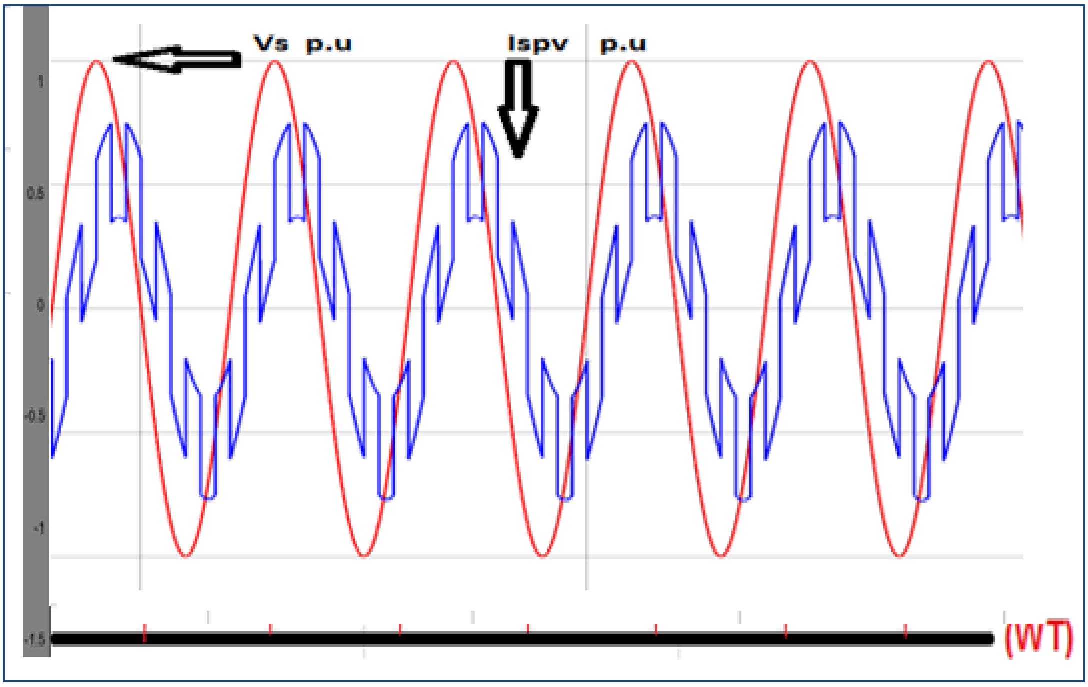

Figure 3.16: Waveforms of source voltage and smart PV system current.

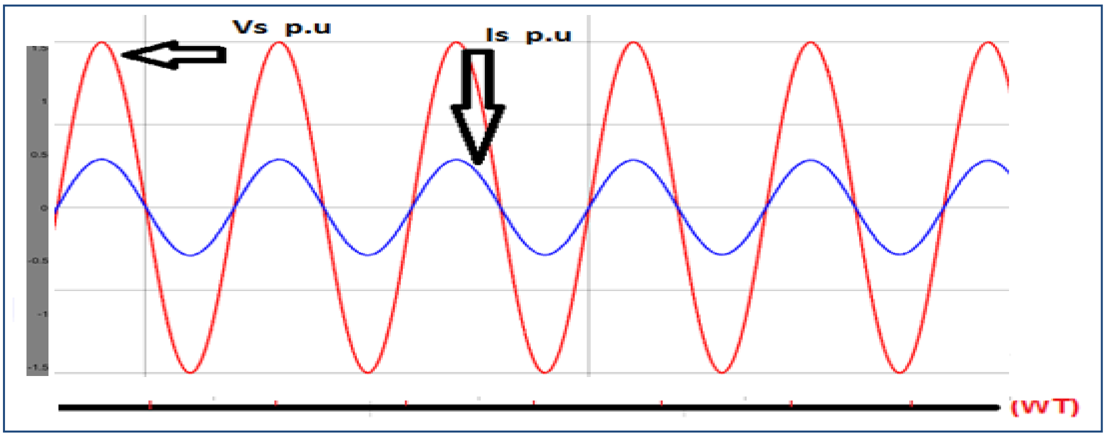

Figure 3.17: Waveforms of source voltage and current.

Figure 3.18 shows waveforms of source voltage and smart PV system current, Figure and Figure 3.19 shows waveforms of source voltage and current.

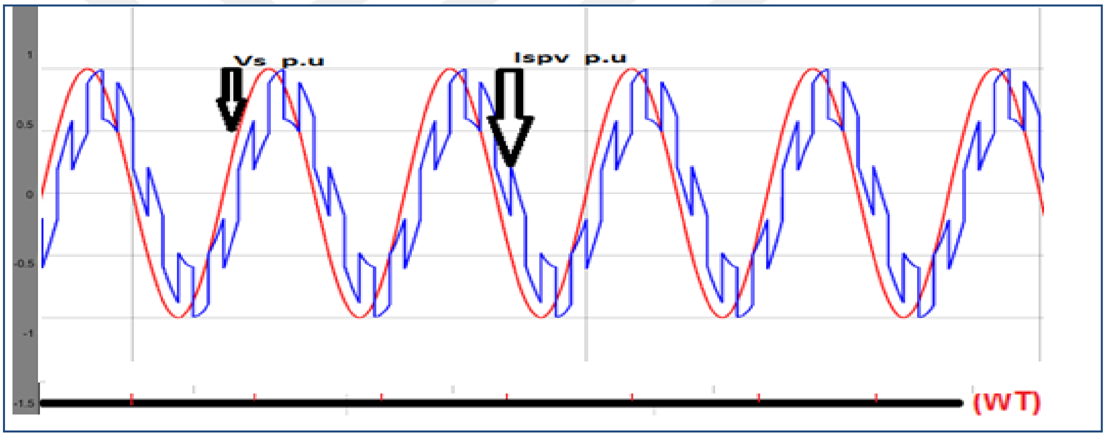

Figure 3.18: Waveforms of source voltage and smart PV system current.

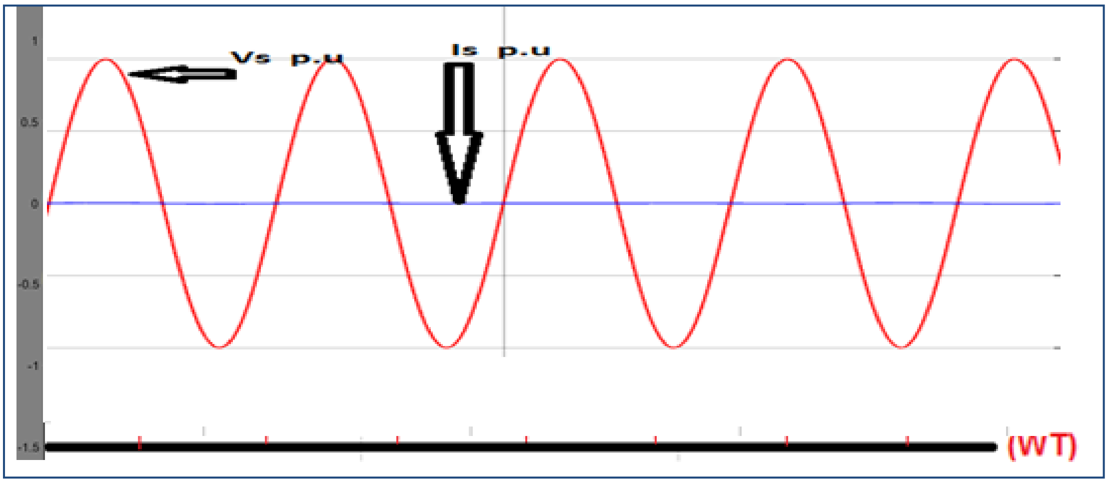

Figure 3.19: Waveforms of source voltage and current.

Figure 3.20 shows waveforms of source voltage and smart PV system current, Figure and Figure 3.21 shows waveforms of source voltage and current in case that the real power produced by the PV system more than load real power.

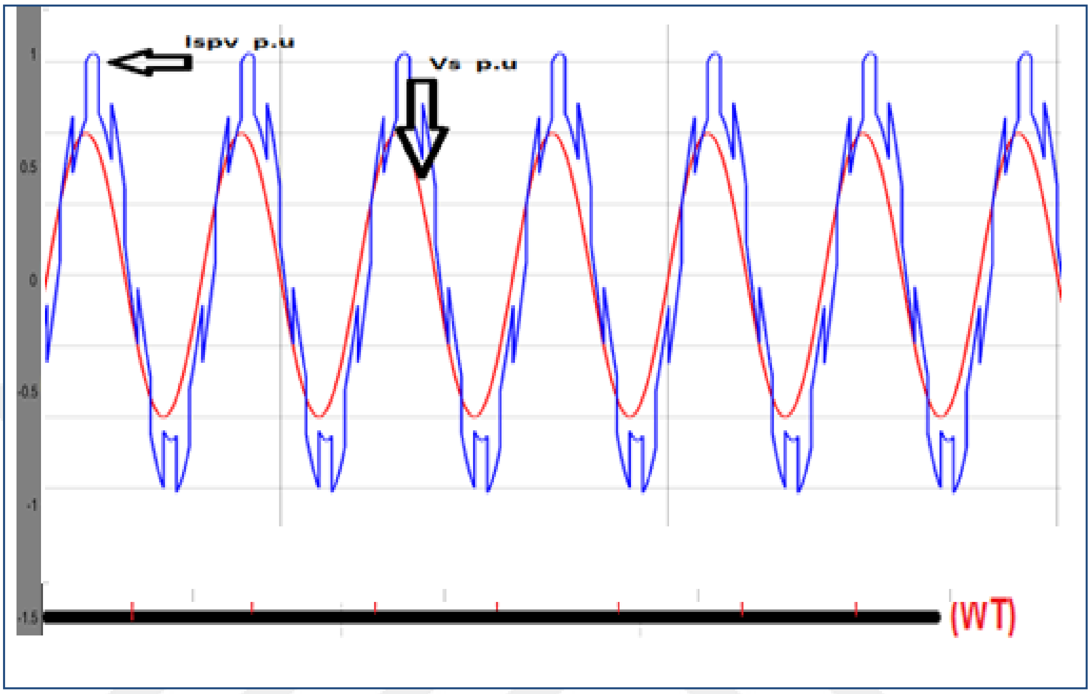

Figure 3.20: Waveforms of source voltage and smart PV system current.

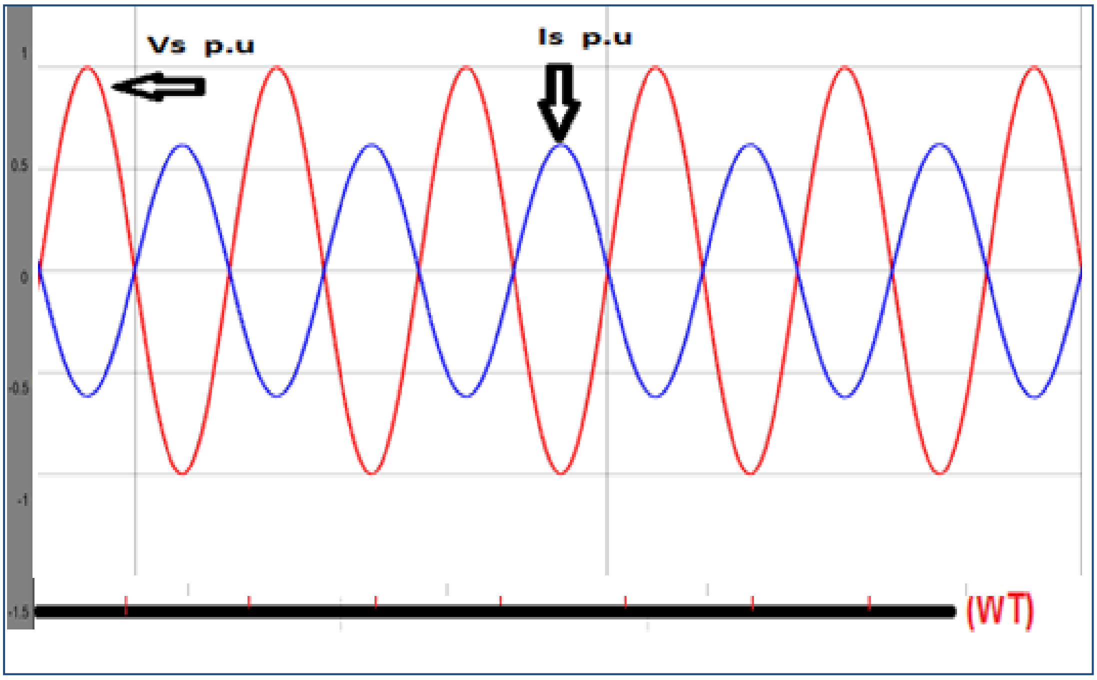

Figure 3.21: Waveforms of source voltage and current.

CHAPTER FOUR

SMART PV SYSTEM SIMULATION

The proposed system was simulated using Matlab/Simulink program.

4.1 Photo Voltaic PV Cell Simulation

To simulate PV cell the equivalent circuit shown in Figure 4.1

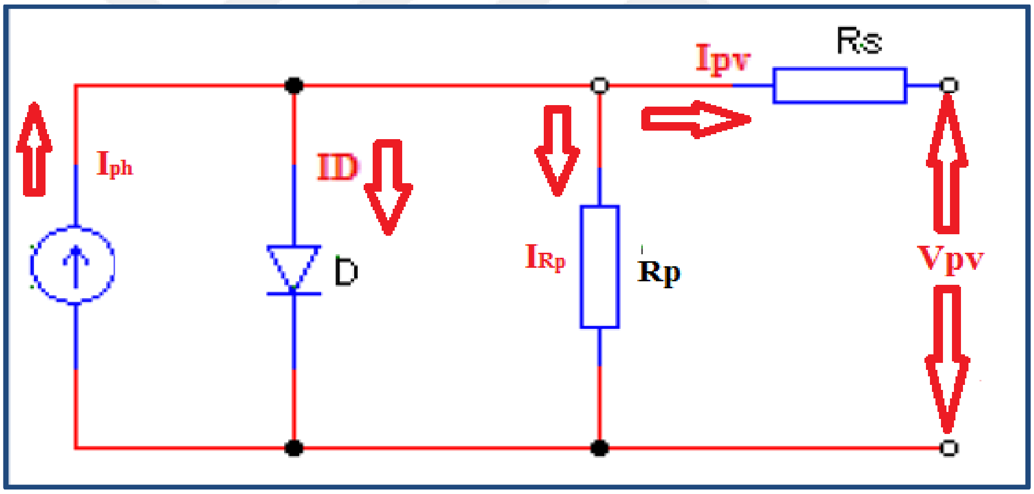

Figure 4.1: PV Cell equivalent circuit.

From figure (4-1) PV equation can be written as:

$$I_{PV} = I_{ph} - I_{Rsh} - I_D \tag{4.1}$$

Where I_D and I_{ph} represent diode and photons currents respectively.

Diode current given by equation 3.2

$$I_D = I_0(e^{\frac{q\,Vpv}{\eta KT}} - 1) \tag{4.2}$$

Where:

η ideality factor for diode

q is the electron charge

k is Boltzmann constant

T is absolute temperature

By substituting diode current equation 4.2 can be re-written as:

$$I_{PV} = I_{ph} - I_0\left(e^{\frac{q\,Vpv}{\eta KT}} - 1\right) - \frac{V_{PV}+I_{PV}R_s}{R_{sh}} \quad (4.3)$$

Always shunt resister effect neglected because of its high value so that equation 4.3 can be written as:

$$I_{PV} = I_{ph} - I_0\left(e^{\frac{q\,Vpv}{\eta KT}} - 1\right) \quad (4.4)$$

The PV cell was simulated using Matlab/Simulink program depending on equation 4.4 as a controlled current source connected in parallel with a diode and series with a resistor, this controlled current source current controlled by the radiance density and temperature. Figures 4.2 and 4.3 the circuit depended in simulation.

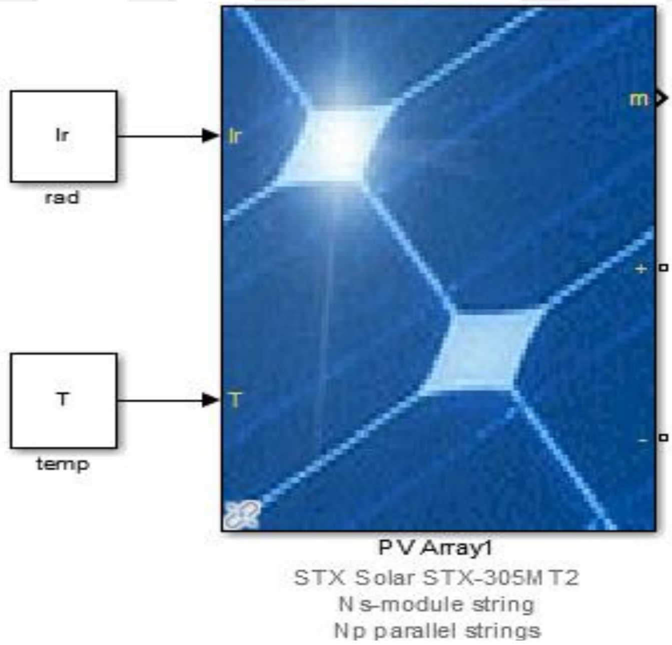

Figure 4.2: Block diagram for PV cell and the values irradiance, and temperature.

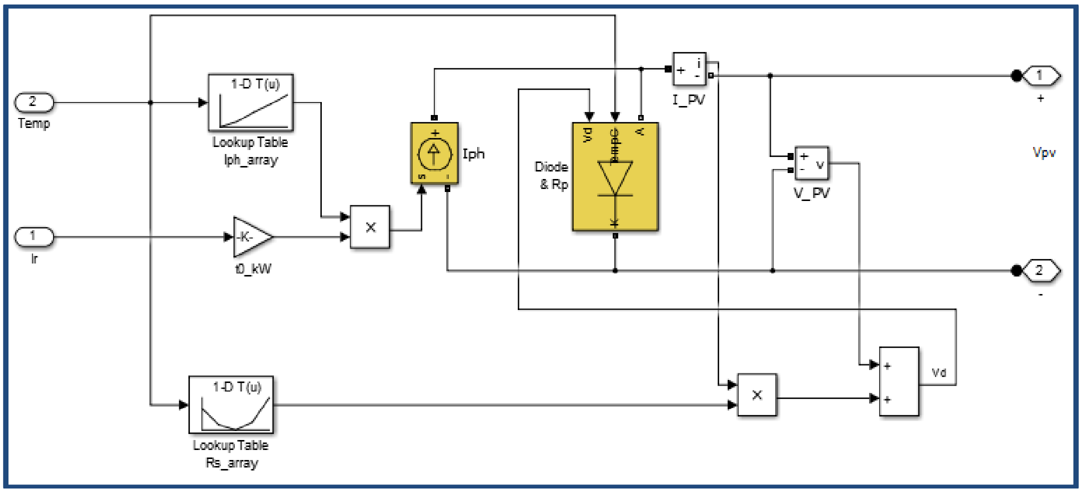

Figure 4.3: Matlab PV equivalent circuit.

While Figure 4.4 shows the circuit used to simulate the diode and shunt resister in the PV cell.

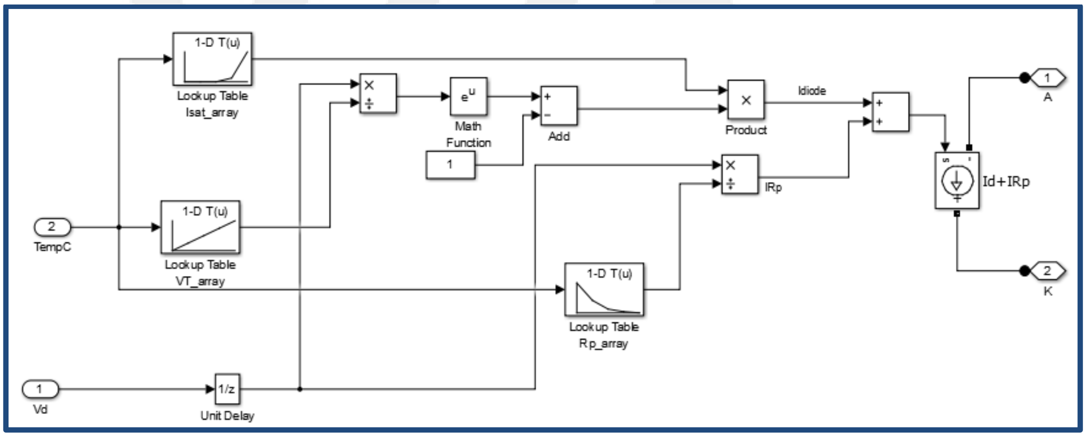

Figure 4.4: Diode and shunt resister circuit.

The power of a single PV cell is low so that it cannot be used as a power source lonely in the proposed application therefore it will be connected as modules which contain many cells connected in series to increase the voltage and in parallel to increase the current. The modules also connected in series and parallel for the same reasons.

Figure 4.5 shows the voltage – current characteristics line for single PV cell in 25 c temperature for different cases of irradiance density. And Figure 4.6 shows the voltage – current and voltage power characteristics lines for PV matrix which contain two groups connected in parallel each group consists of ten modules connected in series.

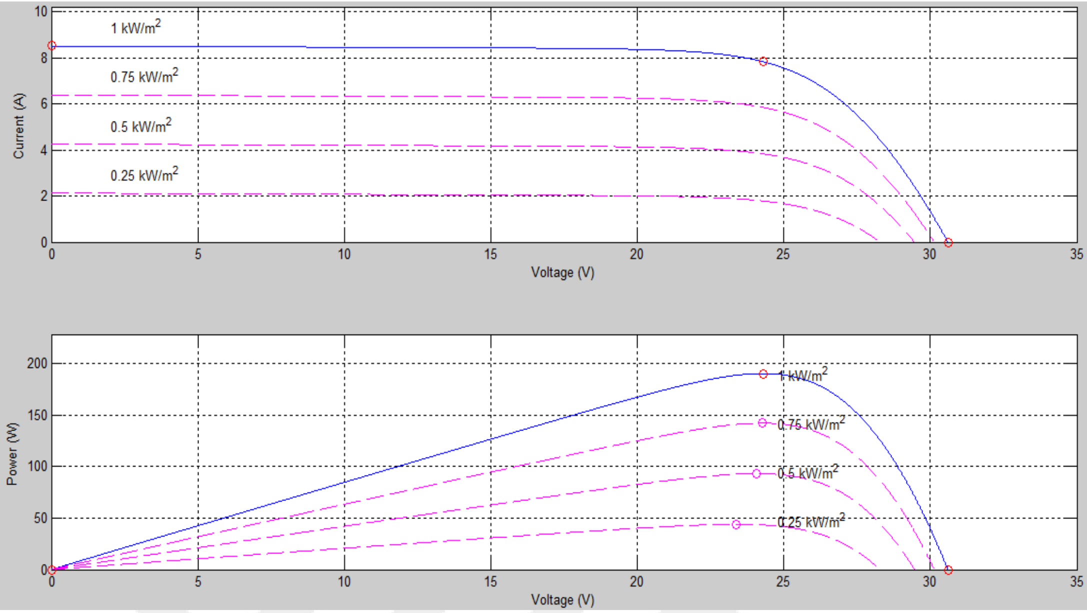

Figure 4.5: V&I and V&P characteristics lines.

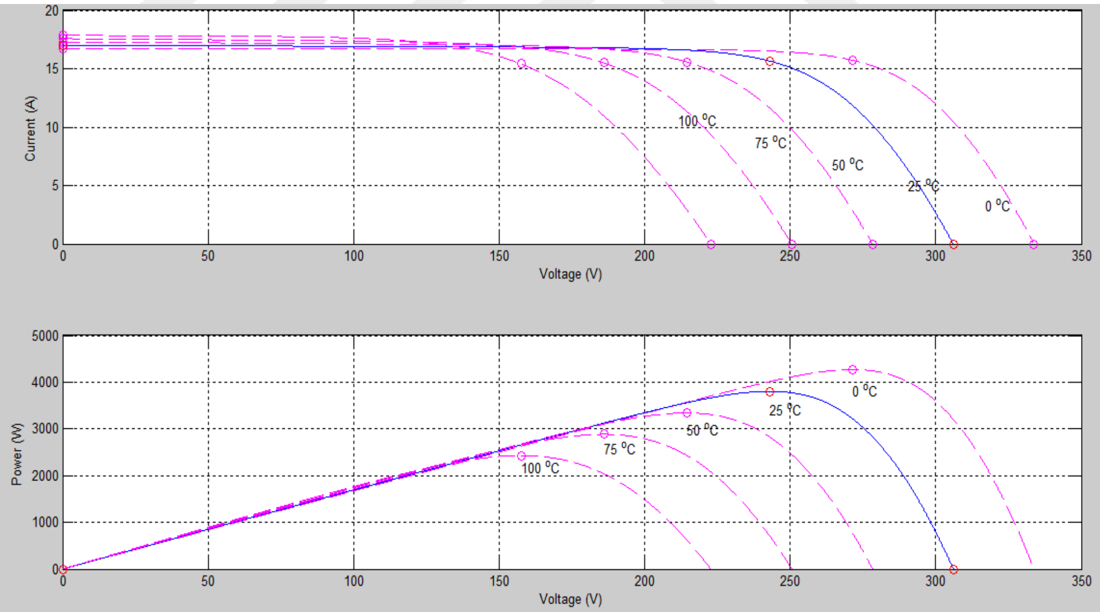

Figure 4.6: V&I and P&V for PV matrix.

Figure 4.7 shows the V&I and V&P characteristics line for PV matrix which explain the effect of irradiance on the matrix current and power in the same temperature.

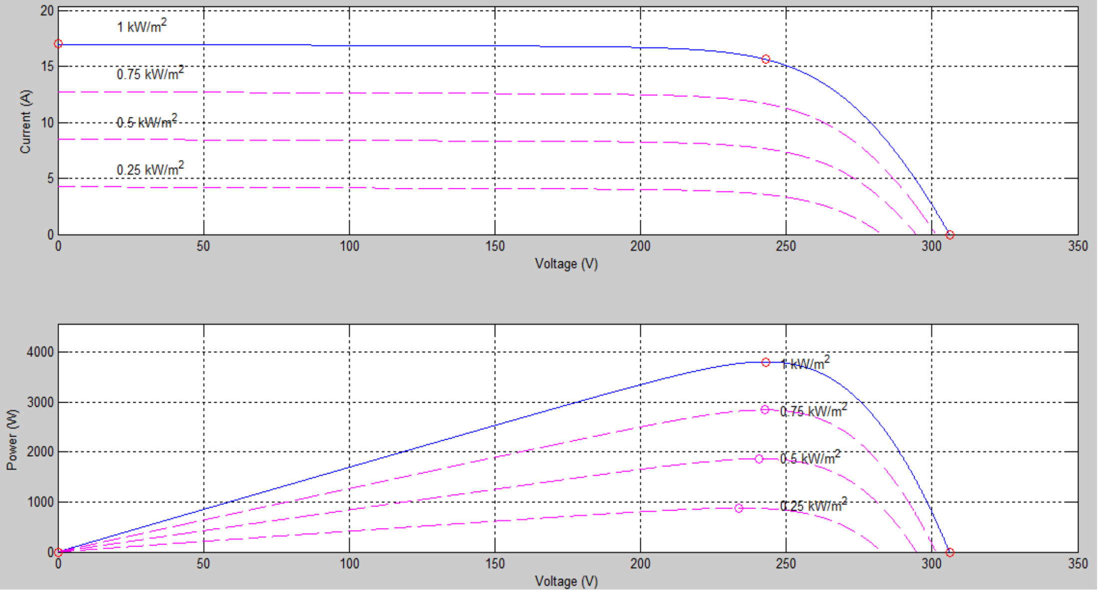

Figure 4.7: V&I and V&P line or the PV matrix.

4.2 Modified System Capacity

The modified system designed to meet the largest number of customs so that it can be used for range (0 – 10 kw) the power calculation as below:

Depending on the number of cells per module the module power can be calculated as below:

Module power = $V_{module} \times I_{module}$

= 54.7 × 5.58

= 305.226 watt

Where:

V_{module} : PV module voltage at maximum power point.

I_{module} : PV module current at maximum power point.

While the total power of the system calculated depending on the number of modules per matrix as below:

Matrix power = N × module power

= 32 × 305.226

= 9.767 KW

4.3 Capacitor Bank

The capacitor bank can be calculated depending on load type so that it can be sufficient for compensation the reactive power of the load, also the ripple in the DC voltage depends on the capacitor size, the capacitor calculated using equation (4.1)[22].

$$C_{dc} >= \frac{P_{out}}{2\pi f \Delta V_{dc} V_{dc}} \tag{4.1}$$

Where:

C_{dc} : The capacitance of capacitor

P_{out} : solar cell matrix power

ΔV_{dc} : the ripple in the DC voltage

V_{dc}: solar cell matrix voltage

f : AC power source frequency Hz

According to equation (4.1) while the solar cell matrix power is 8kw watt at maximum power point, the DC voltage is 325 volts, DC voltage ripple 10 volts and the AC source frequency is 50 Hz.

$$= 784 \text{ x}10^{-3} \text{ Farad}$$

4.4 Single Phase Voltage Source Converter

The voltage source converter used in this system is a full bridge single-phase voltage source converter. The switches used in the simulated system are MOSFET switches because that type has the suitable speed and good rating for such application. The system proposed as a single phase system for many reasons like that it gives the ability to deal with each phase separately and take in consideration that almost home loads are single phase loads and the other reason is the simplicity of implementation and cost reduction. This system is considered as the base of the three single-phase units. Figure (4-8) shows the single-phase full bridge voltage source converter.

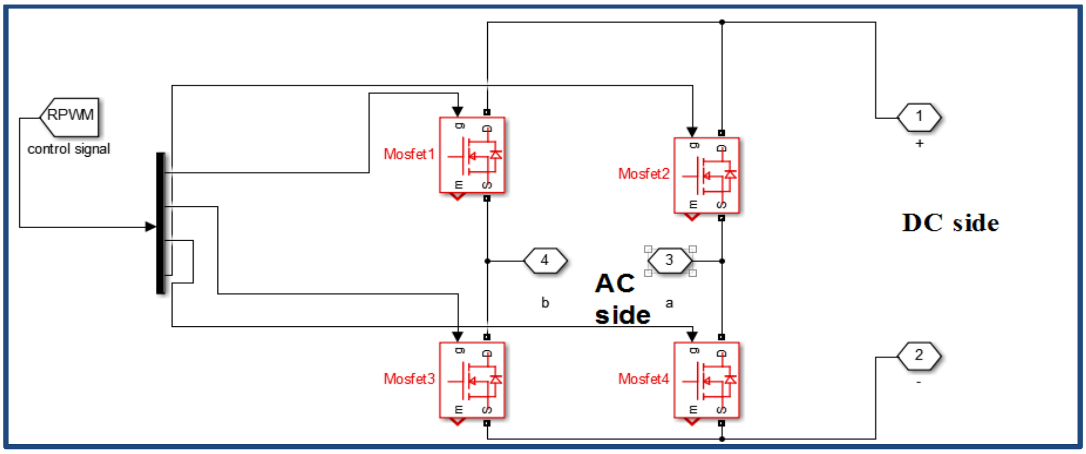

Figure 4.8: Full bridge voltage source converters.

4.5 Power Transistors Switching and Control Circuits

The power transistors driving signal can be estimated instantaneously from many calculations and simulation process that started by analyzing the load current and calculate the PV matrix current so that the wanted smart PV system current can be estimated in magnitude and shape and compare this wanted current with real current of the smart PV system and according to the error signal the modulated signal can be corrected. The modulated signal will change due to the load and PV matrix current change so that it will be a random signal (because it cannot be described previously) therefore this technique will be called Random Pulse Width Modulation RPWM. One advantage of this type of control is the fast response and the ability to deal with the load sudden change without the need for reference signal. This operation is based on equation 2.16 in chapter two. Figure 4.9 shows the circuit used to calculate the modulated signal and Figure 4.10 shows a sample from the modulated signal and Figure 4.11shows the actual and wanted smart PV system currents and the power transistors drive signals all the above signals was to nonlinear inductive load with real power production by the PV matrix. While Figure 4.12 shows the spectrum analysis for the wanted and the actual smart PV system.

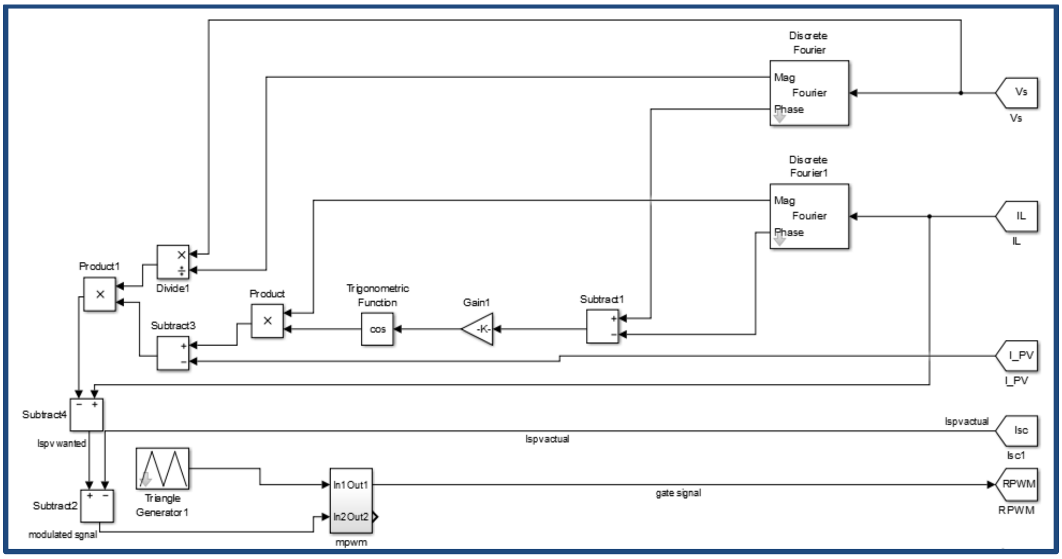

Figure 4.9: Power transistors switching and control circuit.

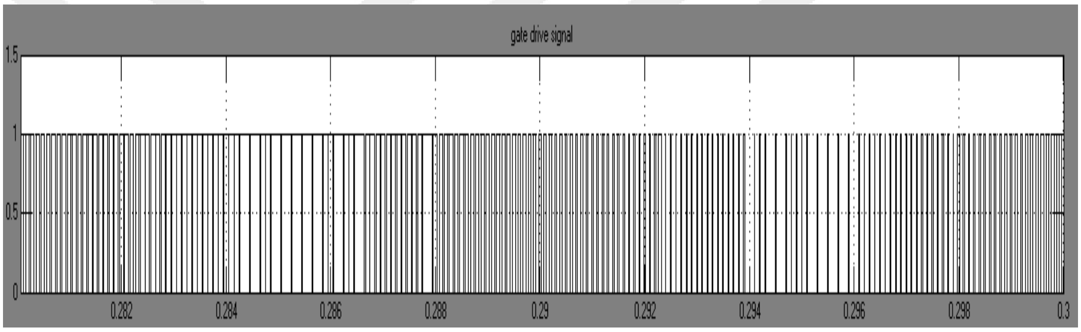

Figure 4.10: Switching signal sample.

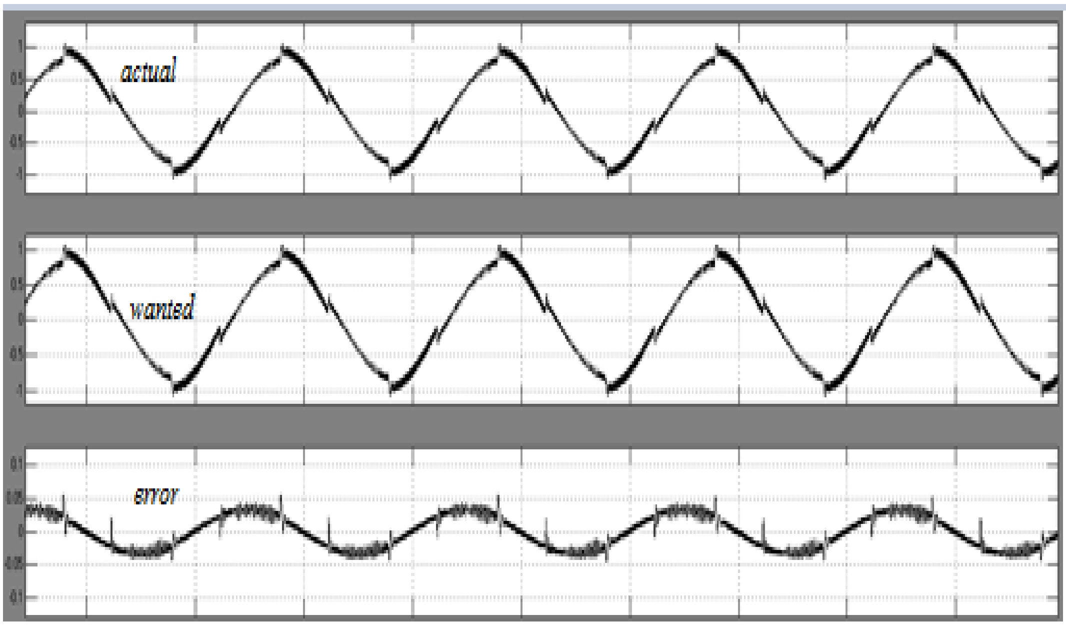

Figure 4.11: Samples for wanted and actual currents and modulated signal.

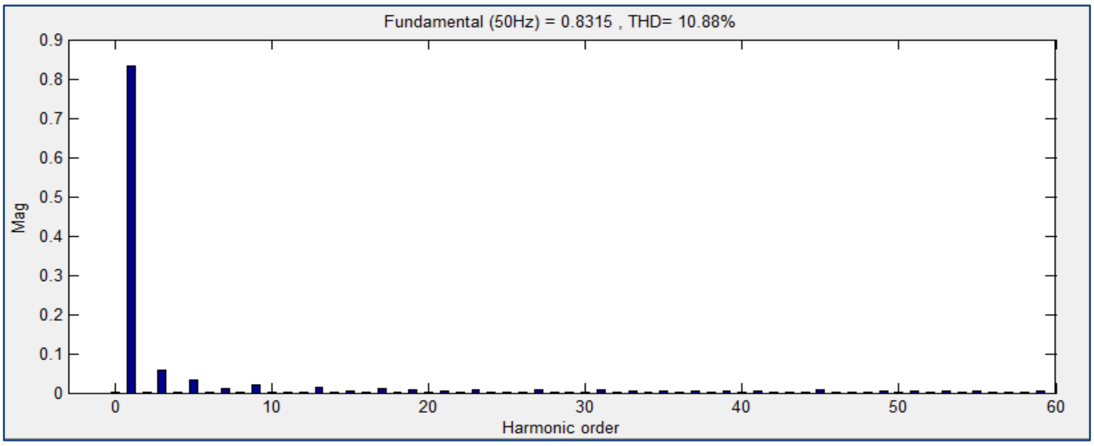

-A-

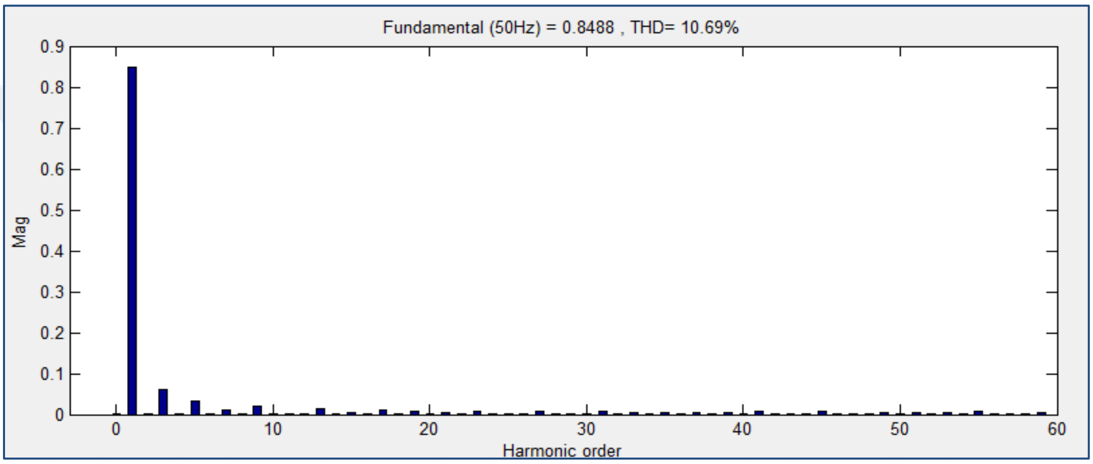

-B-

Figure 4.12: Spectrum analyses for a-actual smart PV system current and b- wanted current.

4.6 AC Power Source

The AC power source simulated by using single phase power source which have the ability to supply and absorb real and reactive power. Figure 4.13 shows overall system, in this all system components presented. The system contains two groups hardware group and software group, the hardware group contains PV system with all related components, capacitor bank which used for compensation, voltage source converter VSC, nonlinear load, coupling inductors, AC power source and monitors. While software group included calculation block where all needed calculations done, control block where load, source and smart PV system currents analyzed so that the wanted firing signals generated.

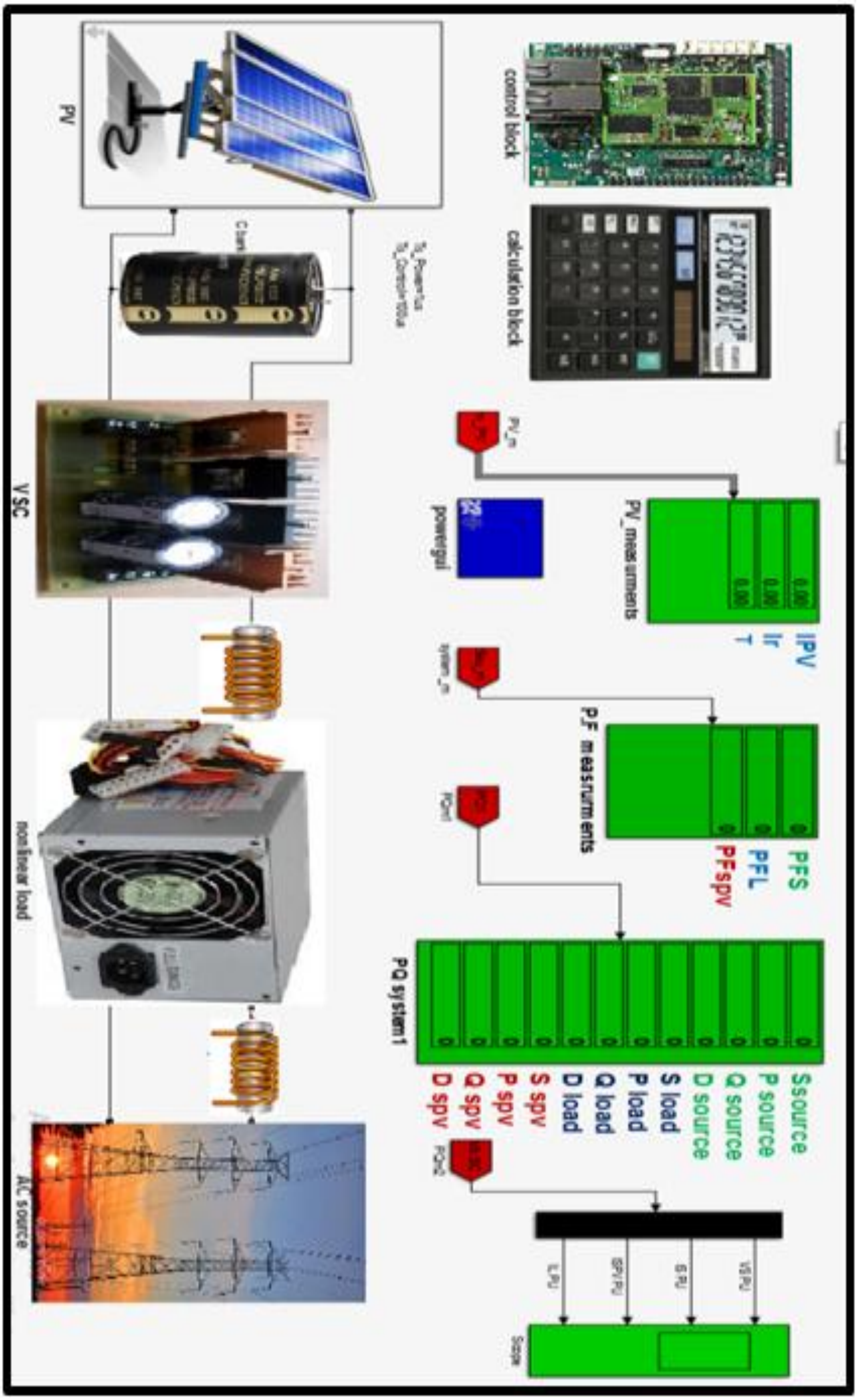

Figure 4.13: Overall system components.

CHAPTER FIVE

SIMULATION RESULTS DISCUSSION

The proposed system was simulated for two types loads, the first of which was with a linear load with and the second a nonlinear load. For four cases, due to the real power production, firstly the PV cells are idle, i.e., there is no real power production. In the second case, the PV system produces real power, but it is less than the load demand. In the third case, the PV system produces real power equal to the load demand, and the fourth case is the PV system producing real power in excess of the load demand. For all the above cases, the smart PV system accomplishes it with a maximum power factor and minimum Total Harmonic Distortion (THD) and it compensates all reactive distortion power which is needed by the load. All components were calculated for load, source and smart PV system

5.1 Linear Load Case

This case include four sub cases which are (produced real power equal to zero, less than load demand , equal to load demand, and more than load demand) :

5.1.1 The First Case Idle PV Cells (in Night)

Table 5.1 shows the power components of the system in cases when the PV cells are idle, while Figure 5.1 shows implementation of the system by the Matlab/Simulink program. Figure 5.2 shows the waveforms of the source voltage, source current, smart PV current, and load PV current. Figures 5.3 and 5.4 show the Fourier analyses (FFT) for both the load current and the source current, respectively. From Table 5.1, we see that the source provides only the real part of the load current while the reactive part is provided by the smart PV system (SPV). Moreover, here we see the all values of THD are less than 5%. By a high power factor, the load specification is reactive power of 2400 var active power1900watt).

Table 5.1: System power components of linear load for first case.

Measured quantity	Load	Source	PV system
Apparent power S p.u	1.000	0.3509	0.937
Real power P p.u	0.3083	0.351	0.04
Reactive power Q p.u	0.9512	0.000	0.956
Distortion power D p.u	0	0.000	0
THD%	0.67	1.35	1.16
Power factor	0.30	1	0.077

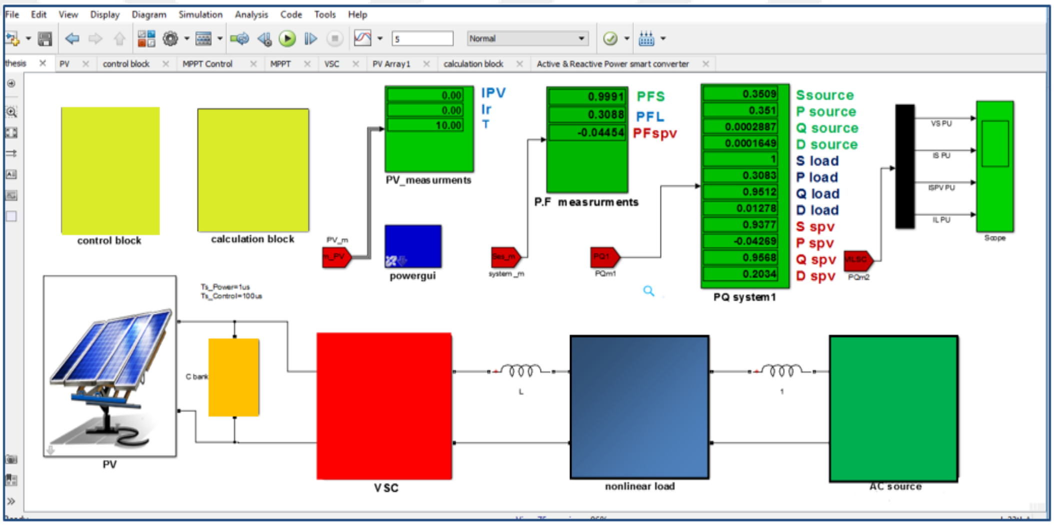

Figure 5.1: Show system implementation by Matlab/ Simulink program.

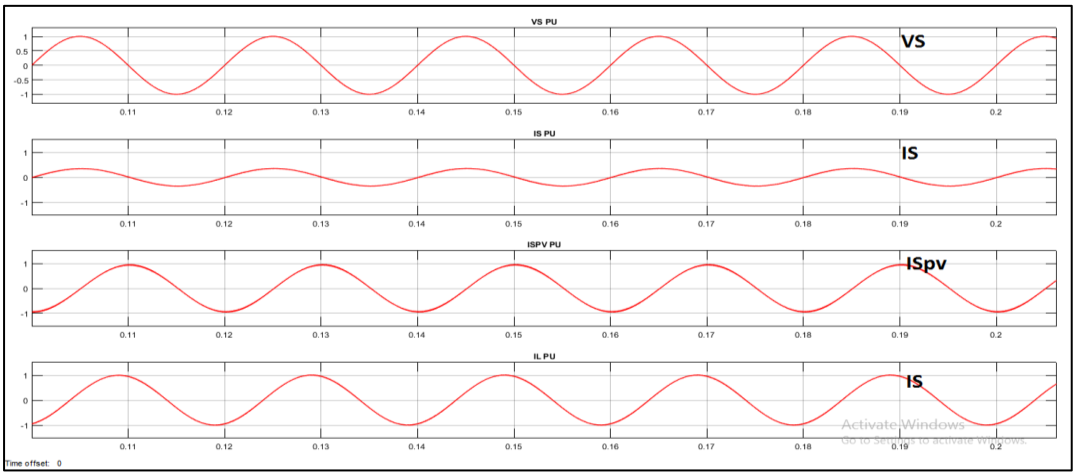

Figure 5.2: Shows the waveforms of source voltage, source current, load current and smart PV current respectively.

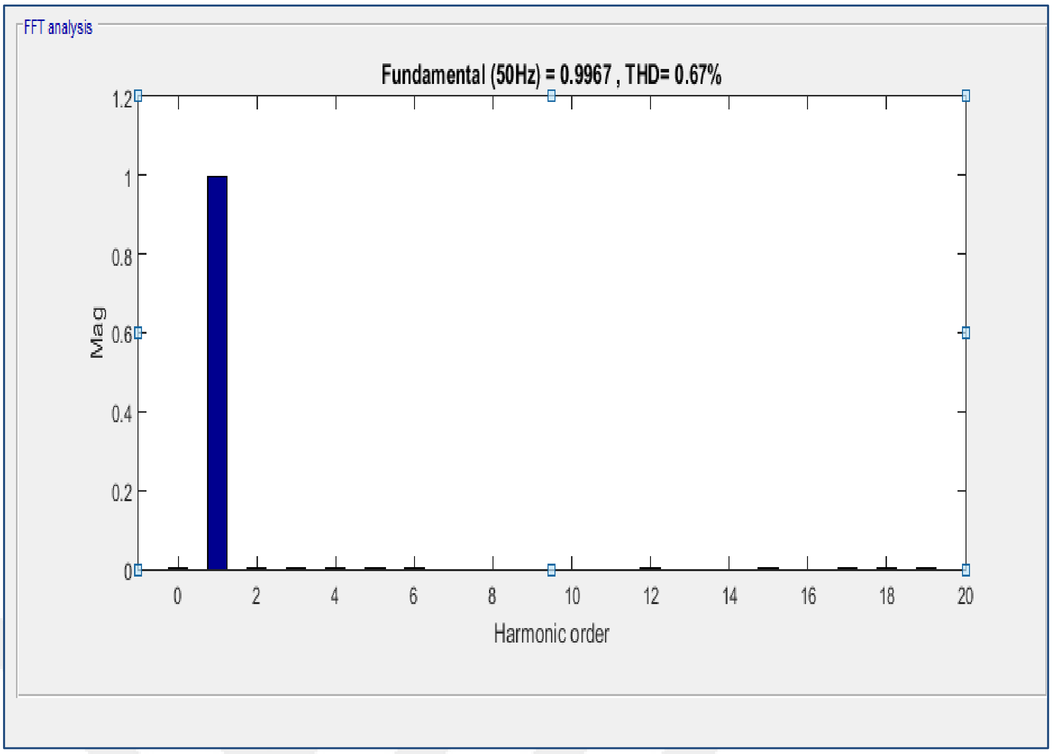

A

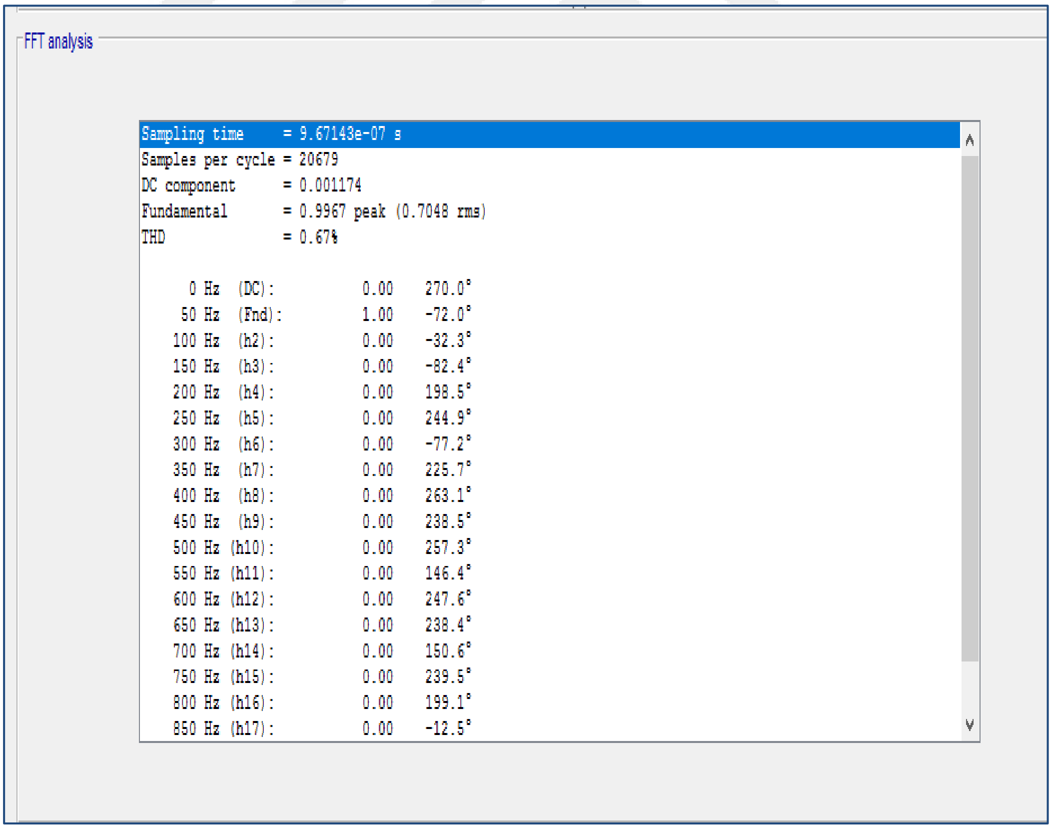

B

Figure 5.3: A and B show FFT analysis of the load current.

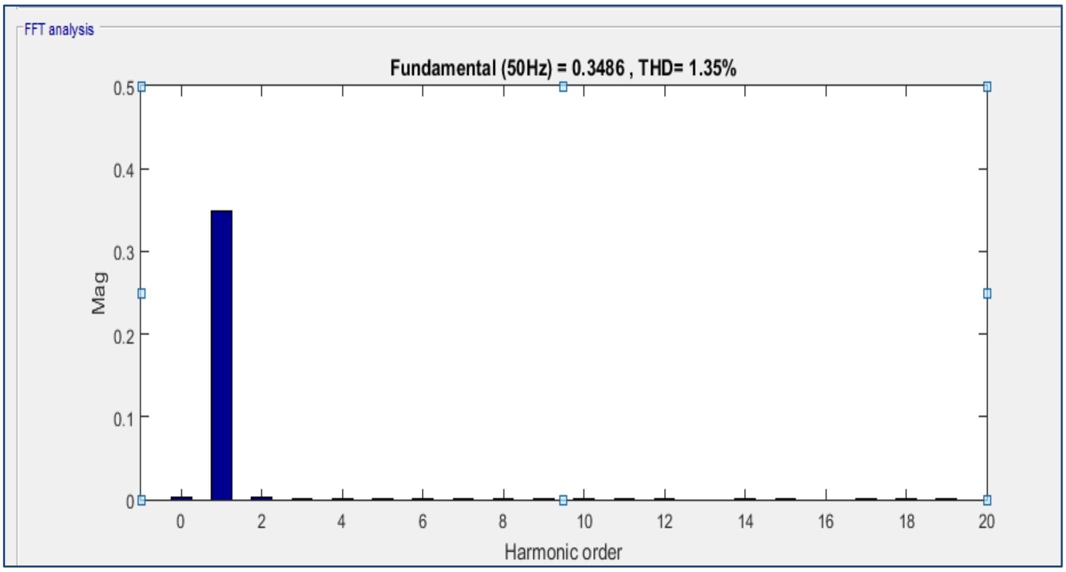

A

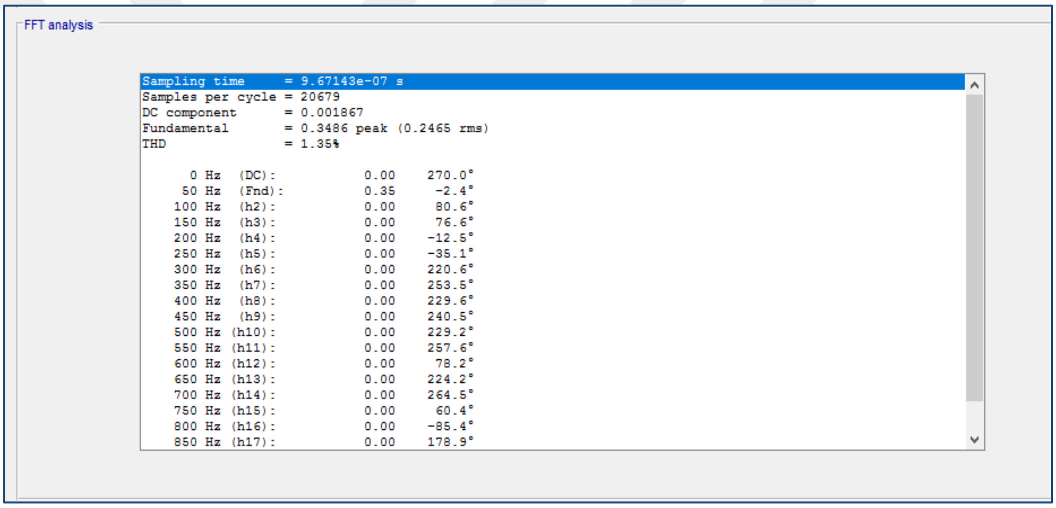

B

Figure 5.4: A and B show FFT analysis for source current.

5.1.2 The Second Case

The system produces real power less than the load demand, this case occurs under the following conditions: temperature 25℃, irradiance density: 200 W/ m^2. The power components for the system in this case shown in table5.2 while the Figure 5.5 show implementation of the system with the Matlab/Simulink program. Figure5.6 shows the waveforms of the source voltage, source current, smart PV current, and 6uboth load current and source current respectively. From table 5.6 we see that the real power part of the load current is provided from the source and the Smart PV

System (SPV) Moreover, also here we see all values of (THD) less than 5%, reactive power 1500var, active power2400watt).

Table 5.2: System power components of linear load for second case.

Measured quantity	Load	Source	PV system
Apparent power S p.u	1.000	0.3731	0.8
Real power P p.u	0.6151	0.3731	0.24
Reactive power Q p.u	0.788	0	0.77
Distortion power D p.u	0	0	0
THD%	0.78	1	1
Power factor	0.615	1	0.29

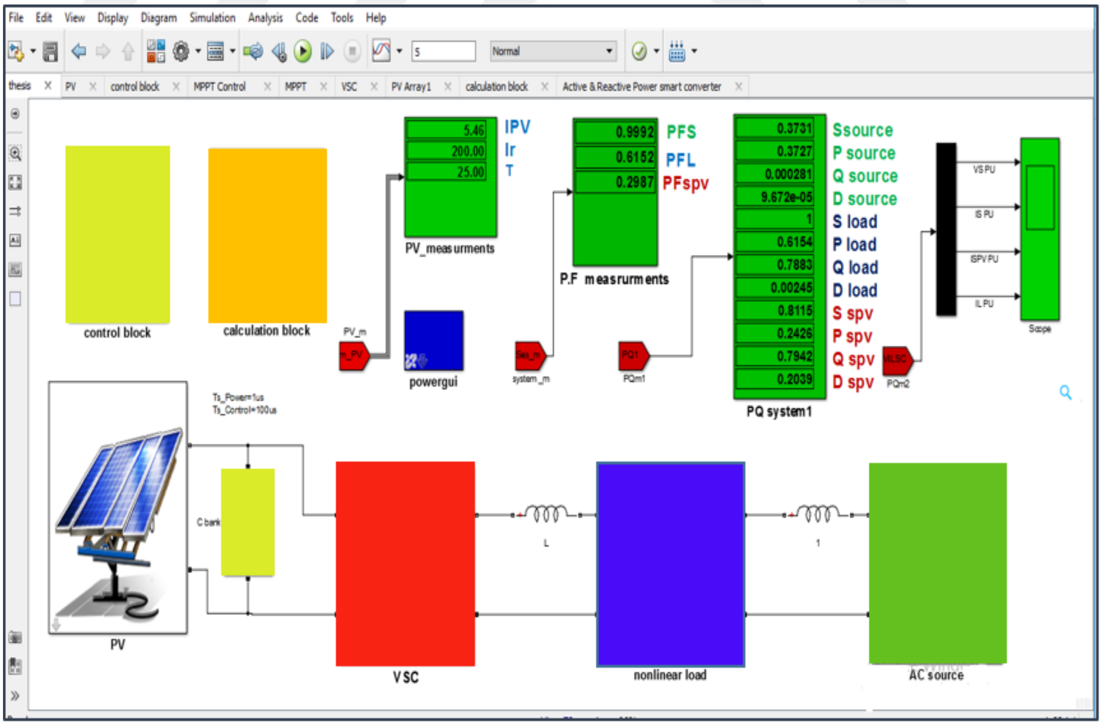

Figure 5.5: Show system implementation by Matlab/ Simulink program.

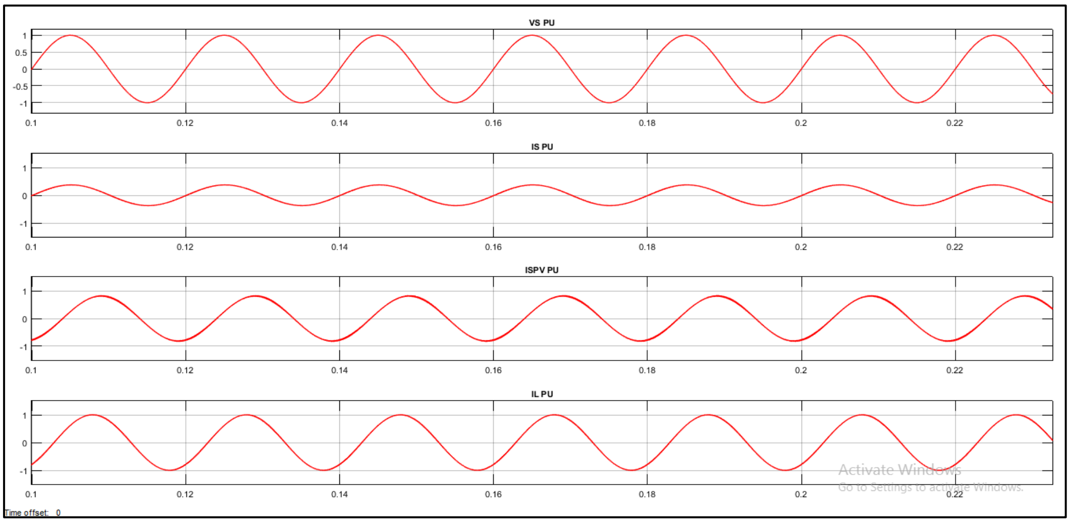

Figure 5.6: Shows the waveforms of source voltage, source current, load current and smart PV current respectively.

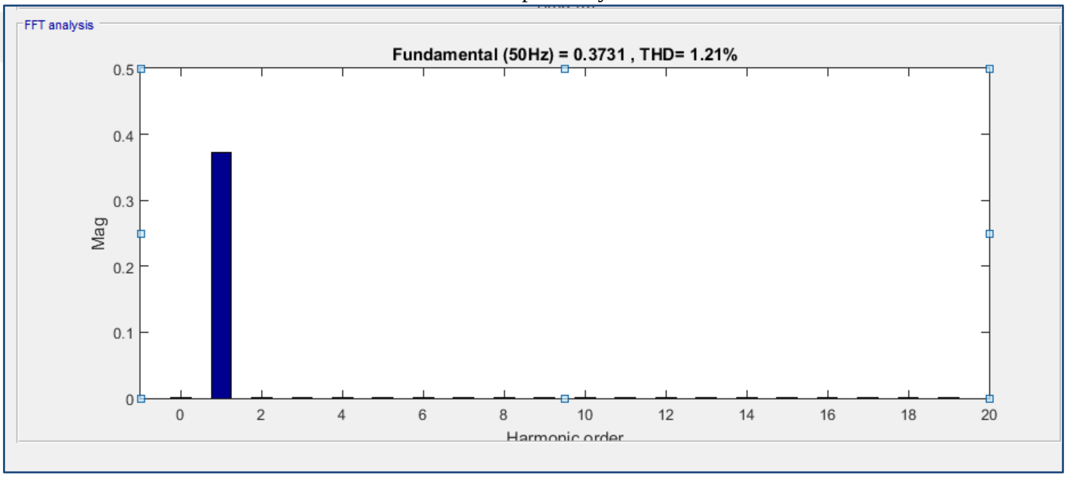

A

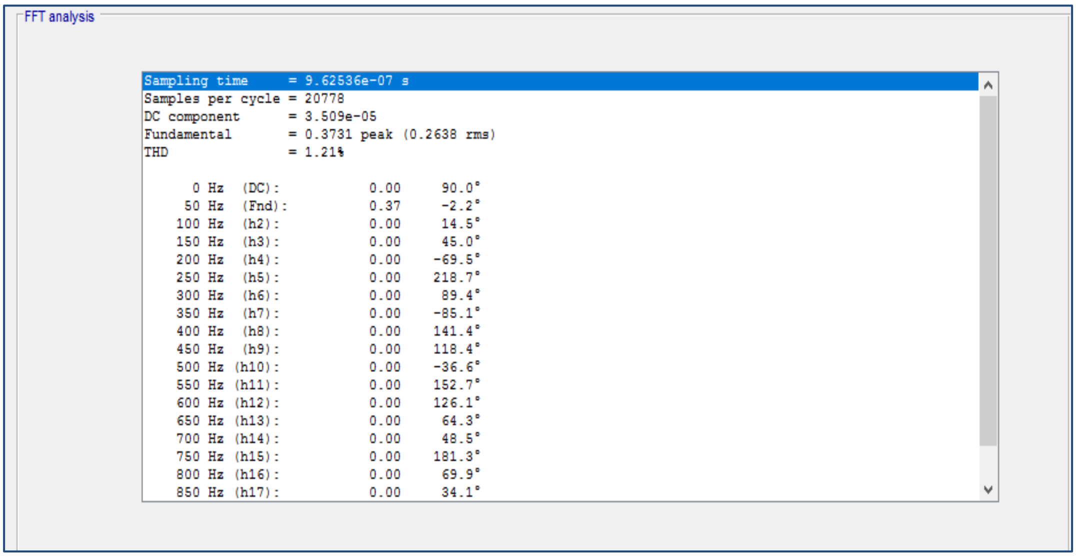


```
Sampling time      = 9.62536e-07 s
Samples per cycle  = 20778
DC component       = 3.509e-05
Fundamental        = 0.3731 peak (0.2638 rms)
THD                = 1.21%

   0 Hz  (DC):        0.00     90.0°
  50 Hz  (Fnd):       0.37     -2.2°
 100 Hz  (h2):        0.00     14.5°
 150 Hz  (h3):        0.00     45.0°
 200 Hz  (h4):        0.00    -69.5°
 250 Hz  (h5):        0.00    218.7°
 300 Hz  (h6):        0.00     89.4°
 350 Hz  (h7):        0.00    -85.1°
 400 Hz  (h8):        0.00    141.4°
 450 Hz  (h9):        0.00    118.4°
 500 Hz (h10):        0.00    -36.6°
 550 Hz (h11):        0.00    152.7°
 600 Hz (h12):        0.00    126.1°
 650 Hz (h13):        0.00     64.3°
 700 Hz (h14):        0.00     48.5°
 750 Hz (h15):        0.00    181.3°
 800 Hz (h16):        0.00     69.9°
 850 Hz (h17):        0.00     34.1°
```

B

Figure 5.7: A and B show FFT analysis for source current.

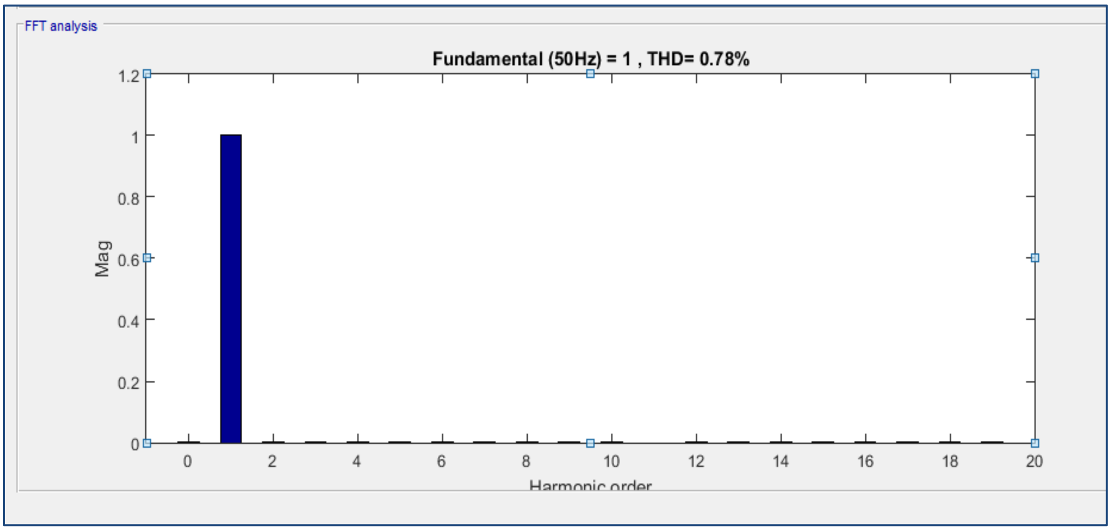

A

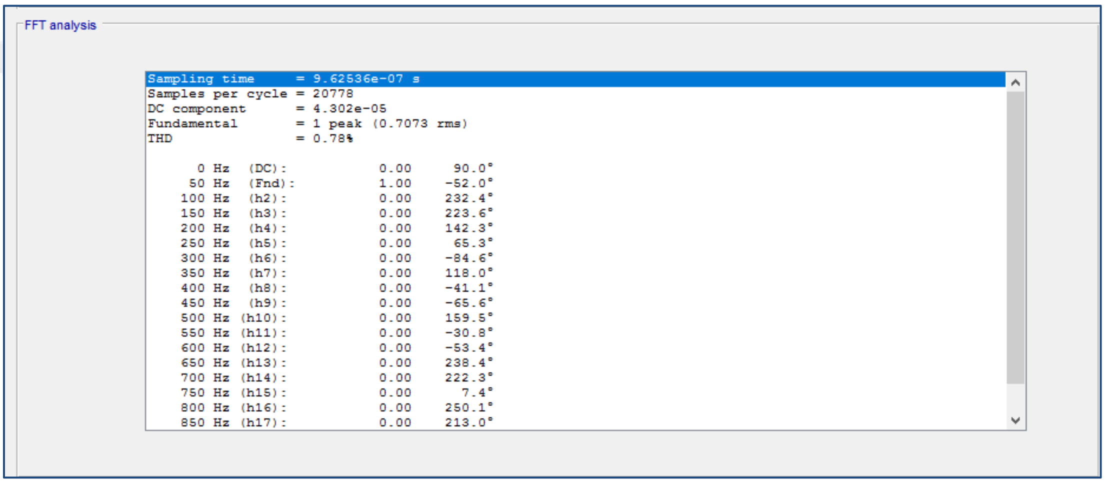

B

Figure 5.8: A and B show FFT for load current.

5.1.3 The Third Case

The system produces real power more than the load demands, this case occurs in the following conditions: temperature 34°C and irradiance density is 1000 W/m^2. Table 5.3 shows power components in this case while the Figure 5.9 show implementation of the system by Matlab/Simulink program, the Figure 5.10 shows the waveforms of the source voltage, source current, smart PV current, and load PV current respectively, the Figures 5.11, 5.12 shows the Fourier analysis FFT for both load current and source current respectively. From table5.3 we see that the real power of the smart PV system is greater than load current demand we the system is injected the overflow from need the load to the electrical grid, while the reactive part was provided by the smart PV system (SPV) and also here we see that acceptable distortion in source current, where all values of (THD) less than 5%, reactive power 2400var, active power600watt).

Table 5.3: System power components of linear load for third case.

Measured quantity	Load	Source	PV system
Apparent power S p.u	1.000	0.5819	1.454
Real power P p.u	0.636	-0.5845	1.22
Reactive power Q p.u	0.773	0.000	0.8
Distortion power D p.u	0.068	0.000	0.131
THD%	0.49	0.92	0.71
Power factor	0.63	-1	0.83

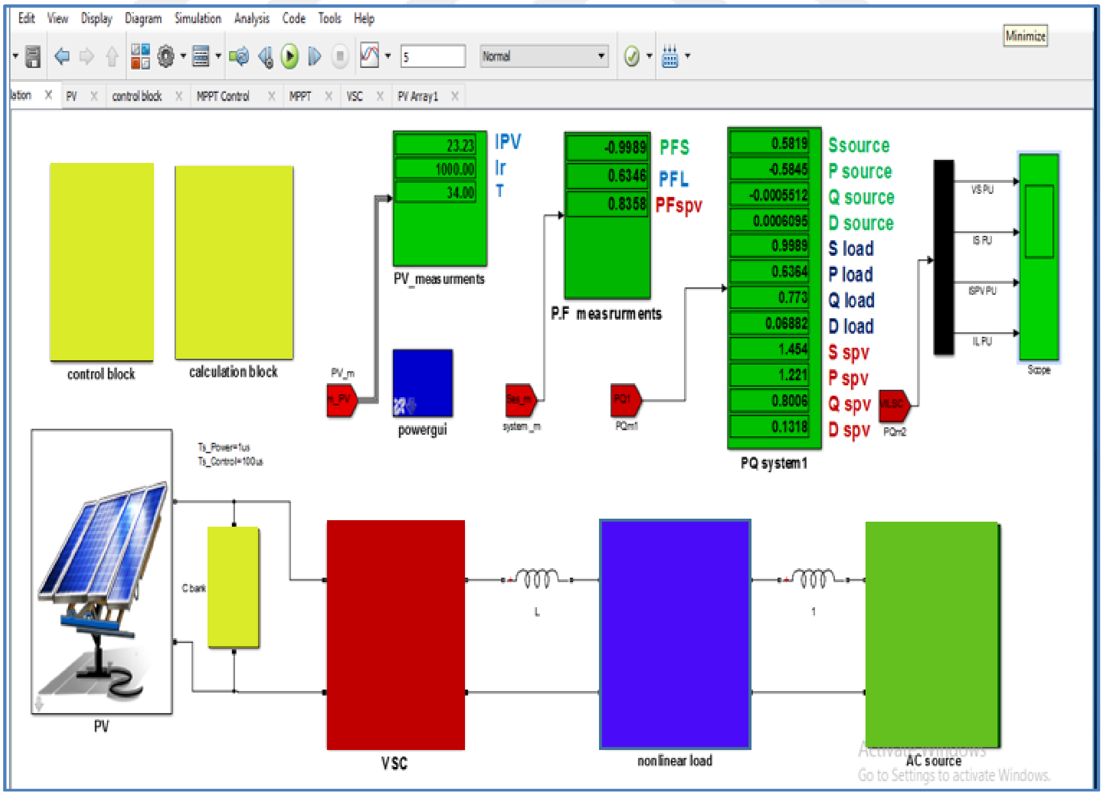

Figure 5.9: Show system implementation by Matlab/Simulink program.

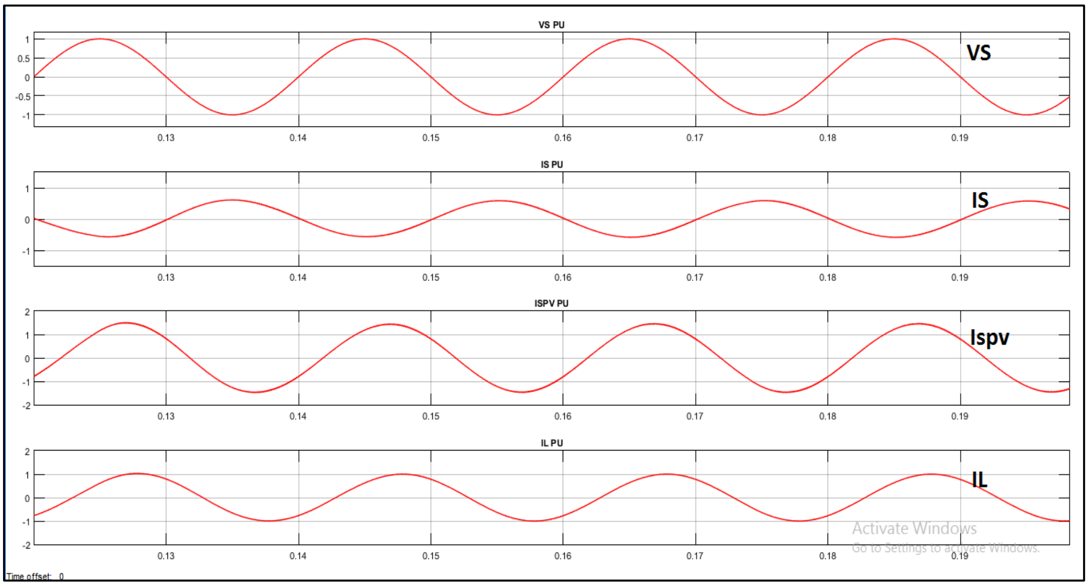

Figure 5.10: Waveforms of source voltage, source current, load current and smart PV current respectively.

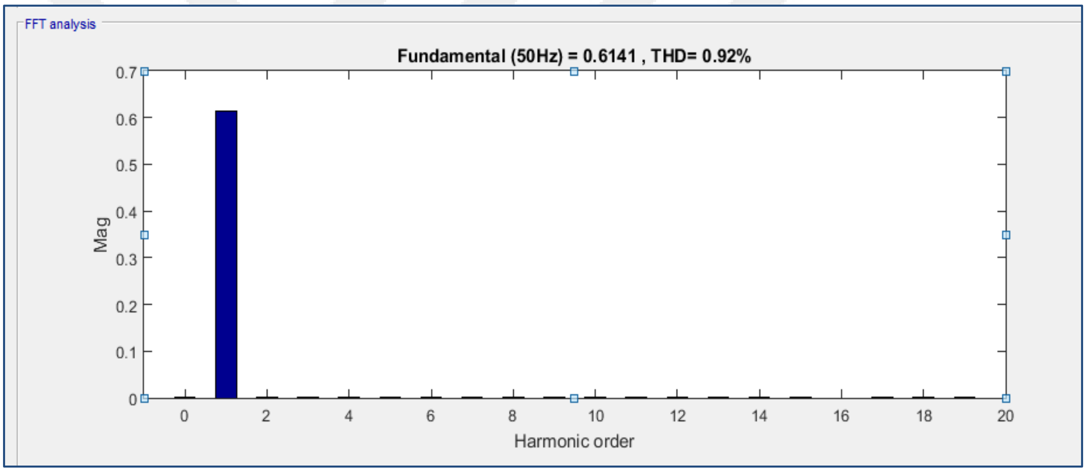

A

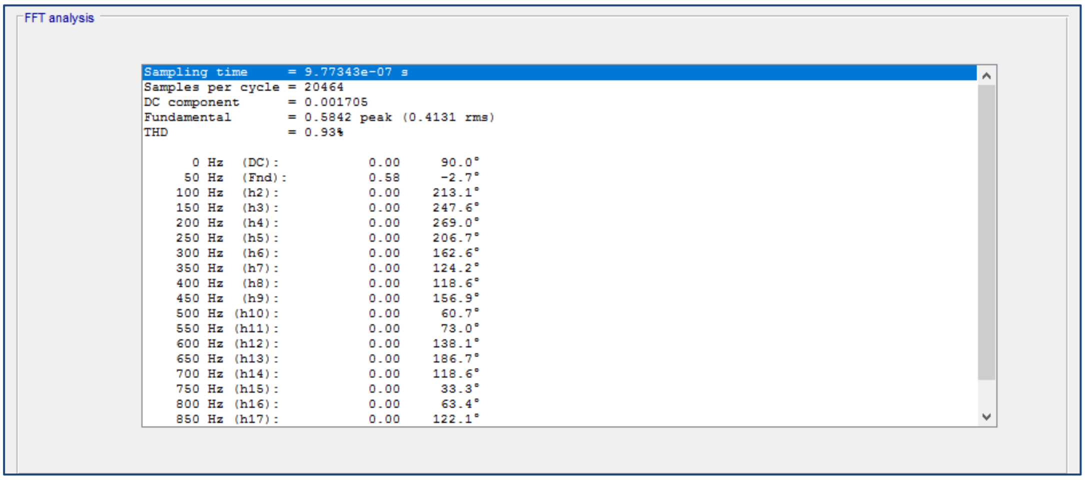
FFT analysis

```
Sampling time      = 9.77343e-07 s
Samples per cycle = 20464
DC component      = 0.001705
Fundamental       = 0.5842 peak (0.4131 rms)
THD               = 0.93%

   0 Hz  (DC):          0.00      90.0°
  50 Hz  (Fnd):         0.58      -2.7°
 100 Hz  (h2):          0.00     213.1°
 150 Hz  (h3):          0.00     247.6°
 200 Hz  (h4):          0.00     269.0°
 250 Hz  (h5):          0.00     206.7°
 300 Hz  (h6):          0.00     162.6°
 350 Hz  (h7):          0.00     124.2°
 400 Hz  (h8):          0.00     118.6°
 450 Hz  (h9):          0.00     156.9°
 500 Hz (h10):          0.00      60.7°
 550 Hz (h11):          0.00      73.0°
 600 Hz (h12):          0.00     138.1°
 650 Hz (h13):          0.00     186.7°
 700 Hz (h14):          0.00     118.6°
 750 Hz (h15):          0.00      33.3°
 800 Hz (h16):          0.00      63.4°
 850 Hz (h17):          0.00     122.1°
```

B

Figure 5.11: A and B show FFT for load current.

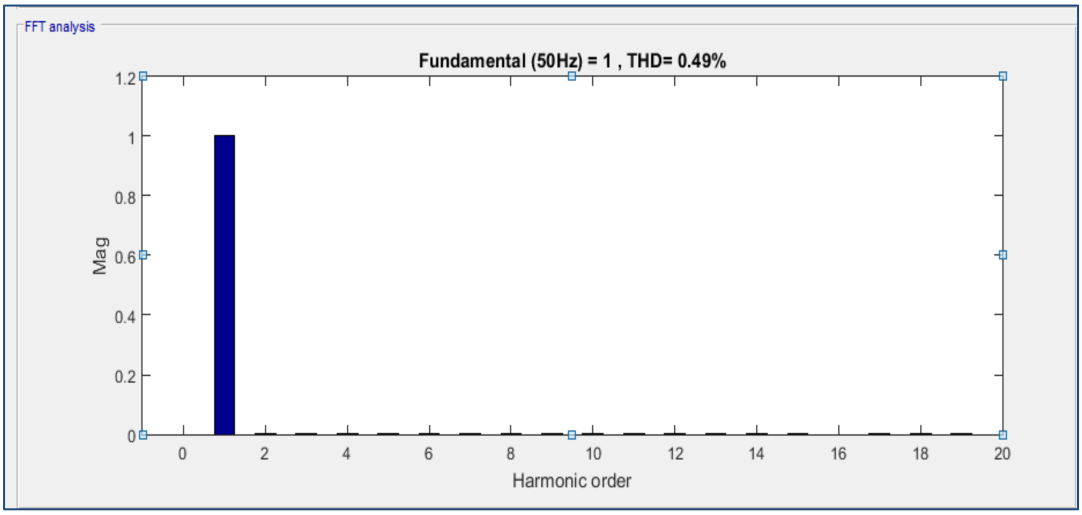

A

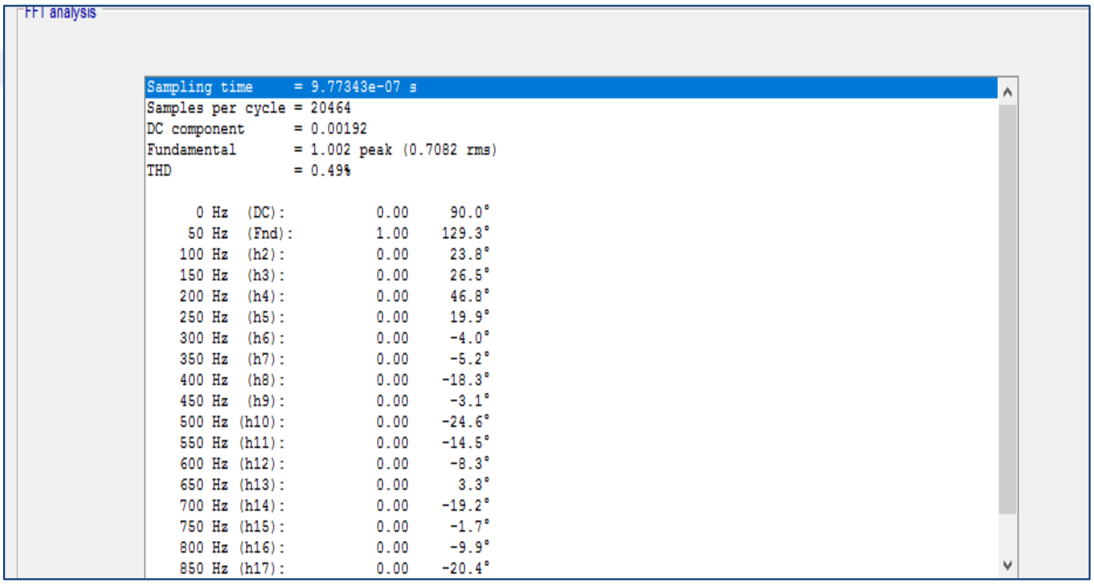

B

Figure 5.12: A and B show FFT for load current.

5.1.4 The Fourth Case

The system produces real power equal to the load demand, this case occurs in the following conditions: temperature 29℃ and the irradiance density 280 W/m^2. Table5.4 shows the power components of the system while the Figure5.13 show implementation of the system by Matlab/Simulink program, the Figure5.14 shows the waveforms of the source voltage, source current, smart PV current, and load PV current respectively, the figures5.15, 5.16 shows the Fourier analysis FFT for both load current and (SPV) current respectively. From table 5.8 we see that the real power of the smart PV system is equal load current demand we see the real power part system is provide from smart PV system only (SPV), while the reactive part was provided by the smart PV system (SPV) and also here we see that acceptable distortion in source current, where all values of (THD) less than 5%, reactive power 1000var, active power1050watt).

Table 5.4: System power components of linear load for fourth case.

Measured quantity	Load	Source	PV system
Apparent power S p.u	1.000	0.01352	1.000
Real power P p.u	0.7267	0.00	0.7344
Reactive power Q p.u	0.6872	0.000	0.7106
Distortion power D p.u	0.01	0.000	0.215
THD%	0.78	-------	1.87
Power factor	0.7266	-------	0.7285

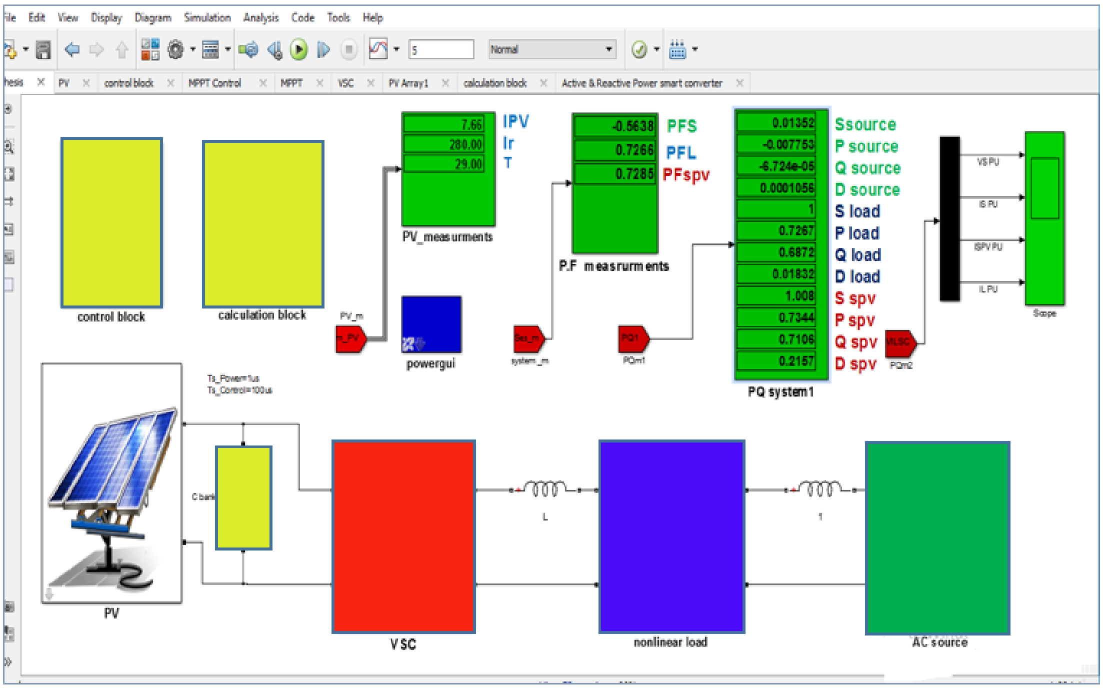

Figure 5.13: Show system implementation by Matlab/ Simulink program.

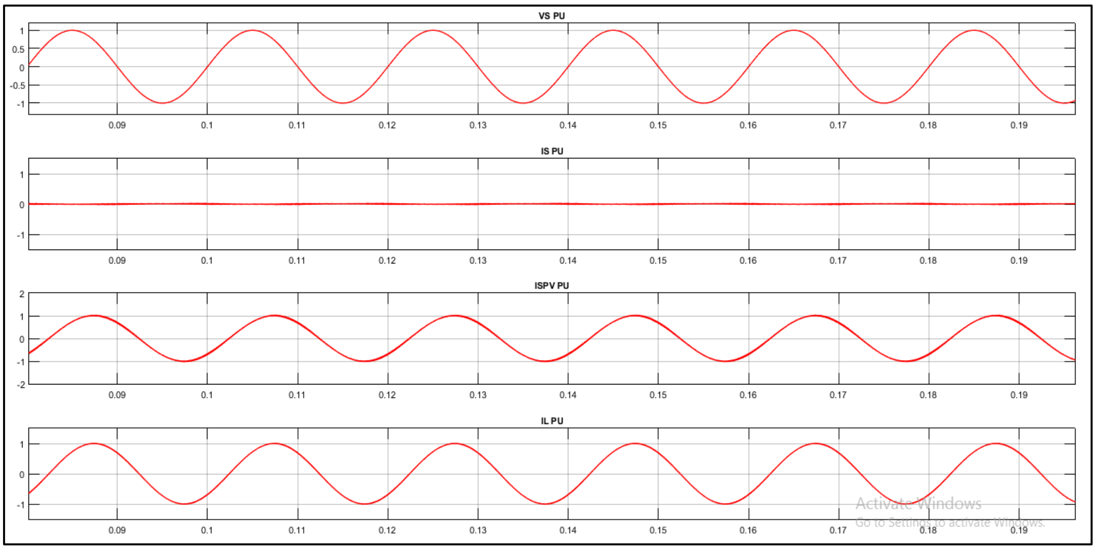

Figure 5.14: shows the waveforms of source voltage, source current, load current and smart PV current respectively.

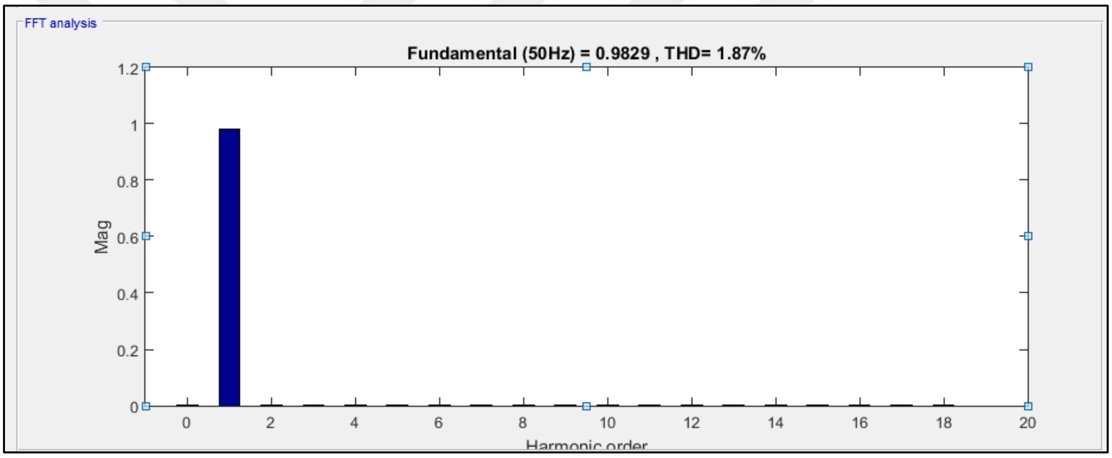

A

FFT analysis

```
Sampling time     = 9.63421e-07 s
Samples per cycle = 20759
DC component      = 0.0007801
Fundamental       = 0.9829 peak (0.695 rms)
THD               = 1.87%

  0 Hz  (DC):        0.00    270.0°
 50 Hz  (Fnd):       0.98    133.1°
100 Hz  (h2):        0.00    116.1°
150 Hz  (h3):        0.00    135.2°
200 Hz  (h4):        0.00     86.4°
250 Hz  (h5):        0.00    250.4°
300 Hz  (h6):        0.00    207.1°
350 Hz  (h7):        0.00     14.1°
400 Hz  (h8):        0.00    235.2°
450 Hz  (h9):        0.00    174.6°
500 Hz (h10):        0.00    144.3°
550 Hz (h11):        0.00     20.3°
600 Hz (h12):        0.00    177.1°
650 Hz (h13):        0.00    147.8°
700 Hz (h14):        0.00    220.5°
750 Hz (h15):        0.00    259.9°
800 Hz (h16):        0.00    130.2°
850 Hz (h17):        0.00     99.4°
```

B

Figure 5.15: A and B show FFT for load current.

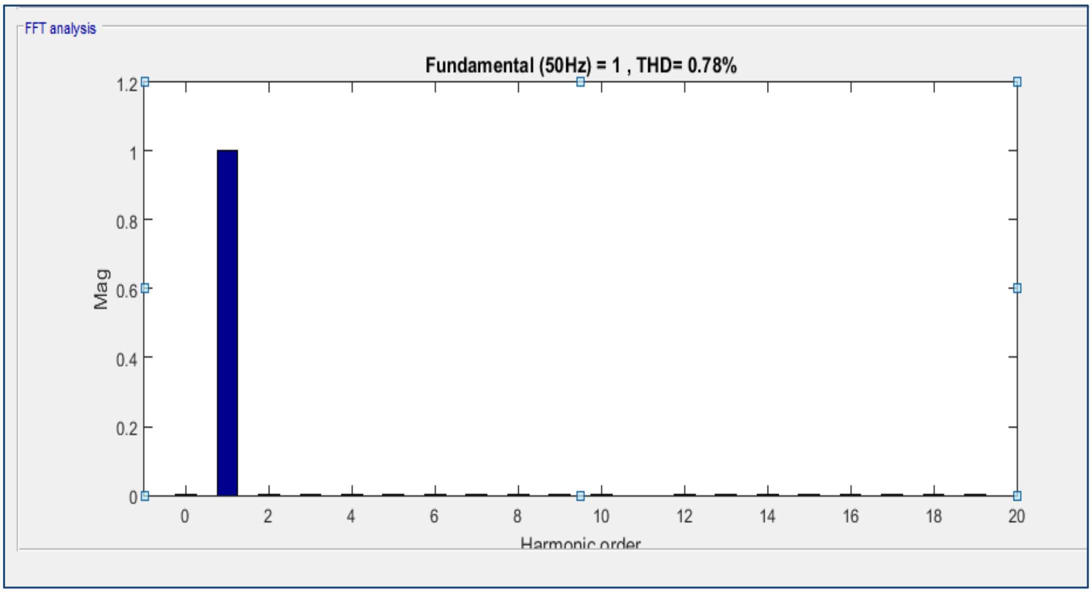

A

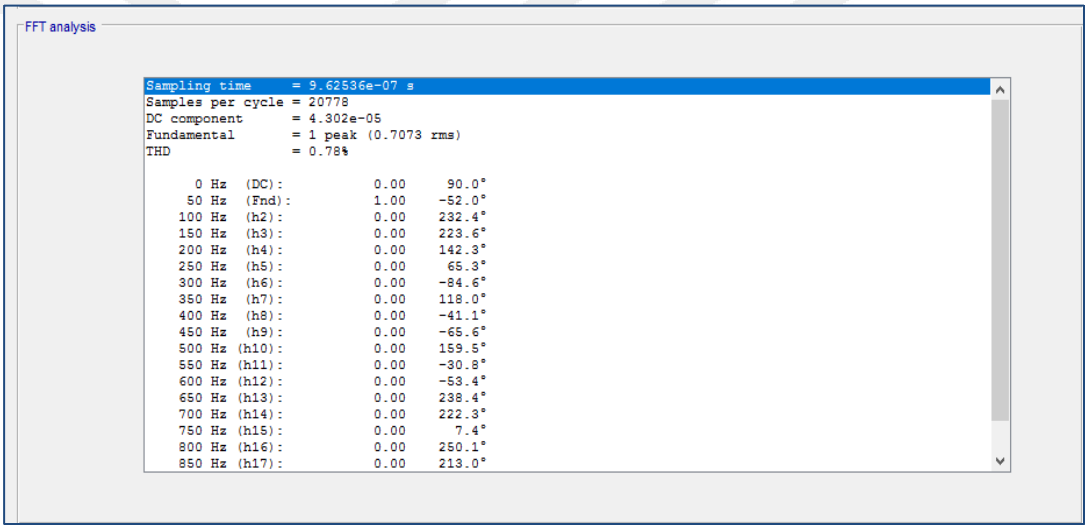


```
Sampling time     = 9.62536e-07 s
Samples per cycle = 20778
DC component      = 4.302e-05
Fundamental       = 1 peak (0.7073 rms)
THD               = 0.78%

   0 Hz  (DC):        0.00     90.0°
  50 Hz  (Fnd):       1.00    -52.0°
 100 Hz  (h2):        0.00    232.4°
 150 Hz  (h3):        0.00    223.6°
 200 Hz  (h4):        0.00    142.3°
 250 Hz  (h5):        0.00     65.3°
 300 Hz  (h6):        0.00    -84.6°
 350 Hz  (h7):        0.00    118.0°
 400 Hz  (h8):        0.00    -41.1°
 450 Hz  (h9):        0.00    -65.6°
 500 Hz (h10):        0.00    159.5°
 550 Hz (h11):        0.00    -30.8°
 600 Hz (h12):        0.00    -53.4°
 650 Hz (h13):        0.00    238.4°
 700 Hz (h14):        0.00    222.3°
 750 Hz (h15):        0.00      7.4°
 800 Hz (h16):        0.00    250.1°
 850 Hz (h17):        0.00    213.0°
```

b

Figure 5.16: A and B show FFT for smart PV current.

5.2 Nonlinear Load Case

The proposed system was simulated for the same four cases as in the nonlinear case which are (produced real power equal to zero, less than load demand, equal to load demand, and more than load demand).

5.2.1 The First Case Idle PV Cells (in Night)

Table 5.5 shows the power components of the system in case that the PV cells are idle while the Figure5.17 show implemented of the system by Matlab/Simulink program, the Figure 518 shows the waveforms of the source voltage, source current, smart PV current, and load PV current respectively, the Figures 5.19, 5.20 shows the Fourier analysis FFT for both load current and source current respectively. From table 5.1 we see that the source provide only the real part of the load current by high power factor, while the reactive part was provided by the smart PV system (SPV) and also here we see all values of (THD) less than 5%, the nonlinear load specification is reactive power 900 var, active power1 950 watt, active power2 500 watt and active power3600 watt). This case occurs under the following conditions: a temperature 10℃, irradiance density is zero.

Table 5.5: System power components of nonlinear and idle PV cells.

Measured quantity p.u	Load	Source	PV system
Apparent power S p.u	1.000	0.6258	0.80
Real power P p.u	0.6345	0.6248	0.000
Reactive power Q p.u	0.8378	0.000	0.832
Distortion power D p.u	0.323	0.000	0.3122
THD%	13.24	0.51	16.14
Power factor	0.5629	1	-------

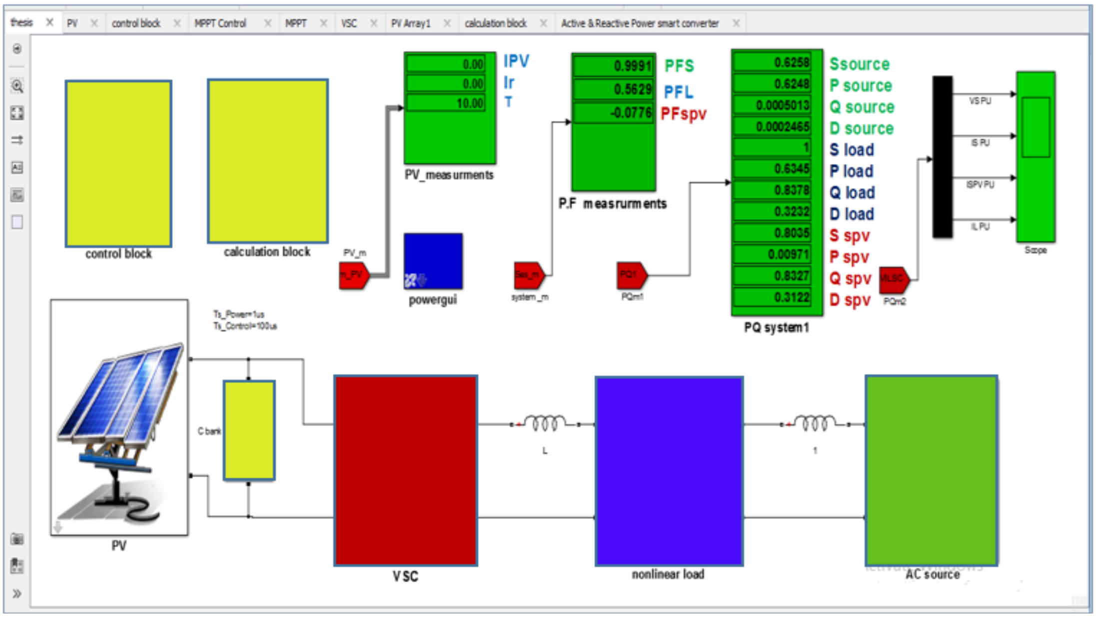

Figure 5.17: Show system implementation by Maltab/Simulink program.

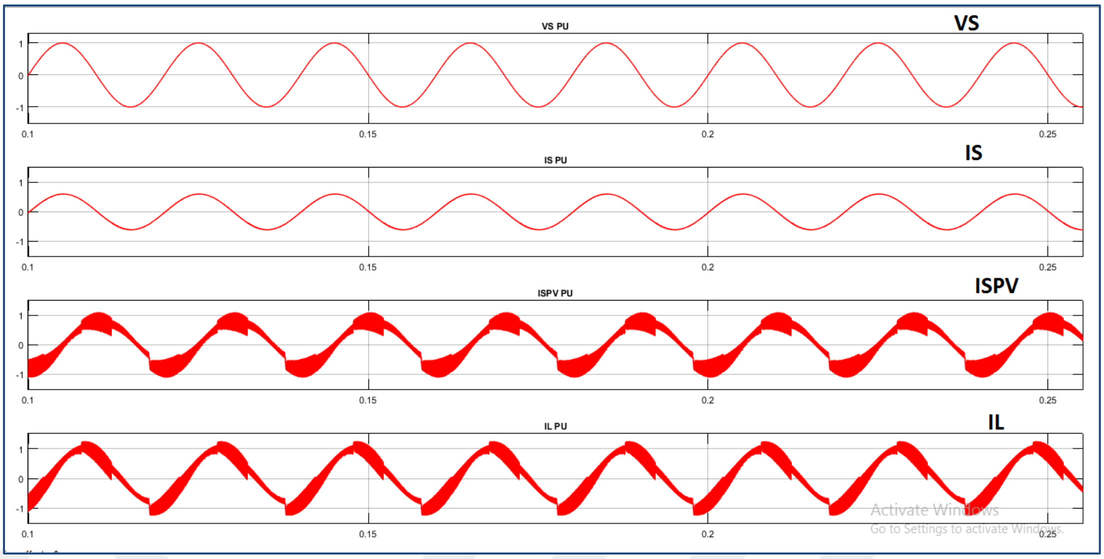

Figure 5.18: Waveforms of the source voltage, source current, smart PV current, and load current respectively.

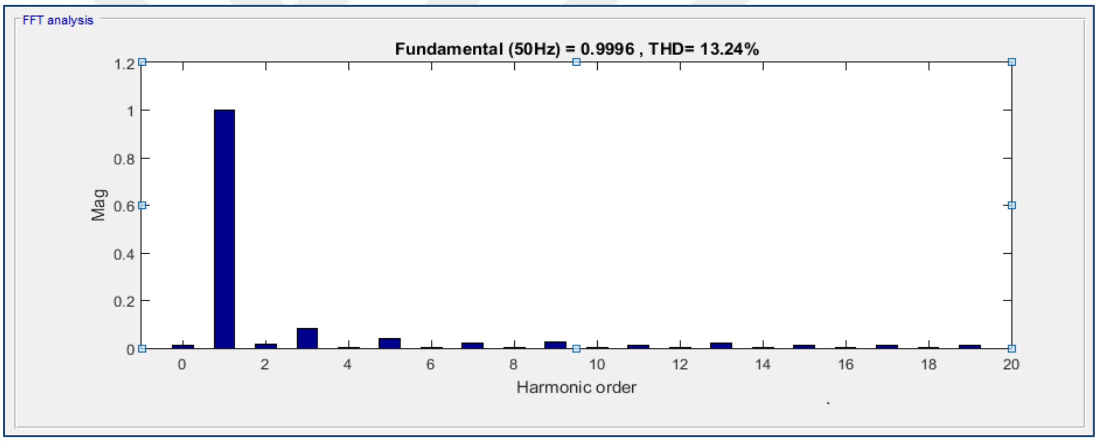

A

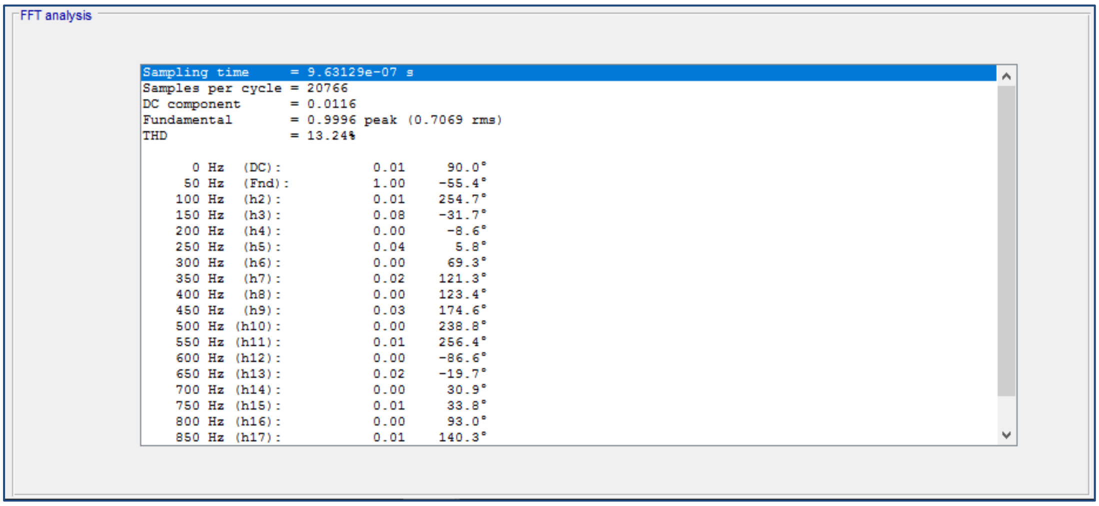


```
Sampling time      = 9.63129e-07 s
Samples per cycle = 20766
DC component       = 0.0116
Fundamental        = 0.9996 peak (0.7069 rms)
THD                = 13.24%

   0 Hz  (DC):          0.01     90.0°
  50 Hz  (Fnd):         1.00    -55.4°
 100 Hz  (h2):          0.01    254.7°
 150 Hz  (h3):          0.08    -31.7°
 200 Hz  (h4):          0.00     -8.6°
 250 Hz  (h5):          0.04      5.8°
 300 Hz  (h6):          0.00     69.3°
 350 Hz  (h7):          0.02    121.3°
 400 Hz  (h8):          0.00    123.4°
 450 Hz  (h9):          0.03    174.6°
 500 Hz (h10):          0.00    238.8°
 550 Hz (h11):          0.01    256.4°
 600 Hz (h12):          0.00    -86.6°
 650 Hz (h13):          0.02    -19.7°
 700 Hz (h14):          0.00     30.9°
 750 Hz (h15):          0.01     33.8°
 800 Hz (h16):          0.00     93.0°
 850 Hz (h17):          0.01    140.3°
```

B

Figure 5.19: A and B FFT of load current.

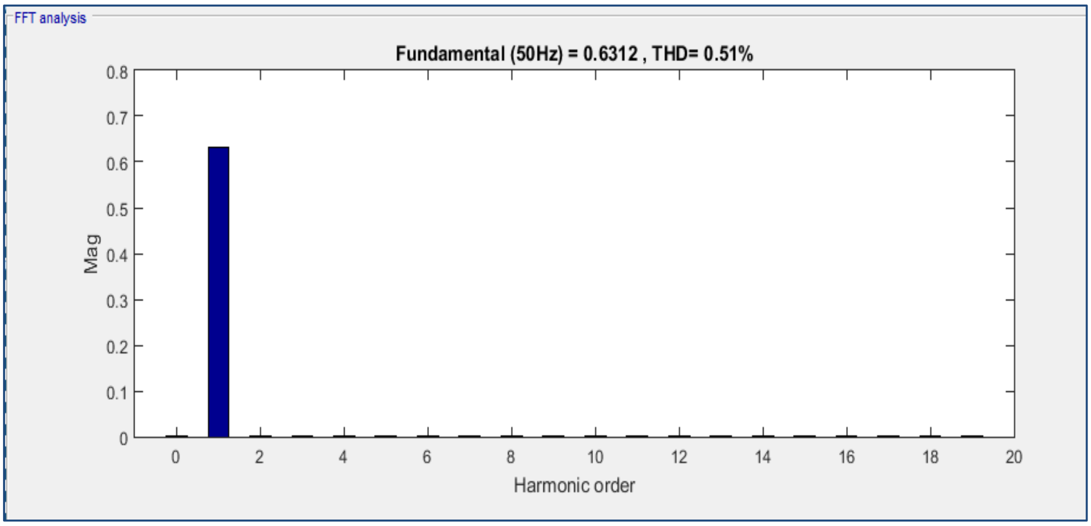

A

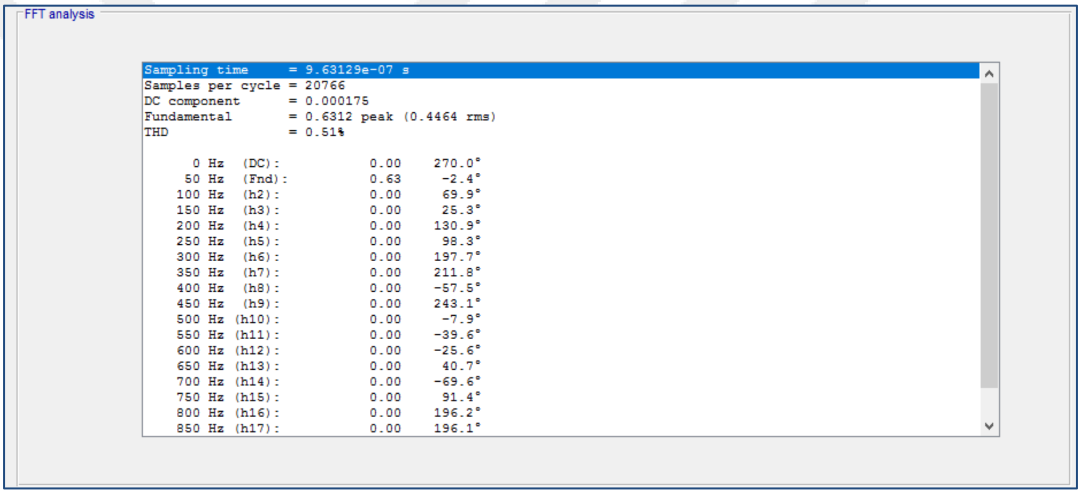
FFT analysis

```
Sampling time     = 9.63129e-07 s
Samples per cycle = 20766
DC component      = 0.000175
Fundamental       = 0.6312 peak (0.4464 rms)
THD               = 0.51%

    0 Hz  (DC):          0.00    270.0°
   50 Hz  (Fnd):         0.63     -2.4°
  100 Hz  (h2):          0.00     69.9°
  150 Hz  (h3):          0.00     25.3°
  200 Hz  (h4):          0.00    130.9°
  250 Hz  (h5):          0.00     98.3°
  300 Hz  (h6):          0.00    197.7°
  350 Hz  (h7):          0.00    211.8°
  400 Hz  (h8):          0.00    -57.5°
  450 Hz  (h9):          0.00    243.1°
  500 Hz (h10):          0.00     -7.9°
  550 Hz (h11):          0.00    -39.6°
  600 Hz (h12):          0.00    -25.6°
  650 Hz (h13):          0.00     40.7°
  700 Hz (h14):          0.00    -69.6°
  750 Hz (h15):          0.00     91.4°
  800 Hz (h16):          0.00    196.2°
  850 Hz (h17):          0.00    196.1°
```

B

Figure 5.20: A and B FFT of source current.

5.2.2 The Second Case

The smart PV system produces real power less than the load demand, this case occurs under the following conditions: temperature 28°C, irradiance density:100 W/m^2. The power components for the system in this case shown in table5.6 while the Figure5.21 show implementation of the system by Matlab/Simulink program, the Figure5.22 shows the waveforms of the source voltage, source current, smart PV current, and load PV current respectively, the Figures 5.23,5.24 shows the Fourier analysis FFT for both load current and source current respectively. From table5.6 we see that the real power part of the load current is provide from the source and the Smart PV System (SPV), while the reactive part was provided by the smart PV system (SPV) and also here we see that acceptable distortion in source current, where all values of (THD) less than 5%, the nonlinear load specification is reactive power 600var, active power11000watt, active power2 200 watt and active power3600 watt).

Table 5.6: System power components of nonlinear load for second case.

Measured quantity	Load	Source	PV system
Apparent power S p.u	1.000	0.5596	0.6739
Real power P p.u	0.7902	0.5594	0.2308
Reactive power Q p.u	0.6739	0.000	0.6717
Distortion power D p.u	0.2804	0.000	0.2209
THD%	15.29	0.71	19.57
Power factor	0.734	1	---------

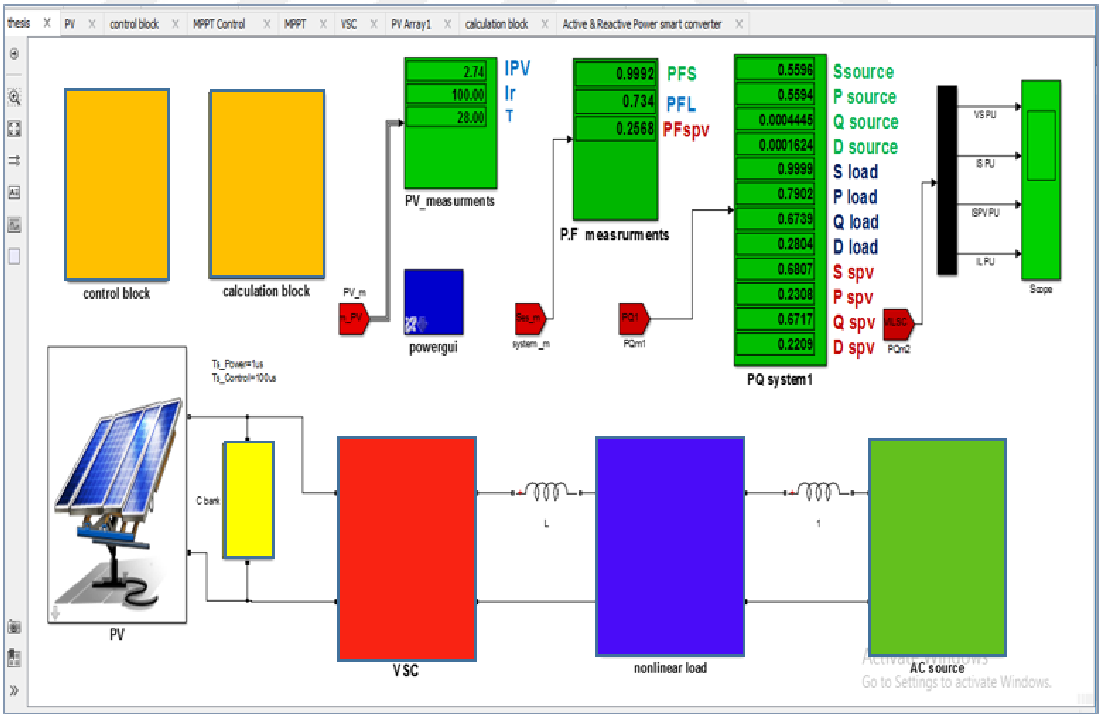

Figure 5.21: Show system implementation by Matlab/Simulink program.

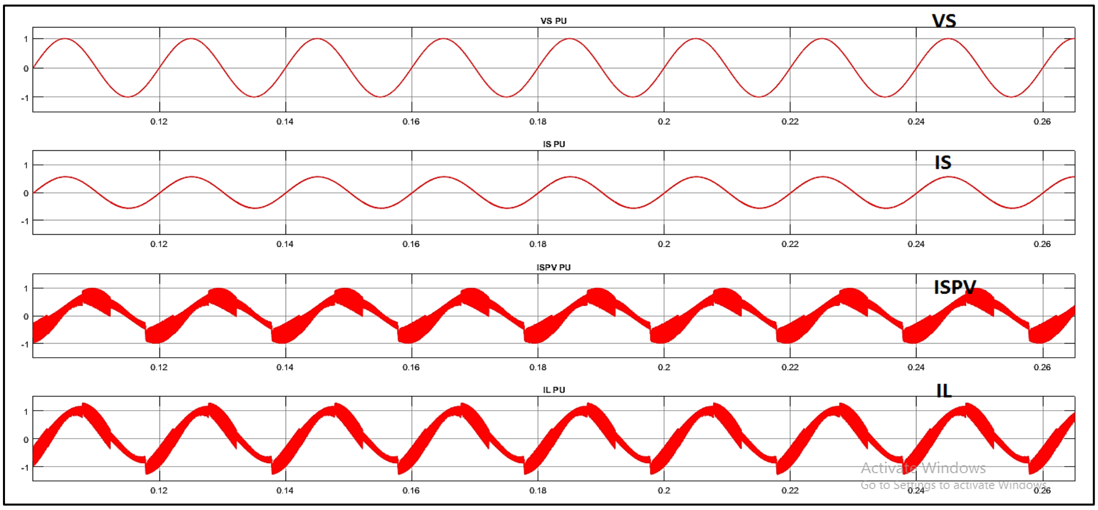

Figure 5.22: Waveforms of the source voltage, source current, smart PV current and load current respectively.

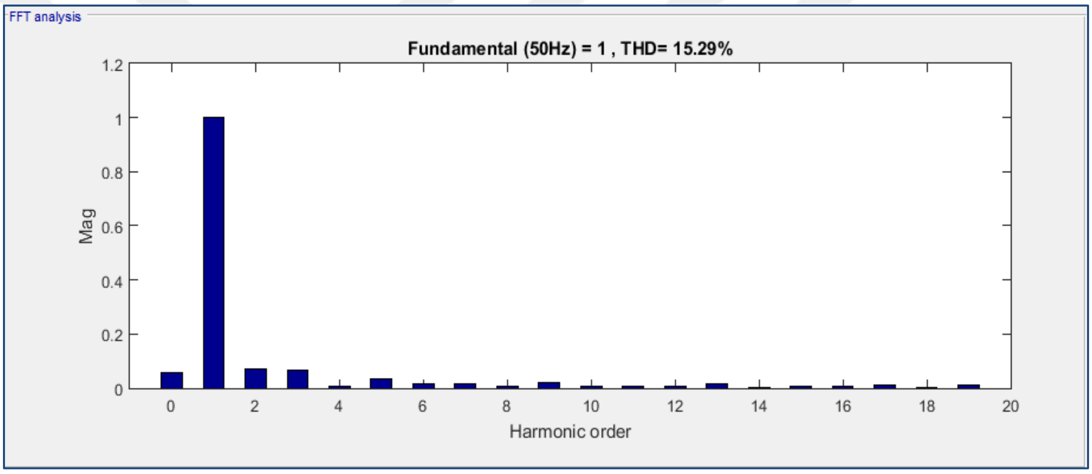

A

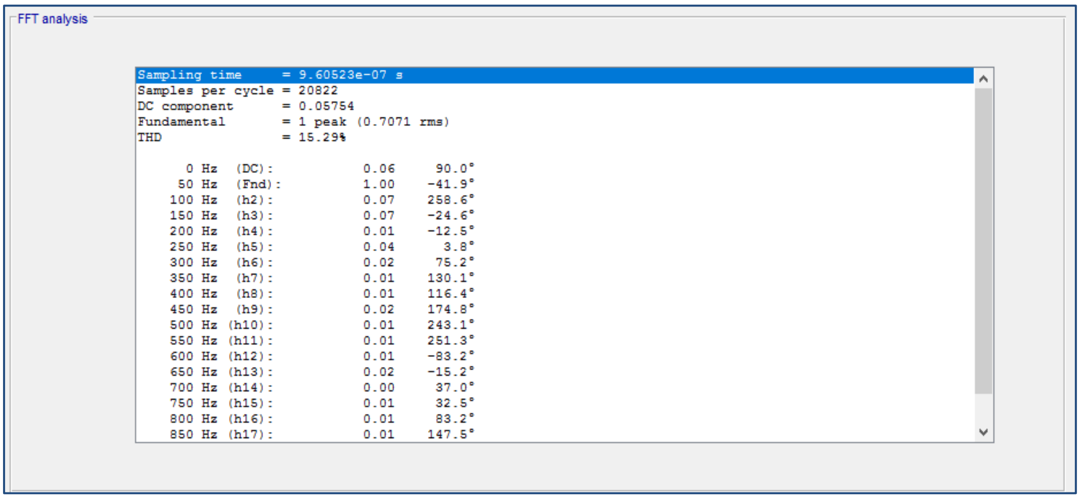
FFT analysis

```
Sampling time     = 9.60523e-07 s
Samples per cycle = 20822
DC component      = 0.05754
Fundamental       = 1 peak (0.7071 rms)
THD               = 15.29%

  0 Hz  (DC):       0.06     90.0°
 50 Hz  (Fnd):      1.00    -41.9°
100 Hz  (h2):       0.07    258.6°
150 Hz  (h3):       0.07    -24.6°
200 Hz  (h4):       0.01    -12.5°
250 Hz  (h5):       0.04      3.8°
300 Hz  (h6):       0.02     75.2°
350 Hz  (h7):       0.01    130.1°
400 Hz  (h8):       0.01    116.4°
450 Hz  (h9):       0.02    174.8°
500 Hz (h10):       0.01    243.1°
550 Hz (h11):       0.01    251.3°
600 Hz (h12):       0.01    -83.2°
650 Hz (h13):       0.02    -15.2°
700 Hz (h14):       0.00     37.0°
750 Hz (h15):       0.01     32.5°
800 Hz (h16):       0.01     83.2°
850 Hz (h17):       0.01    147.5°
```

B

Figure 5.23: A and B FFT of load current

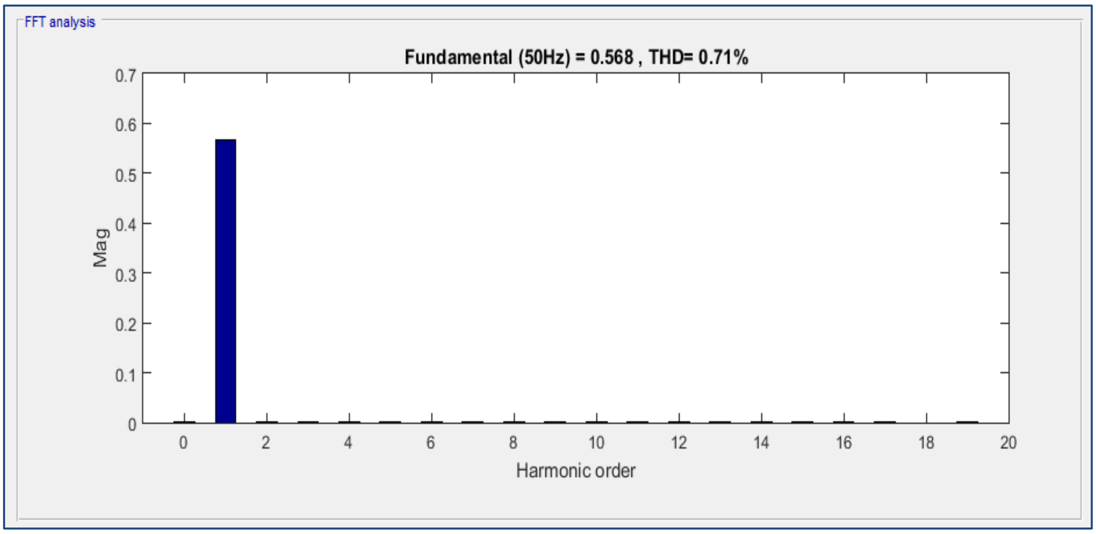

A

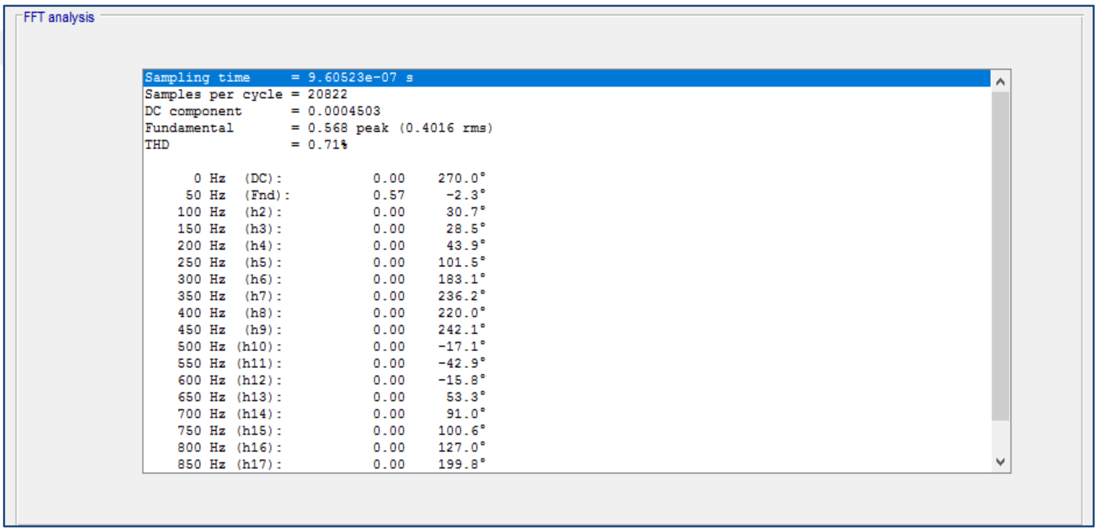

B

Figure 5.24: A and B FFT of source current.

5.2.3 The Third Case

The system (SPV) produces real power more than the load demand, this case occurs in the following conditions: temperature 37°C and irradiance density is 800 W/m^2. Table5.7 shows power components in this case while the Figure5.25 show implementation of the system by Matlab/Simulink program, the Figure5.26 shows the waveforms of the source voltage, source current, smart PV current, and load PV current respectively, the Figures 5.27, 5.28 shows the Fourier analysis FFT for both load current and source current respectively. From table 5.11we see that the real power of the smart PV system is greater than load current demand so that the system will inject the left amount of the real power to the electrical grid by high power factor, while the reactive part was provided by the Smart PV System (SPV) and also here we see that acceptable distortion in source current, where all values of (THD) less than 5%, the nonlinear load specification is reactive power 1300 var, active power1100 watt, active power2 500 watt and active power3 600 watt) .

Table 5.7: System power components of nonlinear for third case.

Measured quantity p.u	Load	Source	PV system
Apparent power S p.u	1.000	0.8527	1.781
Real power P p.u	0.9173	-0.8537	1.772
Reactive power Q p.u	0.5006	0.000	0.5616
Distortion power D	0.3026	0.000	0.6987
THD%	21.75	0.94	23.88
Power factor	0.822	-1	0.93

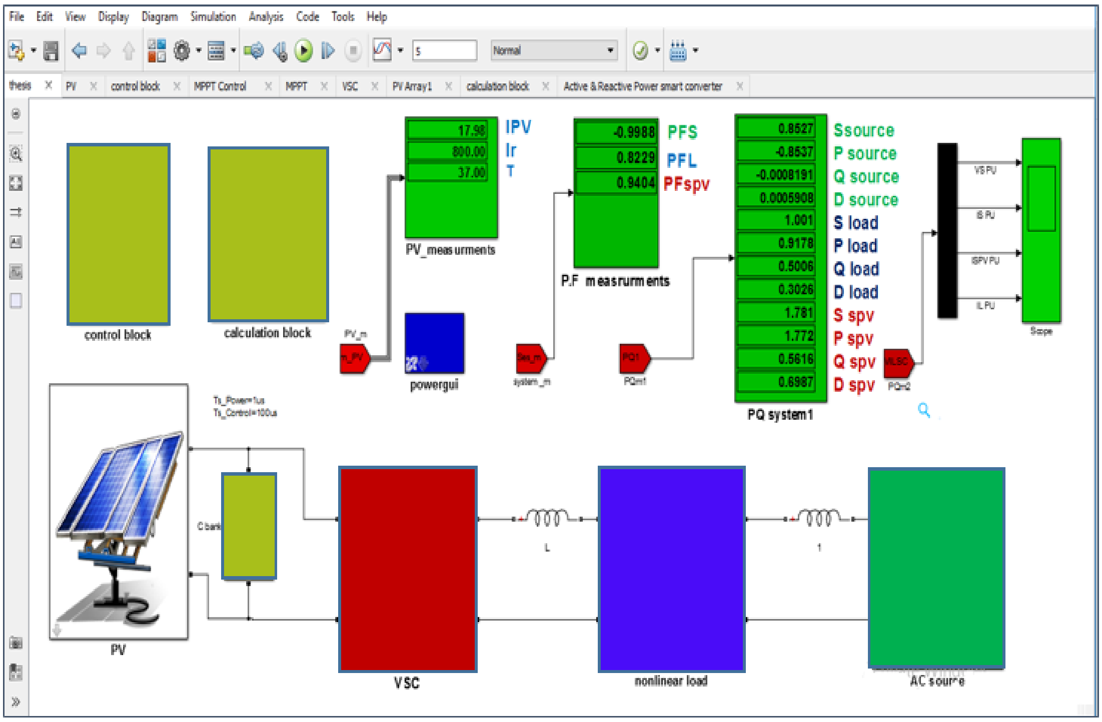

Figure 5.25: System implementation by Matlab/Simulink program.

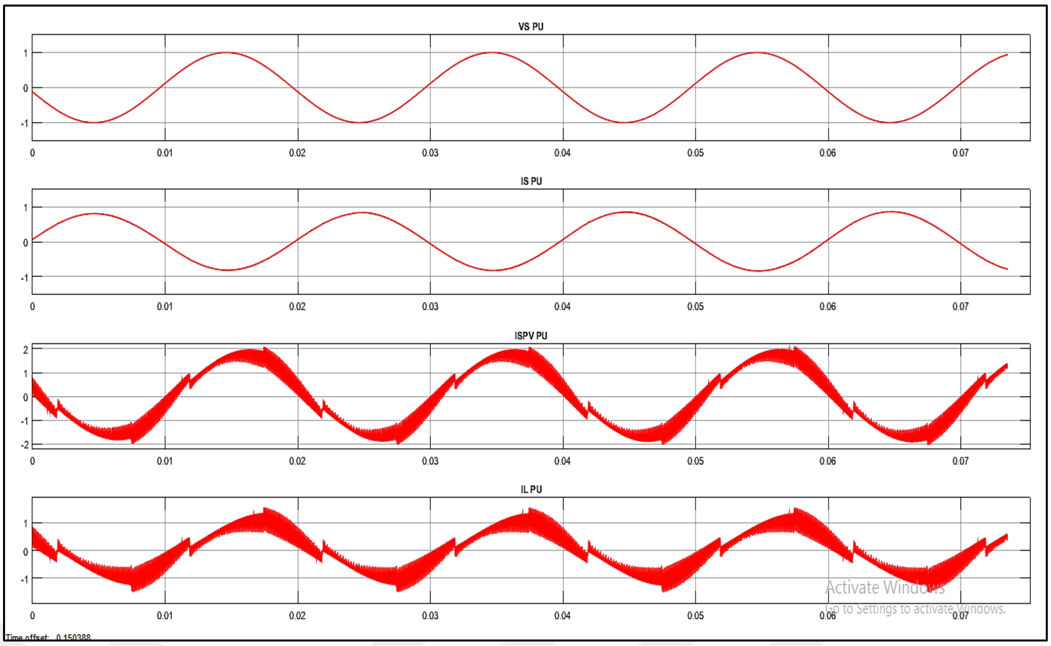

Figure 5.26: Waveforms of the source voltage, source current, load current and smart PV converter current respectively.

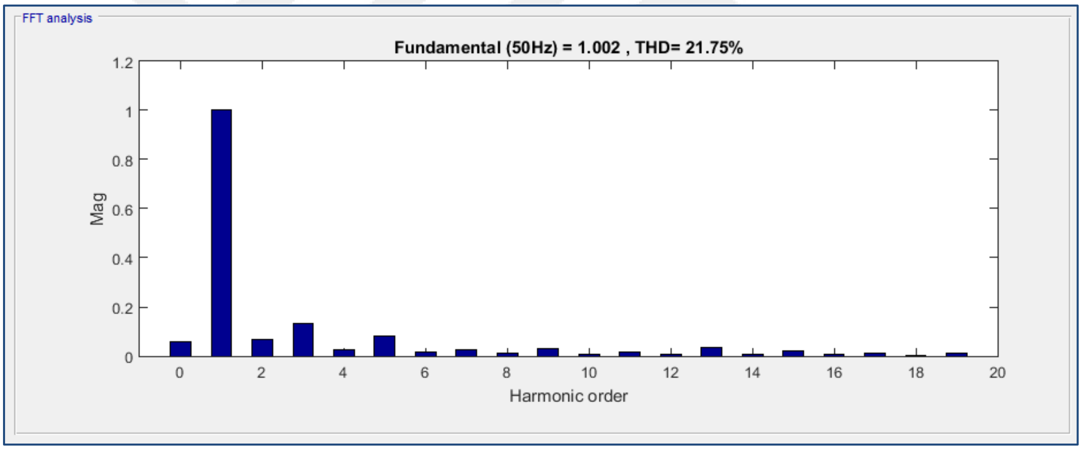

A

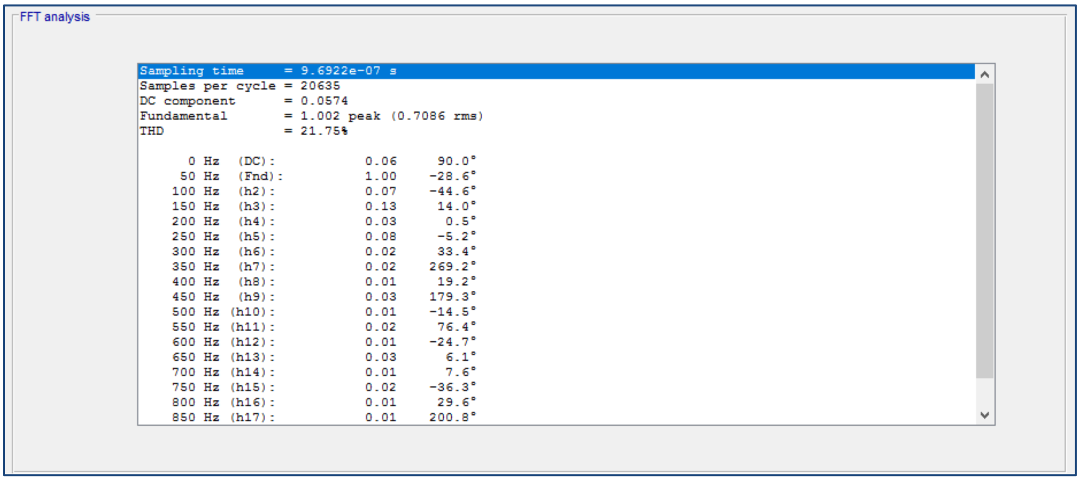
FFT analysis

```
Sampling time      = 9.6922e-07 s
Samples per cycle = 20635
DC component       = 0.0574
Fundamental        = 1.002 peak (0.7086 rms)
THD                = 21.75%
```

0 Hz	(DC):	0.06	90.0°
50 Hz	(Fnd):	1.00	-28.6°
100 Hz	(h2):	0.07	-44.6°
150 Hz	(h3):	0.13	14.0°
200 Hz	(h4):	0.03	0.5°
250 Hz	(h5):	0.08	-5.2°
300 Hz	(h6):	0.02	33.4°
350 Hz	(h7):	0.02	269.2°
400 Hz	(h8):	0.01	19.2°
450 Hz	(h9):	0.03	179.3°
500 Hz	(h10):	0.01	-14.5°
550 Hz	(h11):	0.02	76.4°
600 Hz	(h12):	0.01	-24.7°
650 Hz	(h13):	0.03	6.1°
700 Hz	(h14):	0.01	7.6°
750 Hz	(h15):	0.02	-36.3°
800 Hz	(h16):	0.01	29.6°
850 Hz	(h17):	0.01	200.8°

B

Figure 5.27: A and B show FFT of load current.

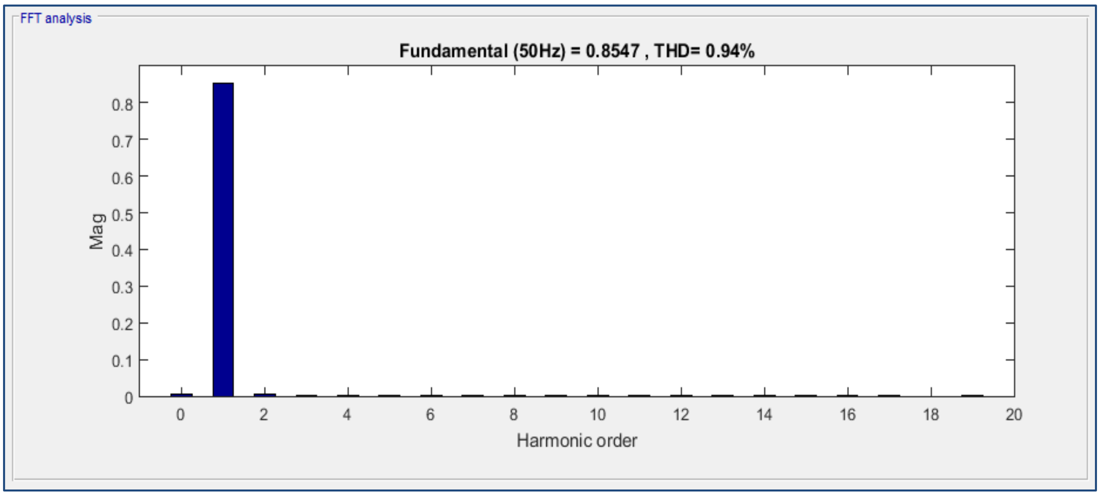

A

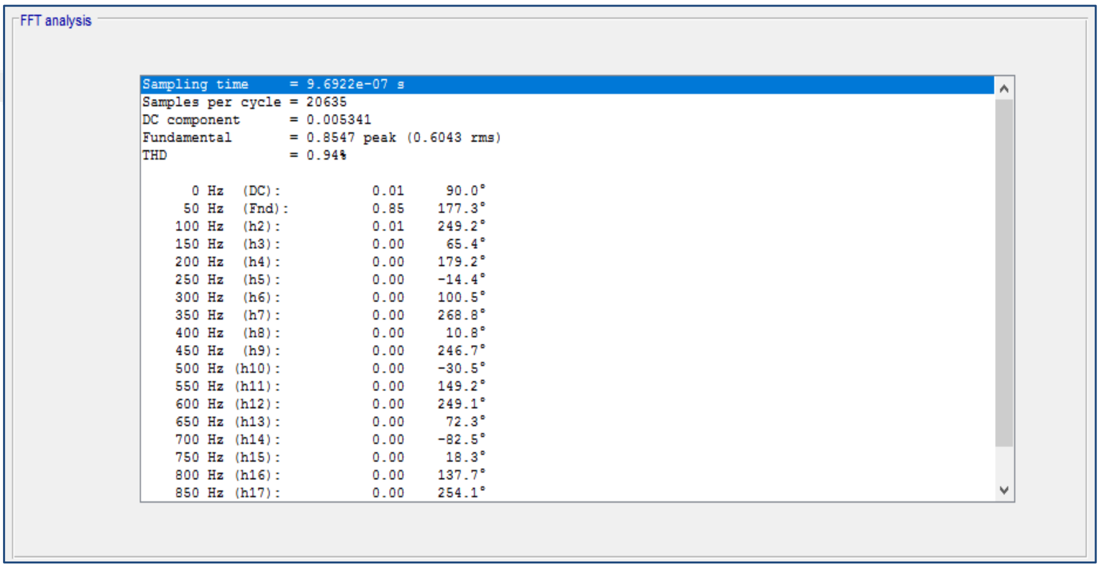

B

Figure 5.28: A and B show FFT of source current.

5.2.4 The Fourth Case

The system produces real power equal to the load demand, this case occurs in the following conditions: temperature 29°C and the irradiance density 280.W/m^2 Table5.8 shows the power components of the system, while the Figure5.29 show implementation of the system by Matlab/Simulink program, the Figure5.30 shows the waveforms of the source voltage, source current, smart PV current, and load PV current respectively, the Figures5.31, 5.32 shows the Fourier analysis FFT for both load current and (SPV) current respectively. From table5.8 we see that the real power of the smart PV system is equal load current demand we see the real power part system is provide from smart PV system only (SPV), while the reactive part was provided by the Smart PV System (SPV) and also here we see that acceptable distortion in source current, where all values of (THD) less than 5%, the nonlinear load specification is reactive power 1200 var, active power1 450 watt, active power2 500 watt and active power3 600 watt).

Table 5.8: System power of nonlinear load for fourth case.

Measured quantity	Load	Source	PV system
Apparent power S p.u	1	0.0064	0.998
Real power P p.u	0.7486	0.0043	0.7443
Reactive power Q p.u	0.7346	0.00005	0.7573
Distortion power D p.u	0.3162	0.00003	0.5
THD%	16.23	---------	16.19
Power factor	0.655	---------	0.652

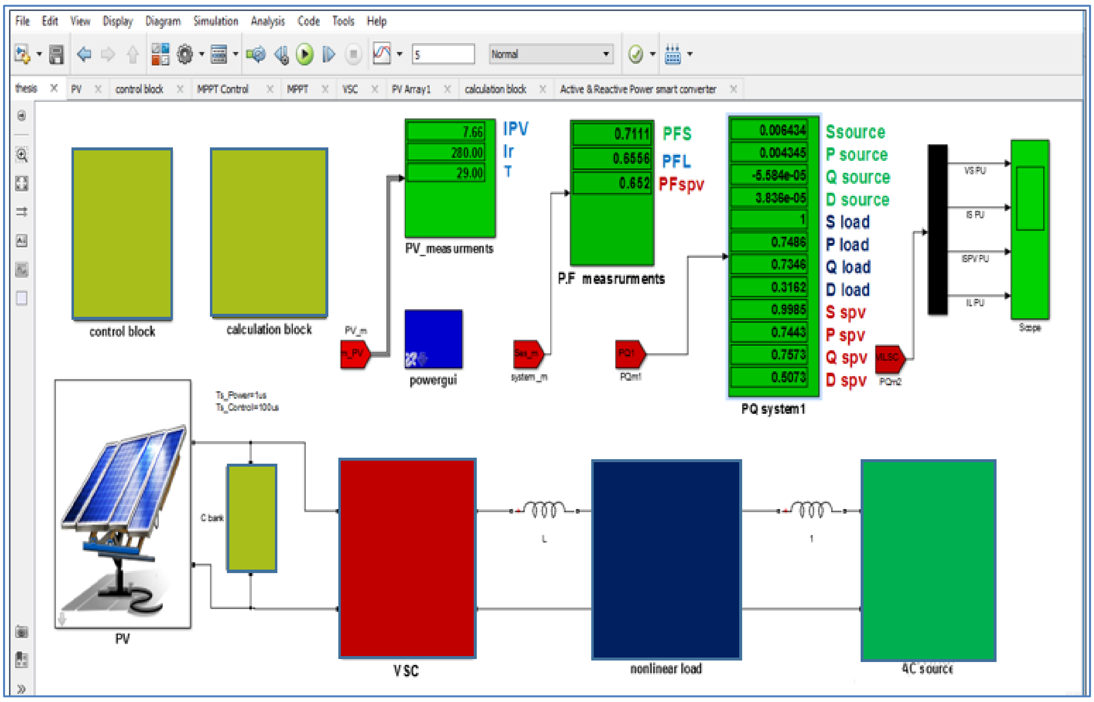

Figure 5.29: System implementation by Matlab/ Simulink program.

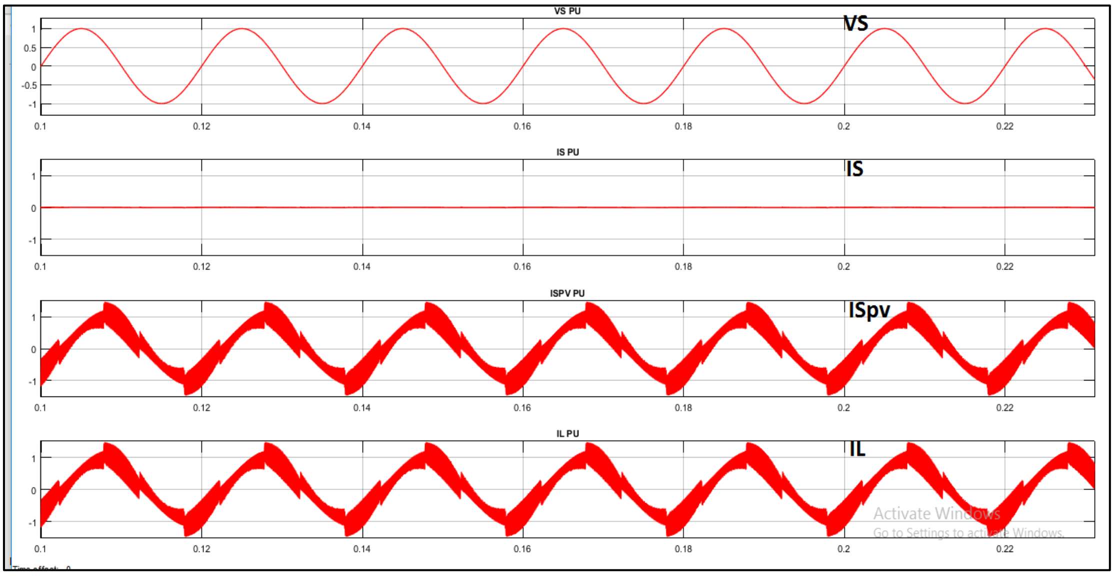

Figure 5.30: Waveforms of source voltage, source current, load current and smart PV current respectively.

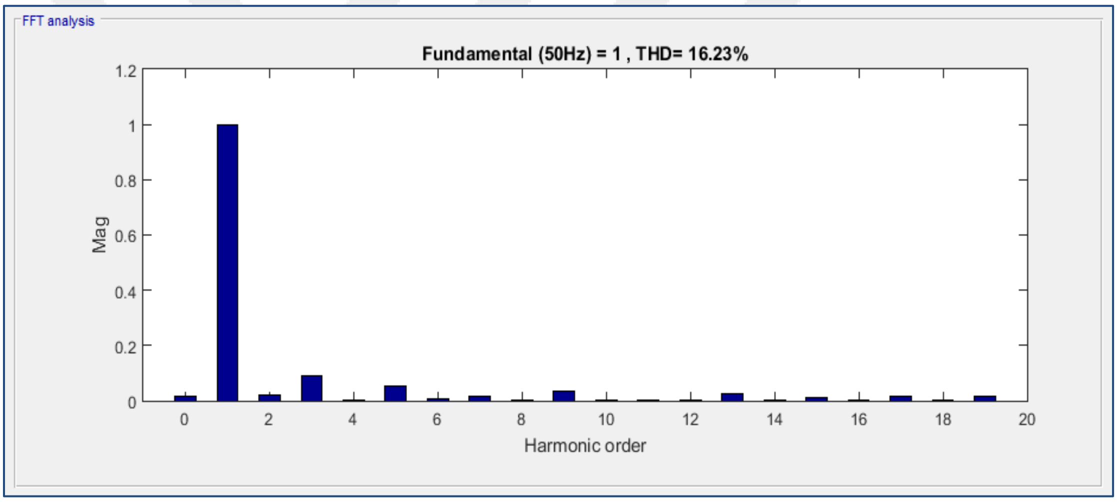

A

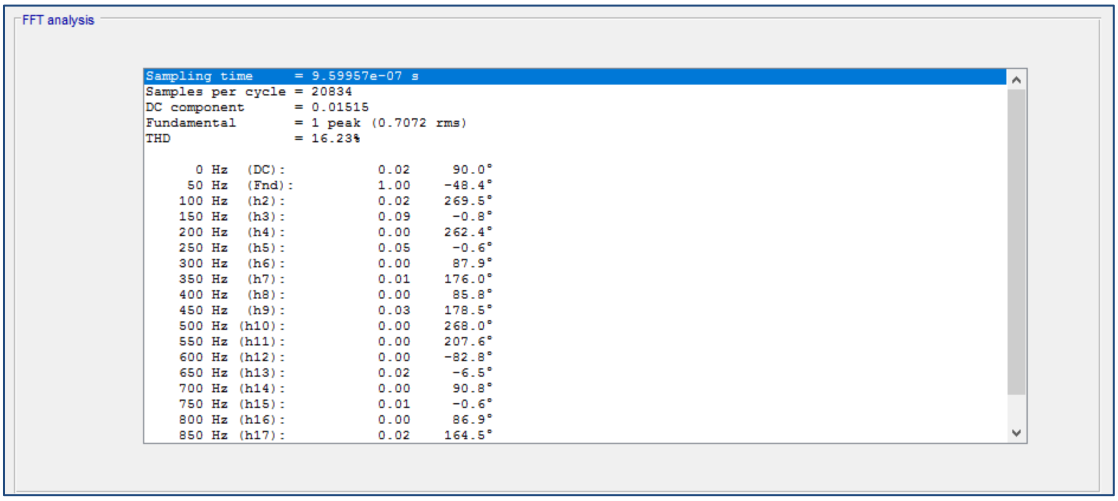

FFT analysis

Sampling time = 9.59957e-07 s
Samples per cycle = 20834
DC component = 0.01515
Fundamental = 1 peak (0.7072 rms)
THD = 16.23%

0 Hz	(DC):	0.02	90.0°
50 Hz	(Fnd):	1.00	-48.4°
100 Hz	(h2):	0.02	269.5°
150 Hz	(h3):	0.09	-0.8°
200 Hz	(h4):	0.00	262.4°
250 Hz	(h5):	0.05	-0.6°
300 Hz	(h6):	0.00	87.9°
350 Hz	(h7):	0.01	176.0°
400 Hz	(h8):	0.00	85.8°
450 Hz	(h9):	0.03	178.5°
500 Hz	(h10):	0.00	268.0°
550 Hz	(h11):	0.00	207.6°
600 Hz	(h12):	0.00	-82.8°
650 Hz	(h13):	0.02	-6.5°
700 Hz	(h14):	0.00	90.8°
750 Hz	(h15):	0.01	-0.6°
800 Hz	(h16):	0.00	86.9°
850 Hz	(h17):	0.02	164.5°

B

Figure 5.31: B and B FFT analysis of the load current.

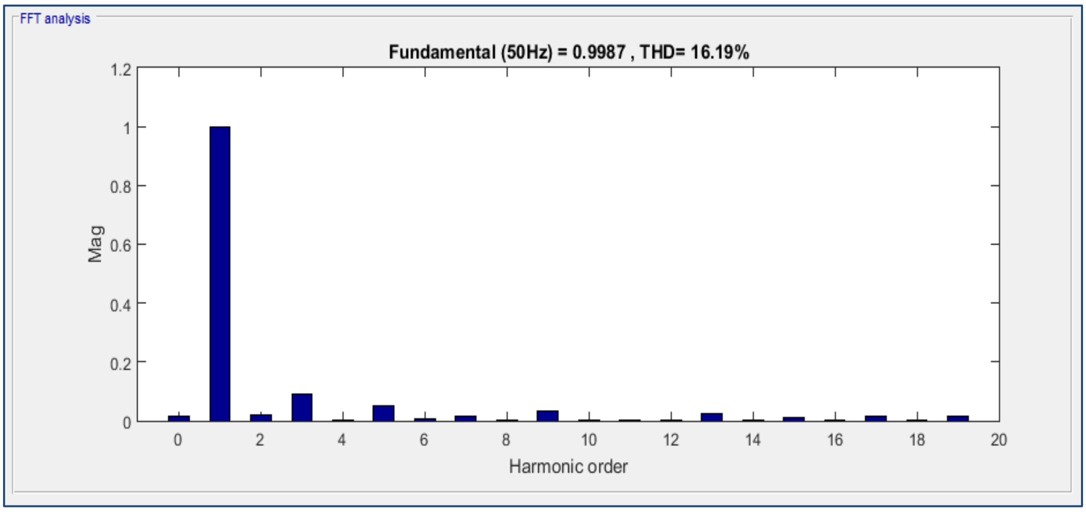

A

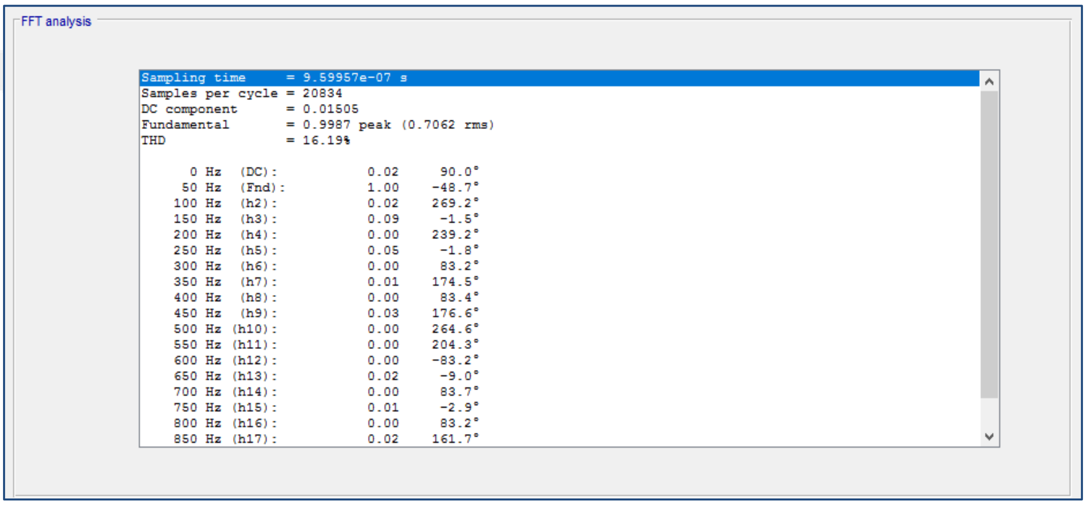

B

Figure 5.32: A and B FFT analysis of the smart PV current.

5.3 Simulated Results Study

From the simulation results the proposed system shows good behavior in dealing in a relax with the variation of load amount and type, temperature and irradiance respectively. in all simulated cases the power factor of the source was near the unity power factor and the total harmonic distortion in all case was less than 5%, also the proposed system shows good behavior in dealing with on line load change and irradiance change as shown in Figures5.33, 5.34 and5.35 respectively which show apparent, real and reactive powers for load, smart PV system and source respectively.

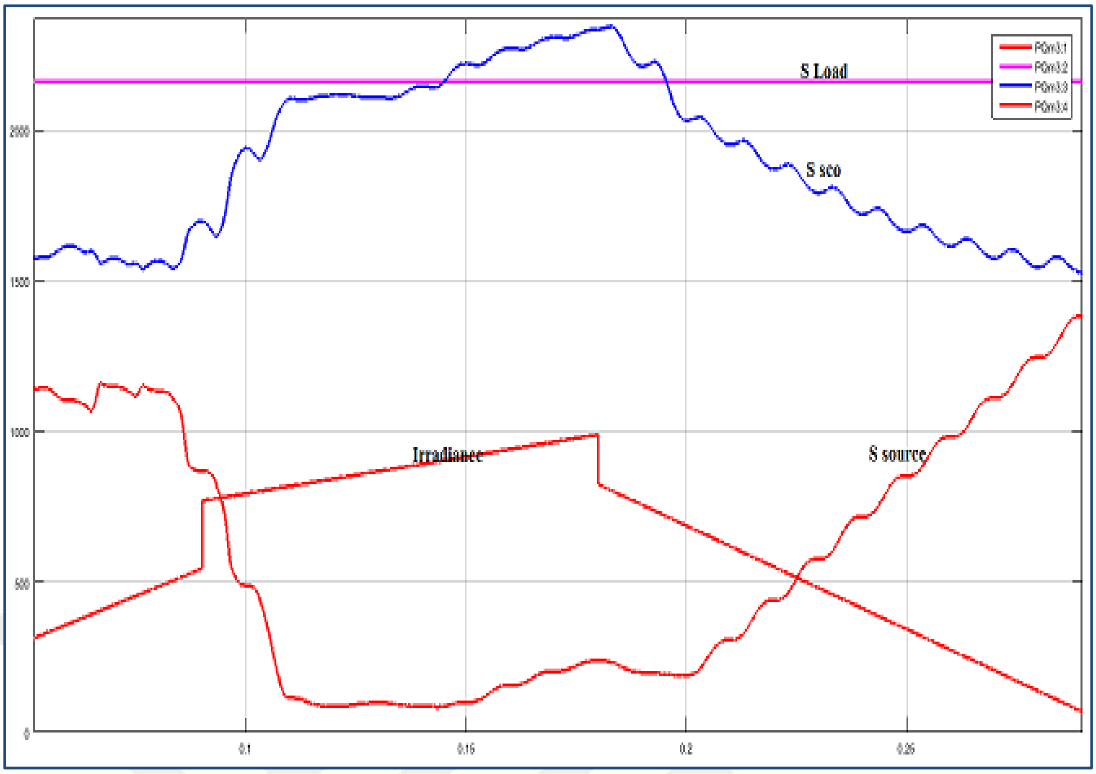

Figure 5.33: Apparent powers waveforms for load, SPV and source.

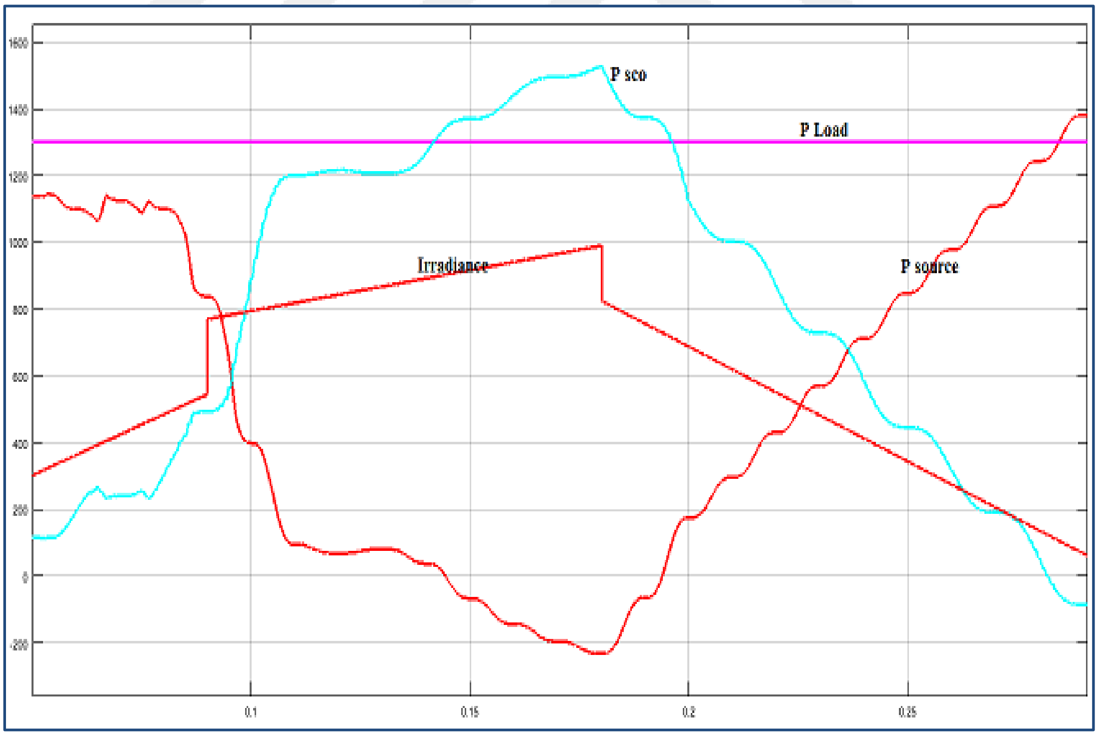

Figure 5.34: Real power waveforms for load, PV and source.

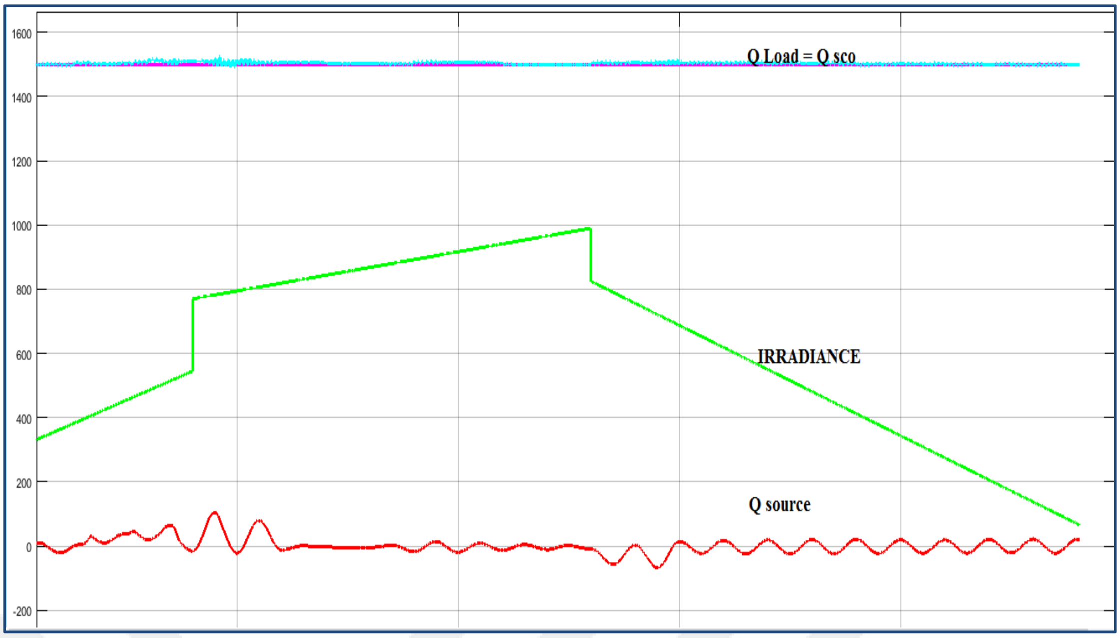

Figure 5.35: Reactive power waveforms for load, SPV and source.

CHAPTER SIX

CONCLUSION AND FUTURE WORKS

The study showed the importance of smart PV systems for power quality improvement through the power components compensation PCC for costumer loads. By presenting mathematical analyses of the modified system, simulate the modified system and finally compare the results obtained in mathematical analysis with those obtained in the simulation. The results convergence was very clear. This convergence in the mathematical and simulation results gives the study its importance.

The smart PV system may be one of the best power quality solutions and one of the best methods for PV system utilization in 24 hours. By inspecting the simulation results, we can see that the total harmonic distortion (THD) in all studied cases was less than 5% and this is acceptable in all electric power quality standards. Moreover, the power factor is also near to unity in all simulated cases. The modified system was utilized for 24 hours so that the modification gave the system its importance.

For future work, this system can be adapted three-phase systems by reducing load unbalance. It can mitigate voltage disturbances due to sudden load changes. The system can be also investigated in the case of short circuit occurrence, and it can be implemented using a multi-level converter in order to reduce switching losses.

REFERENCES

1. MBOUMBOUE Edouard and Donatien NJOMO "Mathematical Modeling and Digital Simulation of PV Solar Panel using MATLAB Software" *International Journal of Emerging Technology and Advanced Engineering* .Volume 3, Issue 9, September 2013.

2. Stuart R. Wenham, Martin A. Green, Muriel E. Watt Richard Corkish and Alistrair. *"Applied Photovoltaic"* Their Edition Earth Scan.

3. Dani Rusirawan *"Energetic modeling of photovoltaic modules in grid – connected systems"* PhD Dissertation Hungary 2012.

4. Muhammad H. Rashid *"Power Electronics Hand Book"* Third Edition, Elsevier Inc. All rights reserved.2011

5. Mohamed E. El-Hawary, *"High Power Converters and AC Drives"* A John Wiley & Sons, Inc., Publication

6. Rajiv K. Varma, Shah Arifur Rahman, Ravi Seethapathy and Tim Vanderheide, Novel Night Time Application of PV Solar Farms as STATCOM (PV-STATCOM)"978-1-4673-2729-9/12/$31.00 © IEEE2012.

7. V. Hima Leela and S. Thai Subha *"Control of Power Converter for Power Quality Improvement in a Grid Connected PV System"* International Conference on Circuits, Power and Computing Technologies [ICCPCT-2013].

8. M. Sai Eswar Rao, K. Obulreddy *"Utilization Of PV Solar Farm As Statcom During Night Hours In A Distribution Network"* INTERNATIONAL JOURNAL OF SCIENTIFIC & TECHNOLOGY RESEARCH VOLUME 3, ISSUE 8, AUGUST 2014.

9. B. Mariappan, B. G. Fernandes and M. Ramamoorty *"A Novel Single Stage Solar Inverter using Active Hybrid Filter with Power Quality Improvement"* 978-1-4799-4032-5/14 IEEE 2014.

10. Prakash Vodapalli, T. Rama Subba Reddy, S. Tara Kalyani *"A New Unified Power Quality Conditioner for Grid Integration of PV System and Power Quality Improvement Feature Distribution System"* 978-1-4799-7678-2/15/$31.00 © IEEE2015.

11. Arun Kumar Venn a, and Bhim Singh *"Harmonics and Reactive Current in a Grid Interfaced PV Distribution System"* 978-1-5090-0128-6/16/$31.00 ©IEEE20 16.

12. Chapman, D.; Power Quality Application Guide - The Cost of Poor Power Quality; Copper Development Association; Version 0b November 2001.

13. The cost of Power Quality Disturbances to Industrial and Digital Economy Companies; Report by Priment; Consortium for Electric Infrastructure to Support a Digital Society (CEIDS), June 2001.

14. *New York Times,* January 2000.

15. *Business Week*, June 17 1996.

16. LAN Times, Category Planning Research, 1997.

17. Abhayrajsinh J. Rana, Mahesh H. Pandya ,Indrajit N. Trivedi, Shaktisinh N. Gohil , Chirag K. Vasoya and Piyushkumar M. Saradva *"Application of D-STATCOM for power quality Improvement in Distribution Line"* International Conference on Computation of Power, Energy Information and Communication (ICCPEIC) , 2016.

18. Bhim Singh, Abrish Chadra and Kamal Al Haddad *"Power Quality Problems and Mitigation Techniques"* India 1 2015.

19. B. Brusilowicz, J. Szafran and Wisniewski *"Reactive power compensation of nonlinear load"* 13th International Conference on Development in Power System Protection (DPSP), Pages: 1 - 6, DOI: 10.1049/cp.2016.0095, 2016.

20. Tanaka, T. and Akagi, H. (1991) *"A new combined system of series active and shunt passive filters aiming at harmonic compensation for large capacity thyristor converters."* Proceedings of IEEE IECON'91, pp. 723–7.

21. N. Ozog , W. Xiao , and W. G. Dunford *"Topology study of photovoltaic interface for maximum power point tracking"* IEEE trans. Ind. Electron , vol 54, no.3,pp.1696-1704, Jun. 2007.

22. Hsu-Chin Wu, Chia-Hsi Chang and Yaow-Ming Chen, *"DC-link capacitor selections for the single-phase grid-connected PV system"* IEEE Conference Publications, International Conference on Power Electronics and Drive Systems (PEDS), Pages: 72 - 77, DOI: 10.1109/PEDS.2009.5385801, 2009.

CURRICULUM VITAE

PERSONAL INFORMATION

Nationality	:	Iraqi
Date and Place of Birth	:	10.5.1979, Slah Al Deen, Iraq
Phone	:	05060549882
Email	:	eng.raaddahi79@gmail.com

EDUCATION

High School	:	AL-Dulueiuh Secondary School, 1998.
Undergraduate	:	University of Diyala / College of Engineering / Electrical Engineering Department, 2002.

WORK EXPERIENCE

Year	:	2003- Present
Place	:	Iraqi Ministry of Electricity/ Energy Production Office

FOREIGN LANGUAGE

English, Turkish